CHARACTERIZING PATTERNS IN ENDANGERED CETACEAN POPULATIONS OF THE HAWAIIAN ARCHIPELAGO USING PASSIVE ACOUSTIC DATA

A DISSERTATION SUBMITTED TO THE GRADUATE DIVISION OF THE UNIVERSITY OF HAWAIʻI AT MĀNOA IN PARTIAL FULFILLMENT OF THE REQUIREMENTS FOR THE DEGREE OF

DOCTOR OF PHILOSOPHY

IN

MARINE BIOLOGY

December 2020

By

Yvonne M. Barkley

Dissertation Committee:

Erik C. Franklin, Chairperson
Erin M. Oleson
Jeffrey Polovina
Margaret McManus
Eva M. Nosal

Keywords: cetacean ecology, passive acoustic monitoring, classification, localization, species distribution models

DEDICATION

To Oma

ACKNOWLEDGMENTS

I would like to thank my advisor, Erik Franklin, for guiding me through my interdisciplinary research and helping me build my quantitative skills. I would also like to thank my committee members, Erin Oleson, Margaret McManus, Jeff Polovina, and Eva Nosal for fostering a positive learning environment where I felt encouraged and supported to pursue my research interests and persevere through any challenges. I would like to express my gratitude to my lab mates who were always willing to relate their analytical skills in fisheries science to my analyses of cetacean acoustic data.

Thank you to everyone involved in collecting the passive acoustic data during the cetacean surveys. My research would not have been possible without your patience, cooperation, and dedication. Special thanks to the Cetacean Research Program for their professional and moral support over the years.

I would like to express my appreciation for Robin Baird and Jim Carretta for their insight and feedback on Chapter 2, Pina Gruden and Fabio Casagrande Hirono for their expertise and detailed revisions of Chapter 3, and Taiki Sakai and Zack Oyafuso for their patience and enthusiasm when discussing the nitty gritty details of Chapter 4.

A special thanks goes to Sheldon Plentovich and Amanda Bradford for cheering me on throughout each stage of my graduate school experience and celebrating the milestones with me. To my parents and my sister, thank you for always supporting me from afar and being proud of me.

Finally, to my loving husband, Erik Norris, whose steadfast belief in me kept me moving in the right direction even through the most difficult times. I could not imagine a better partner by my side throughout this arduous process. Thank you for your genuine excitement about my work, our late-night discussions, and your endless support in helping me achieve my goals in graduate school and in life.

ABSTRACT

Cetaceans play a vital ecological role in the marine environment as highly mobile top predators, but many species lack sufficient baseline data required for effective management and conservation. Cetacean population studies rely on the ability to accurately detect and identify the species, determine their location, estimate the number of animals or groups, and evaluate patterns in distribution. For endangered cetacean species, this information can be critical to their survival. Vessel-based visual observer surveys are the primary methods for studying cetacean populations, but these methods are limited by daylight, cetacean behavior, and poor weather conditions. Passive acoustic monitoring provides a technological approach for studying cetaceans using their vocalizations that is complementary to traditional visual observation methods. For this dissertation work, I developed and applied analytical methods that advance the use of acoustic data for cetacean population studies of endangered false killer whales (*Pseudorca crassidens*) and sperm whales (*Physeter macrocephalus*) in the Hawaiian Archipelago. My research addressed three components: (1) the utility of acoustic data to discriminate whistle characteristics of sympatric false killer whale populations, (2) the development of a localization algorithm for shallow towed linear arrays to improve the accuracy of 3-D positional estimates of cetaceans, and (3) a comparison of the environmental factors that predict the distribution of foraging versus non-foraging sperm whales. Each component of this research contributes important information for these endangered cetacean populations and guides future use of acoustic data in cetacean population studies.

TABLE OF CONTENTS

Page

LIST OF TABLES

Page

LIST OF FIGURES

Page

CHAPTER 1

INTRODUCTION

1.1 Motivation

A diverse community of cetacean species resides in the waters surrounding the Hawaiian Archipelago. Cetaceans are marine apex predators comprised of odontocetes (toothed whales) and mysticetes (baleen whales), with at least 25 species occurring within the Hawaiian Archipelago year-round (Carretta *et al.*, 2020). Odontocetes and mysticetes differ biologically and ecologically, but both influence the structure and function of the marine ecosystem (Estes *et al.*, 2016). Cetaceans affect the behavior and distribution of their prey and competitors, as well as contribute to nutrient recycling and the modification of benthic habitats as part of their ecological role (Bowen, 1997; Kiszka *et al.*, 2015; Estes *et al.*, 2016). We are in a period of unprecedented ecological change. Increasing baseline knowledge about these species now provides our best chance of implementing effective management and conservation plans to sustain future populations.

The Hawaiian Archipelago is situated near the center of the North Pacific Subtropical Gyre (NPSG), where the abiotic and biotic environmental conditions coalesce to create suitable cetacean habitat. The NPSG is an oligotrophic environment characterized by low nutrient levels and primary production (Mann and Lazier, 2006). However, mesoscale oceanographic processes (e.g., eddies and fronts) greatly enhance the productivity of the NPSG resulting in patchy areas of nutrient-rich waters that benefit the base of the food web and, in turn, support cetaceans and other higher tropic level organisms (Polovina *et al.*, 2000; Seki *et al.*, 2002; Woodworth *et al.*, 2012; Abecassis *et al.*, 2015). Food-web dynamics are also influenced by an increase in phytoplankton biomass near the islands and atolls within the Hawaiian Archipelago, i.e., Island Mass Effect (Doty and Oguri, 1956). For example, the micronekton species within the mesopelagic boundary layer community feed on the increased food resources near shore, and are consumed by cetaceans and other pelagic predators that are attracted to these areas of enhanced prey (Benoit-Bird and Au, 2003; Gove *et al.*, 2015).

Sound propagates approximately five times faster through the ocean than through air. With the majority of their time spent underwater, cetaceans have adapted to utilize sound for

every aspect of their lives. Odontocetes produce high-frequency pulsed clicks (echolocation clicks) for foraging and navigation (Au and Hastings, 2008; Zapetis and Szesciorka, 2018). They engage in complex social interactions and behaviors using whistles, which are frequency-modulated calls (Riesch and Deecke, 2011; Janik and Sayigh, 2013). Mysticetes produce lower frequency vocalizations for long-range communication during social interactions and mating (Edds-Walton, 2012). The use of sound is critical for the survival of all cetacean species.

Hawaiian cetaceans endure numerous anthropogenic impacts throughout the island chain. Anthropogenic noise from boating, commercial shipping, and military exercises contributes to increased ocean noise levels that alter cetaceans' habitat and interferes with their ability to communicate, causes hearing loss, and disrupts foraging dives (Hildebrand, 2005; Weilgart, 2007; Tyack *et al.*, 2011; Southall *et al.*, 2016). Disturbance from marine tourism operators and swimmers can alter behavioral states (Scarpaci *et al.*, 2000; Timmel *et al.*, 2008; Wiener *et al.*, 2009). Cetacean prey species are also targeted by commercial and recreational fishers, which can lead to interactions between cetaceans and fishing gear resulting in serious injury or death (Nitta and Henderson, 1993; Forney, 2000; Forney *et al.*, 2011; Baird *et al.*, 2014). Cetaceans are also at risk for bioaccumulating persistent organic pollutants that are linked to reductions in reproductive success and the disruption of endocrine and immune systems (Ylitalo *et al.*, 2009; Bachman *et al.*, 2014).

Fortunately, all cetacean populations in U.S. waters are protected under the U.S. Marine Mammal Protection Act (MMPA) to regulate the unintentional take of cetaceans and other marine mammals that result from anthropogenic activities. The primary objectives of the MMPA are to maintain populations above their optimum sustainable population level and as functioning elements of their ecosystem. Stock assessment reports are required to periodically update the status of a population (or stock) to support management and conservation decisions. Under the MMPA, human-caused mortalities are regulated through the calculation of potential biological removals (PBR) for each population, defined as the maximum number of animals that may be removed from the population while still allowing for levels of abundance to meet or exceed a certain population size (Taylor *et al.*, 2000). The PBR requires estimates of abundance as one element of the PBR calculation. Additionally, the U.S. Endangered Species Act (ESA) applies to cetaceans listed as endangered or threatened and mandates a recovery plan and the designation of critical habitat to prevent the extinction of imperiled species.

The National Marine Fisheries Service (NMFS) conducts shipboard line-transect surveys to study the distribution and estimate the abundance of cetacean populations to inform stock assessments. The surveys are designed according to distance sampling methods and require a team of scientists to collect observational data of cetacean species and oceanographic measurements of their habitat (Buckland *et al.*, 2001; Yano *et al.*, 2018). Visual data collection methods require accurate species identification and entail collecting photo-identification data to count individuals (Durban *et al.*, 2005; Urian *et al.*, 2015), deploying satellite tags to study animal movement (Baird *et al.*, 2011; Straley *et al.*, 2014; Abecassis *et al.*, 2015), and obtaining tissue samples for genetic analyses (Hoelzel, 1992; DeSalle and Amato, 2004; Chivers *et al.*, 2010; Mesnick *et al.*, 2011; Martien *et al.*, 2014). Valuable information about cetacean ecology has been gained through visual observations. Parameters measured from visual observation data are incorporated into abundance estimation and include the distance of the animals from the trackline and group size estimates (estimated number of animals within a group). However, animal behavior may introduce bias to abundance estimation if missed due to cryptic surface behavior or foraging at depth for prolonged periods of time. In both cases, abundance may be underestimated for certain species (Barlow, 1999, 2015).

Passive acoustic monitoring (PAM) has been around for decades to record and analyze animal sounds from all taxa (e.g., marine mammals, (Schevill and Lawrence, 1949; Poulter, 1963); terrestrial mammals, (Lieberman, 1968; Huetz and Aubin, 2012); birds, (Brough, 1969; Catchpole and Slater, 2008); fish, (Myrberg, 1980; Gannon, 2008); amphibians, (Loftus-Hills and Littlejohn, 1971; Gerhardt, 1994); insects, (Alexander, 1962; Tishechkin, 2014); and bats, (Simmons and Stein, 1980; Smotherman *et al.*, 2016). Underwater microphones, i.e., hydrophones, are capable of recording all known frequencies of cetacean vocalizations (Stafford *et al.*, 1998; Merkens *et al.*, 2018). Several types of PAM methods exist to study cetacean populations and the configuration of the PAM system depends on the research question (Mellinger *et al.*, 2007; Van Parijs *et al.*, 2009; Marques *et al.*, 2013).

A towed line array of hydrophones has become a standard PAM method for collecting passive acoustic data from vocalizing cetaceans to complement visual observation methods during line-transect surveys for abundance estimation (Rankin, Oswald, *et al.*, 2008; Rankin *et al.*, 2013). This PAM method is useful for real-time detection, tracking, and localization of vocalizing animals to assist visual observers in finding cetacean groups (Leaper *et al.*, 2000;

Evans and Hammond, 2004; Barlow, 2006). Towed line array acoustic data can be used to measure distances to cetacean groups and are effective for detecting deep-diving and highly cryptic species that may be missed visually (Barlow and Taylor, 2005; Rankin, Barlow and Oswald, 2008). However, many species cannot be accurately identified using acoustic characteristics of their vocalizations and the inability to estimate group size preclude the data from being incorporated into cetacean abundance estimates for stock assessments. Acoustic data collection using towed line arrays is an integral operation during line-transect surveys, but there are limited analytical techniques for deriving important information that could be utilized for studying the abundance and distribution of cetaceans.

This dissertation research produces novel analytical methods to study patterns in cetacean populations using passive acoustic data, specifically advancing the use of towed line array acoustic data for classification, localization, and distribution modeling. The Hawaiian populations of false killer whales (*Pseudorca crassidens*) and sperm whales (*Physeter macrocephalus*) were included in this research due to their endangered status and the fact that their vocalizations can be reliably identified to species (Backus and Schevill, 1966; Whitehead and Weilgart, 1990; Rendell *et al.*, 1999; Oswald *et al.*, 2007; Barkley *et al.*, 2011). Methods and results developed here may be applied to other cetacean populations to improve baseline knowledge and further our understanding of their ecological importance.

1.2 Outline

The false killer whale population associated with the Main Hawaiian Islands (MHI) is listed as endangered and is one of three genetically distinct populations that occur in Hawaiian waters, including a population associated with the Northwestern Hawaiian Islands (NWHI) and a pelagic population dispersed throughout offshore waters (Baird *et al.*, 2008, 2010; Chivers *et al.*, 2010; Baird *et al.*, 2013a; Martien *et al.*, 2014). Abundance estimates for the MHI population are low; less than 200 individuals are estimated to exist from mark-recapture analyses (Bradford *et al.*, 2012). Visual observer surveys of the MHI population have been generally restricted to nearshore waters on the leeward sides of islands, but satellite tag data revealed high-use areas throughout the islands where animals are presumed to spend time foraging (Baird *et al.*, 2012).

Chapter 2 develops a method to distinguish between the three sympatric populations using characteristics of their whistles. Whistles were extracted and measured from towed line

array acoustic data collected during five line-transect cetacean surveys and incorporated into Random Forest classification models to examine the variation in whistle characteristics between and within the three Hawaiian Islands false killer whale populations. Using acoustic data of these populations offers an additional means for studying their distribution in conjunction with visual observations.

Sperm whales in the Hawaiian Archipelago are present year-round and include all demographic groups (Thompson and Friedl, 1982; Mesnick *et al.*, 2011; Baird *et al.*, 2013). Sperm whales produce high-amplitude, low frequency echolocation clicks and buzzes while foraging and socializing (Papastavrou *et al.*, 1989; Weilgart and Whitehead, 1993; Miller *et al.*, 2004; Oliveira *et al.*, 2013). During foraging dives, sperm whales can spend over an hour underwater and descend to depths of nearly 2000 m searching for prey consisting primarily of different cephalopod species (Clarke *et al.*, 1993; Clarke and Young, 1998; Evans and Hindell, 2004; Watwood *et al.*, 2006; Teloni *et al.*, 2008; Irvine *et al.*, 2017; Foskolos *et al.*, 2020). This foraging behavior can result in groups being missed by visual observers during typical line-transect survey operations. However, echolocation clicks can be detected and identified acoustically, providing opportunity to enhance visual survey data with detections from a joint towed array survey.

Several studies report abundance estimates using towed line array acoustic data from line-transect surveys (Gillespie and Leaper, 1997; Taylor *et al.*, 2000; Lewis *et al.*, 2007; Yack *et al.*, 2016). However, distance estimates were derived without accounting for animal depth or uncertainties associated with the acoustic data (i.e., hydrophone movement, sound propagation effects, errors in the time of arrival differences) potentially biasing abundance estimates. Chapter 3 develops a semi-automated, model-based localization approach to analyze towed line array acoustic data of sperm whales to improve upon existing two-dimensional localization methods typically applied to deep-diving cetaceans. This approach accounts for sources of error and animal depth for three-dimensional localization with error estimates. The localization method is evaluated and demonstrated using simulated and empirical sperm whale acoustic data. By integrating the uncertainties associated with towed line array acoustic data of deep-divers, more robust location and distance estimates are achieved with this model-based localization approach. This research also provides a better understanding of factors influencing localization results in

general, which is helpful for improving acoustic data collection methods for all cetaceans using towed line arrays.

Understanding the distribution of a species is important for effective management and conservation but knowing where individuals are located at any given time is challenging. Species distribution models (SDMs) are a quantitative tool used to predict the distribution of a species by correlating the presence or abundance of a species with their associated geographic and environmental habitat features (Elith and Leathwick, 2009). Sighting data are the predominant observational data used for predicting cetacean distribution in SDMs. While many line-transect cetacean surveys use towed line arrays to collect passive acoustic data for cetaceans, relatively few studies incorporate the data into SDMs for several reasons. Many cetaceans cannot be accurately identified to species based solely on their vocal characteristics, which restricts the application of SDMs to only certain cetacean species. Acoustic data often require multiple stages of processing to extract the necessary information for models, which can be labor-intensive and time-consuming. Furthermore, it is not currently possible to accurately estimate the number of animals in a group for most species using acoustic data, precluding its use in models designed to predict density and abundance (Redfern *et al.*, 2006). However, there is value in developing SDMs to incorporate all available data to study spatial distribution patterns of cetaceans, especially when acoustic data complement the sighting data (Fleming *et al.*, 2018).

Chapter 4 develops methods to incorporate sighting and acoustic data from four line-transect surveys into SDMs to better understand the spatial patterns of sperm whale groups. This work also evaluates the effectiveness of including disparate data types in SDMs. Information derived from the type of echolocation clicks present in the acoustic data allowed for sperm whale groups to be categorized as foraging or non-foraging to create separate SDMs based on sperm whale behavior. Comparing results from SDMs using sighting and acoustic data showed some differences in the spatial patterns and significant environmental predictors. The behavioral SDMs resulted in substantially different spatial patterns, highlighting areas where the foraging whales were more prevalent in the northwestern region of the study area. This study emphasizes the value of including all available data when deciphering patterns in distribution since different data types provide complementary information about a population.

CHAPTER 2

WHISTLE CLASSIFICATION OF SYMPATRIC FALSE KILLER WHALE POPULATIONS IN HAWAIIAN WATERS YIELDS LOW ACCURACY RATES

Barkley, Y., Oleson, E. M., Oswald, J. N. and Franklin, E. C. (2019) 'Whistle classification of sympatric false killer whale populations in Hawaiian waters yields low accuracy rates', *Frontiers in Marine Science*, 6, pp. 1–27. doi:10.3389/fmars.2019.00645.

Abstract

Cetaceans are ecologically important marine predators, and designating individuals to distinct populations can be challenging. Passive acoustic monitoring provides an approach to classify cetaceans to populations using their vocalizations. In the Hawaiian Archipelago, three genetically distinct, sympatric false killer whale (*Pseudorca crassidens*) populations coexist: a broadly distributed pelagic population and two island-associated populations, an endangered main Hawaiian Islands (MHI) population and a Northwestern Hawaiian Islands (NWHI) population. The mechanisms that sustain the genetic separation between these overlapping populations are unknown but previous studies suggest that the acoustic diversity between populations may correspond to genetic differences. Here, we investigated whether false killer whale whistles could be correctly classified to population based on their characteristics to serve as a method of identifying populations when genetic or photographic-identification data are unavailable. Acoustic data were collected during line-transect surveys using towed hydrophone arrays. We measured 50 time and frequency parameters from whistles in 16 false killer whale encounters identified to population and used those measures to train and test random forest classification models. Random forest models that included three populations correctly classified 42% of individual whistles overall and resulted in a low kappa coefficient, $\kappa = 0.15$, indicating low agreement between models and the true population. Whistles from the MHI population showed the highest correct classification rate (52%) compared to pelagic and NWHI whistles (42% and 36%, respectively). Pairwise random forest models classifying pelagic and MHI whistles proved slightly more accurate (62% accuracy, $\kappa = 0.24$), though a similar pelagic-NWHI model did not (56% accuracy, $\kappa = 0.12$). Results suggest that the time-frequency whistle characteristics are not suitable to confidently classify encounters to a specific false killer whale

population, although certain features of whistles produced by the endangered MHI population allow for overall higher classification accuracy. Inclusion of other vocalization types, such as echolocation clicks, and alternative whistle variables may improve correct classification success for these sympatric populations.

2.1 Introduction

Cetaceans are top predators widely distributed throughout the world's oceans and can play specific roles in maintaining ecosystem function and structure due to their higher trophic level (Estes *et al.*, 1998; Roman and McCarthy, 2010; Roman *et al.*, 2014). Changes to their abundance and distributions have cascading effects that affect complex interactions between multiple trophic levels within the oceanic food web (Heithaus *et al.*, 2008; Baum and Worm, 2009; Estes *et al.*, 2011; Kiszka *et al.*, 2015). Conservation and management efforts for cetaceans are complicated by the inherent challenges associated with studying animals that live primarily underwater. Most statistical analyses for estimating cetacean density, abundance, and distribution only include data collected by visual observers (Buckland *et al.*, 2001; Durban *et al.*, 2005; Palacios *et al.*, 2013; Urian *et al.*, 2015; Bradford *et al.*, 2017). Visual observations contribute valuable information about cetacean distribution, abundance, and population structure, but poor weather conditions, lack of daylight, and high sea state can limit their effectiveness (Barlow *et al.*, 2001; Barlow, 2015). Some species are also missed by visual observers due to long dive periods or cryptic surface behavior, which then biases the statistical results (Buckland, 2004).

Fortunately, various research tools have emerged to improve empirical data collection for cetaceans, such as unmanned aerial vehicles (UAVs; Aniceto *et al.*, 2018; Torres *et al.*, 2018), satellite and multisensory tags (Woodworth *et al.*, 2012; Citta *et al.*, 2017), and passive acoustic monitoring (PAM; Mellinger *et al.*, 2007; Van Parijs *et al.*, 2009; Bittle and Duncan, 2013). PAM methods are complementary to visual observer methods during shipboard line-transect surveys (Evans and Hammond, 2004; Barlow and Taylor, 2005; Rankin, *et al.*, 2008). and do not depend on weather or daylight, nor do they require direct interactions with the animals. Current PAM technology can record all frequencies of known cetacean vocalizations, offering an alternative method for assessing cetacean biodiversity, distribution and occurrence patterns, and behavior.

Acoustic-based detection and classification methods continue to improve for many cetacean species (Charif and Clark, 2009; Delarue *et al.*, 2009; Roch *et al.*, 2011; Baumann-Pickering *et al.*, 2013; Rankin *et al.*, 2017). Many dolphin species can be identified based on characteristics of their whistle and click vocalizations, and in some cases, population-level differences are evident (Rendell *et al.*, 1999; Oswald *et al.*, 2007; Soldevilla *et al.*, 2008; Gannier *et al.*, 2010; Azzolin *et al.*, 2014; Baumann-Pickering *et al.*, 2015). For example, dolphin whistles vary geographically in many species, including striped dolphins (*Stenella coeruleoalba*), short-beaked common dolphins (*Delphinus delphis*), Guiana dolphins (*Sotalia guianensis*), common bottlenose dolphins (*Tursiops truncatus*), and Indo-Pacific bottlenose dolphins (*Tursiops aduncas*) with variation found in duration, number of contour inflections points, and the beginning or maximum frequency of whistles (Morisaka *et al.*, 2005; Rossi-Santos and Podos, 2006; May-Collado and Wartzok, 2008; Azzolin *et al.*, 2013; Papale *et al.*, 2013). Killer whales (*Orcinus orca*) in the temperate coastal waters of the eastern North Pacific have sympatric ecotypes with corresponding differences in vocal repertoires between social groups (Ford, 1991; Yurk *et al.*, 2002; Saulitis *et al.*, 2005; Deecke *et al.*, 2010; Riesch and Deecke, 2011). Methods to acoustically distinguish reproductively and socially isolated sympatric dolphin populations, such as killer whales, are useful for assessing the population status of these highly mobile marine predators. Differentiation in dolphin whistle characteristics between and within dolphin populations suggest fine-scale adaptations may be driven by different context-specific factors, such as environmental conditions, behavioral states, group composition, or ambient noise levels (Norris et al., 1994; Nowacek, 2005; Oswald et al., 2008; Henderson et al., 2012).

False killer whales, *Pseudorca crassidens*, (Owen, 1846) are a large, highly social dolphin found throughout tropical and semi-tropical waters. In the Hawaiian Archipelago, three genetically differentiated populations of false killer whales are recognized and managed, including a pelagic population dispersed throughout offshore waters, an insular population associated with the Northwestern Hawaiian Islands (NWHI), and an endangered insular population associated with the main Hawaiian Islands (MHI) (Baird *et al.*, 2008; Chivers *et al.*, 2010; Baird, Oleson, *et al.*, 2013; Martien *et al.*, 2014). Abundance estimates for the pelagic, NWHI, and MHI populations indicate population sizes of 1,540, 617, and 167 individuals, respectively (Bradford et al., 2015, 2018). Several years of photo-identification data coupled

with genetic analyses and telemetry data from satellite-tagged individuals suggest the populations are demographically independent and do not readily interbreed despite overlapping habitat use (Baird *et al.*, 2010; Martien *et al.*, 2014; Baird, 2016), including areas where the pelagic population overlaps with both island-associated populations and an offshore area near Kauai where all three populations overlap (Bradford *et al.*, 2015). Additionally, individuals from the MHI population associate at a finer scale in five social clusters that also overlap in their habitat ranges with some genetic differentiation (Baird et al., 2012; Martien et al., 2014; pers. comm. R. Baird, October 12, 2018). The mechanisms maintaining the separation between and within these disparate, yet overlapping, populations are unknown.

The three Hawaiian false killer whale populations face threats from multiple human activities, including fisheries interactions (Shallenberger, 1981; Nitta and Henderson, 1993; Baird and Gorgone, 2005; Forney *et al.*, 2011). False killer whales primarily feed on fish and squid, and many of the same fish species are also targeted by Hawaii-based fisheries (Baird, 2009, 2016). Interactions between the longline and other hook-and-line fisheries and Hawaii's false killer whales have been documented for decades and led to death or serious injuries of individuals incidentally hooked or entangled (Baird and Gorgone, 2005; Gilman *et al.*, 2006; Baird *et al.*, 2014; Bradford and Forney, 2014; Bradford and Lyman, 2019). The currently estimated ranges of all three of the Hawaiian populations overlap the commercial longline fisheries and recreational fisheries (Bradford *et al.*, 2015; Bayless *et al.*, 2017). As long as the Hawaii-based fisheries continue to target the same fish species as false killer whales and the full ranges of the false killer whale populations are uncertain, these marine predators remain at risk.

Because of human-caused threats to this species, and given the endangered status of the MHI population (Oleson *et al.*, 2010), it is critical to track false killer whale abundance in Hawaiian waters at the population level. False killer whales are primarily monitored by collecting abundance and distribution data during shipboard visual and acoustic line-transect surveys but require genetic samples and photo-identification data to confirm the population identity of sighted individuals, data which are often unavailable due to the challenges inherent to sampling cetaceans. Hawaiian false killer whales are particularly challenging to study due to their low densities, dispersed subgrouping behavior, and tendency to approach research vessels from behind (Bradford *et al.*, 2014). Fortunately, they are vocally active, commonly detected using PAM methods during line-transect surveys (Barlow and Rankin, 2007; Bradford *et al.*,

2014) and their whistles can be classified correctly to species with a high level of certainty compared to other dolphin species (Oswald *et al.*, 2007; Barkley *et al.*, 2011). No studies have examined and compared the characteristics of each Hawaiian false killer whale population's whistle repertoire. If population-level differences exist between the whistles of the different populations, PAM could provide a method for determining their abundance, ranges, and occurrence patterns.

In this study, we examine the variation in whistle characteristics between and within the three Hawaiian Islands false killer whale populations and build classification models utilizing random forest (RF) classification methods (Breiman, 2001; Liaw and Wiener, 2002). Advancing PAM methods to identify populations of marine predators enhances our ability to address more complex research questions to further understand the distributions and ecological roles of cetacean populations for more robust management and conservation (Fleming *et al.*, 2018; von Benda-Beckmann *et al.*, 2018).

2.2 Methods

2.2.1 Data Collection

Acoustic recordings and visual sighting data were collected during several line-transect cetacean abundance surveys conducted by the Pacific Islands Fisheries Science Center (PIFSC) of the National Oceanic and Atmospheric Administration (NOAA) aboard the NOAA Ship *Oscar Elton Sette* in 2012, 2013, and 2016. This study also included data from surveys organized by PIFSC and the NOAA Southwest Fisheries Science Center (SWFSC) in 2010 and 2017. All efforts used consistent protocols to search for cetaceans and collect sighting data, methods developed by SWFSC in the 1980s (Kinzey *et al.*, 2000; Bradford *et al.*, 2017). In brief, three marine mammal observers searched for cetaceans 180º forward of the ship from the flying bridge. The port and starboard observers used 25 × 150 binoculars and the third observer in the center searched with unaided eyes or 7× binoculars and acted as the data recorder. When cetaceans were sighted within 5.6 km (3 nmi) of the transect line, the ship diverted from the transect line to estimate group size and identify the species present. A small boat was launched on some cetacean groups to collect photo-identification images, biopsy samples, and deploy satellite telemetry tags when possible.

Continuous acoustic recordings were collected during daylight hours using custom-built hydrophone arrays towed at approximately 4–10 m deep, 300 m behind the ship while traveling at 18.5 km/h (10 kt). Trained acousticians monitored the hydrophones aurally with headphones and visually using spectrographic software (ISHMAEL, Mellinger, 2002; PAMGuard, Gillespie et al., 2008). When cetacean vocalizations were detected, a phone-pair bearing algorithm in ISHMAEL or PAMGuard was used to calculate the direction of the sound source relative to the bow of the ship. These bearings were plotted using a mapping software with a GPS interface, either Whaltrak or PAMGuard, and target motion analysis was used to localize the animals based on the convergence of plotted bearings with left/right ambiguity. The ambiguity in the acoustic location estimate was often resolved either by turning the ship or matching the bearings to an associated sighting by the visual observers (Rankin, *et al.*, 2008). Each survey used a different array of hydrophones made up of 4–7 hydrophone elements from various manufacturers, but all had a flat frequency response from 2kHz to at least 40 kHz and acoustic data were digitized with sampling rates of 192 kHz or 500 kHz, providing sufficient bandwidth for capturing dolphin whistles in their entirety (Table 2.1).

Table 2.1. Specifications of towed hydrophone array data collected during each survey.

	HICEAS 2010 (PIFSC/SWFSC)	PICEAS 2012 (PIFSC)	PACES 2013 (PIFSC)	HITEC 2016 (PIFSC)	HICEAS 2017 (PIFSC/SWFSC)
NOAA ship & Sail Dates	*Oscar Elton Sette*: September 2 – October 29, 2010 *McArthur II*: August 13 – December 1, 2010	*Oscar Elton Sette*: April 23 – May 17, 2012	*Oscar Elton Sette*: May 7 – June 5, 2013	*Oscar Elton Sette*: June 28 – July 27, 2016	*Oscar Elton Sette*: July 6 – October 10, 2017 *Reuben Lasker*: August 17 – December 1, 2017
Total Acoustic Effort (hours)	371 1074	263	293	350	857 886
Population recorded	Pelagic, NWHI	Pelagic	Pelagic	MHI	MHI
Hydrophone	EDO EC65	EDO EC65	APC 42-1021	HTI-96-MIN	HTI-96-MIN
Hydrophone flat response range	2–40 kHz	2–40 kHz	2–40 kHz	2–85 kHz	2–85 kHz
A/D converter	MOTU mK3	MOTU mK3	MOTU mK3	SA Instrumentation SAIL DAQ	SA Instrumentation SAIL DAQ
Sampling rate	192 kHz	192 kHz	192 kHz	500 kHz	500 kHz
Recorder bit-depth /resolution	16-bit	16-bit	16-bit	16-bit	16-bit
Pre-amplifier flat response range	> 2 kHz	> 2 kHz	> 2 kHz	> 2 kHz	2–50 kHz
High pass filter	1.5 kHz	1.5 kHz	1.5 kHz	1.5 kHz	1.5 kHz

A two-phase protocol specific to false killer whale sightings and acoustic detections was developed to reduce bias in abundance estimates introduced by their subgrouping behavior (Bradford *et al.*, 2014; Yano *et al.*, 2018). All acoustic recordings included in this analysis were collected during the first phase, when the ship traveled in a straight line through the entire false killer whale group. Visual observers estimated the number of individuals in the group (when possible), their initial behavior, and identified the group to the level of species and population (pelagic, NWHI, MHI) using photo-identification analysis, genetic analysis, and/or satellite telemetry data.

2.2.2 Whistle Selection and Measurement

Acoustic recordings of false killer whales were organized into acoustic encounters, defined as the total length of recording time during the first phase of the associated false killer whale sighting. Recordings were decimated to 192 kHz to maintain consistency in measurements for all surveys. An equal subset of whistles from each acoustic encounter was randomly selected to avoid oversampling individuals and obtain a representative sample of whistle characteristics across the populations. The number of whistles selected for each subset was determined by considering prior whistle classification studies in which total selected whistles ranged between 35 and 811 whistles per acoustic encounter (Bazúa-Durán and Au, 2004; Oswald *et al.*, 2007; May-Collado and Wartzok, 2008) and the constraints of this data set. Initially, we selected 100 whistles per encounter based on the acoustic encounter with the shortest duration (3540 s), which equaled approximately one whistle every 35 s. Selected whistles had signal-to-noise ratios ranging from 0.5 to 8.8 dB and all had clearly visible continuous contours and distinct start and end frequencies for accurate measurement of whistle variables. The recordings were partitioned into 100 equal time increments (in seconds) and the first clear whistle was selected from a spectrogram of each time increment using Raven Pro (4096 FFT, Hann window, 50% overlap, version 1.5; Bioacoustics Research Program, 2017). If a time increment did not include whistles, a whistle was chosen from a different, randomly selected, time increment. Fifty additional whistles were included from randomly selected time increments to increase the sample size for each acoustic encounter.

After whistles were selected and annotated using Raven Pro, whistle contours were manually traced from spectrograms (4096 FFT, Hann window, 50% overlap) using the Real-time Odontocete Call Classification Algorithm (ROCCA) module (Oswald and Oswald, 2013) within PAMGuard (version 1.15.1; Gillespie *et al.*, 2008). ROCCA contains several semi-automated whistle classifiers, including one for eight delphinid species recorded in the eastern tropical Pacific Ocean with particularly high accuracy for false killer whales (Barkley *et al.*, 2011). ROCCA automatically measures 50 time and frequency measurements from traced whistle contours, which can be used in other analyses (Table 2.2; Oswald, 2013).

Table 2.2. Fifty time and frequency whistle variables measured by the Real-Time Odontocete Call Classification Algorithm (ROCCA) were considered in the random forest models.

Variable Name	Description	Units	Type
MaxFreq	maximum frequency of whistle	Hertz	continuous
MinFreq	minimum frequency	Hertz	continuous
Duration	duration of whistle in time	seconds	continuous
BegFreq	frequency at the beginning of the whistle	Hertz	continuous
EndFreq	frequency at the end of the whistle	Hertz	continuous
FreqRange	frequency range for the entire whistle	Hertz	continuous
MeanDC	mean duty cycle (proportion of time signal 'on' vs 'off')	seconds	continuous
StdDevDC	standard deviation of the duty cycle	seconds	continuous
MeanFreq	mean frequency of whistle	Hertz	continuous
StdDevFreq	standard deviation of the frequency	Hertz	continuous
MedFreq	median of the frequency	Hertz	continuous
CenterFreq	frequency at the center of the whistle	Hertz	continuous
FreqRelBW	frequency of the relative bandwidth	Hertz	continuous
MaxMinRatio	ratio of the max and min frequencies	NA	continuous
BegEndRatioFreq	ratio of the beginning and end frequencies	NA	continuous
QuarterFreq1	frequency of the first quarter of the whistle	Hertz	continuous
QuarterFreq2	frequency of the second quarter of the whistle	Hertz	continuous
QuarterFreq3	frequency of the third quarter of the whistle	Hertz	continuous
FreqSpread	frequency spread	Hertz	continuous

Table 2.2. (Continued) Fifty time and frequency whistle variables measured by the Real-Time Odontocete Call Classification Algorithm (ROCCA) were considered in the random forest models.

CoeffFreqMod	coefficient of frequency modulation: take 20 frequency measurements equally spaced in time, then subtract each frequency value from the one before it. COFM is the sum of the absolute values of these differences, all divided by 10000 (McCowan and Reiss, 1995)	NA	continuous
StepsUpFreq	number of steps that have increasing frequency	NA	count
StepsDwnFreq	number of steps that have decreasing frequency	NA	count
StepsTotal	total number of steps	NA	count
MeanSlope	frequency of overall mean slope calculated every three contour points	Hertz	continuous
MeanAbsSlope	frequency of absolute mean slope calculated every three contour points	Hertz	continuous
MeanPosSlope	frequency of mean positive slope calculated every three contour points	Hertz	continuous
MeanNegSlope	frequency of mean negative slope calculated every three contour points	Hertz	continuous
PosNegSlopeRatio	ratio of positive and negative mean slope	Hertz	continuous
BegSwpFreq	frequency of the beginning of the sweep	Hertz	continuous
BegUpFreq	frequency as slope begins to go up	1 = beginning slope is positive, 0 = beginning slope is negative	Binary
MeanNegSlope	frequency of mean negative slope calculated every three contour points	Hertz	continuous
PosNegSlopeRatio	ratio of positive and negative mean slope	Hertz	continuous

Table 2.2. (Continued) Fifty time and frequency whistle variables measured by the Real-Time Odontocete Call Classification Algorithm (ROCCA) were considered in the random forest models.

BegSwpFreq	frequency of the beginning of the sweep	Hertz	continuous
BegUpFreq	frequency as slope begins to go up	1 = beginning slope is positive, 0 = beginning slope is negative	Binary
BegDwnFreq	frequency as slope begins to go down	1 = beginning slope is positive, 0 = beginning slope is negative	binary
EndSwpFreq	frequency of the end of the sweep	1 = ending slope is positive, –1 = ending slope is negative, 0 = ending slope is 0	categorical
UpEndFreq	frequency of the up end	1 = beginning slope is positive, 0 = beginning slope is negative	binary
DownEndFreq	frequency of the down end	1 = beginning slope is positive, 0 = beginning slope is negative	binary
NumInflPosToNeg	number of inflection points that go from positive slope to negative slope	NA	count
NumInflNegToPos	number of inflection points that go from negative slope to positive slope	NA	count

2.2.3 Model Configuration

The ROCCA whistle measurements were used as the predictor variables in RF classification models (Breiman, 2001; Liaw and Wiener, 2002) to test whether the three false killer whale populations could be distinguished based on their whistles. The RF algorithm is a non-parametric statistical method capable of modeling complex interactions among ordinal and nominal predictor variables (Cutler *et al.*, 2007). The RF models are an ensemble of decision trees designed to recursively partition data based on the values of the predictor variables (e.g., whistle measurements). Decision trees are grown from a bootstrap sample of the model data with approximately 1/3 of the data omitted as the Out-of-Bag (OOB) sample for cross-validating the classification accuracy of the model (Efron and Tibshirani, 1997). At each node, predictor variables are selected from a random subset of the predictor variables to split the data into the most homogeneous daughter nodes until the trees are grown to their maximum depth. Data are classified to a target variable (e.g., population) based on the majority vote of the predictions of all trees. The output of RF models includes variable importance measures, a ranking of the predictor variables based on their importance in predicting the outcome. We calculated variable importance as the mean decrease in accuracy by permuting each variable and comparing the OOB error rates of the model before and after permutation. Here, RF classification models were developed in the R programming environment (version 3.5.2; R Core Team, 2018) using the *randomForest* package (version 4.6-14; Liaw and Wiener, 2002).

We developed two RF model configurations to classify the whistle measurement data: one configuration incorporated all false killer whale populations (RF_PNM) and the second configuration was composed of pairwise models incorporating only two populations. The pairwise configurations only applied to regions of the archipelago assumed to be inhabited by two of the three populations, resulting in two pairwise RF models: one for the pelagic and insular northwest Hawaiian populations (RF_PN) and the other for the pelagic and insular main Hawaiian populations (RF_PM). We assumed that no region existed in the archipelago inhabited by only the insular MHI and insular NWHI populations.

Figure 2.1 provides a schematic diagram detailing the sampling and processing procedures of the whistle measurement data to configure each RF model. For each RF model, an equal number of acoustic encounters (including all 150 whistles) were randomly selected from

each population. Next, we performed a correlation analysis on the data to measure the linear dependence between pairs of whistle variables, removing variables if the Pearson's correlation coefficient exceeded ±0.8. Typically, model overfitting due to correlation does not occur with RFs (Cutler *et al.*, 2012). However, studies have shown that correlated variables strongly bias the ranking of important variables, making it difficult to interpret the results (Strobl *et al.*, 2008; Gregorutti *et al.*, 2017). The subset of whistle data with uncorrelated variables was then partitioned by acoustic encounter into independent training and test data sets for each population, with 75% of the acoustic encounters included in the training data and 25% included in the test data. The RF model configurations include two parameters that can be adjusted to achieve the highest accuracy rate from the model training data: the number of variables randomly selected at each node (*mtry*) and the number of trees in the forest (*ntree*). The number of variables was set to the default (the square root of the total number of whistle measurements) and the number of trees was optimized. Optimized RF models sampled 100 different combinations of acoustic encounters (with replacement) to train and test the model configurations and obtain average classification rates.

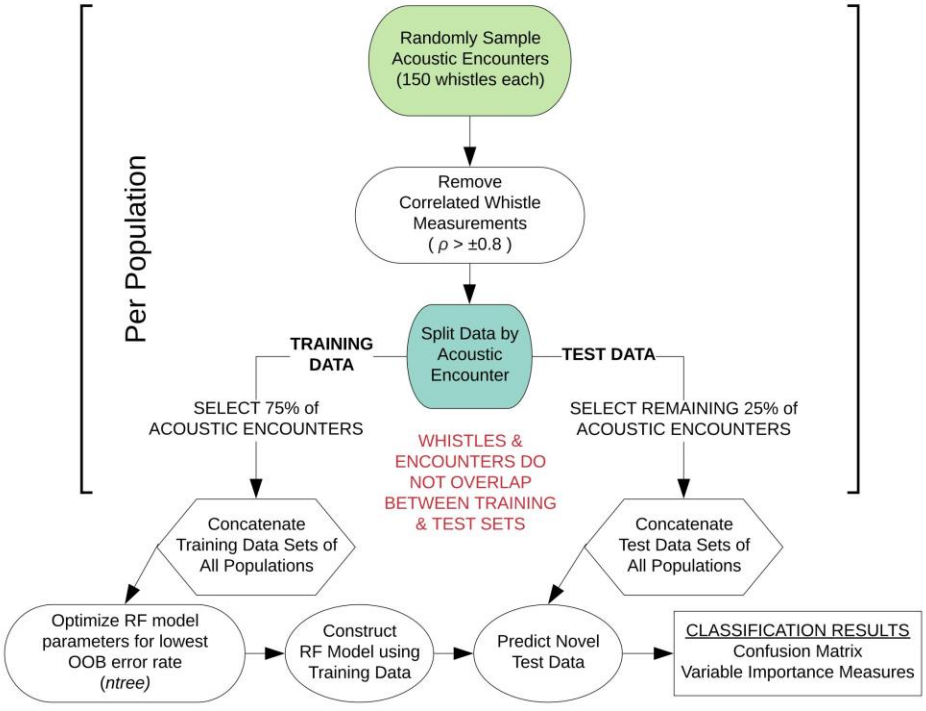

Figure 2.1. Schematic diagram outlining the modelling approach for sub-sampling the whistle measurement data for each random forest model configuration. This workflow was performed 100 times for each model configuration.

The RF models used the whistle measurement data to classify individual whistles to a population to obtain overall classification rates. Then, since the MHI population associates in social clusters and any form of stable social groups are unconfirmed for the pelagic and NWHI populations, we also examined the variability of whistle measurements within populations in two ways. First, whistles were classified to a given acoustic encounter instead of a population by creating separate RFs per population using the same steps described for classifying individual whistles to a population. Second, acoustic encounters were classified to a population based on the majority of individual whistle classifications within encounters.

2.2.4 Model Evaluation

Classification results for all RF models were summarized in confusion matrices, which included the proportion of correctly and incorrectly classified whistles by population. Cohen's Kappa statistic, κ, was calculated to evaluate model performance by comparing the classification results of the test data (observed accuracy) to random chance (expected accuracy) (Cohen, 1960). The strength of agreement for κ coefficients is outlined by Landis and Koch (1977) as the following: 0.01–0.20 slight, 0.21–0.40 fair, 0.41–0.60 moderate, 0.61–0.80 substantial, and 0.81–100 nearly perfect. This is a statistic originally used to measure interrater reliability, but is also commonly used for evaluating results of machine learning classification methods as a more informative metric as it accounts for random chance versus only reporting the observed accuracy (Titus *et al.*, 1984; Garzón *et al.*, 2006; Cutler *et al.*, 2007; García *et al.*, 2009).

Variable importance was measured using the mean decrease in accuracy (MDA) calculated by permuting each variable in the RF model and comparing OOB accuracies for models with and without permutation. We summarized variable importance using the minimum, maximum, and median MDAs for the 10 most important variables from all iterations of each model configuration to better understand which variables contributed the most to the classification results. Pairwise Kolmogorov-Smirnov tests compared cumulative frequency distributions of the most important whistle variables to examine which whistle characteristics significantly differed between populations.

2.3 Results

A total of 40.7 hours of recordings were analyzed from 16 acoustic encounters of false killer whales identified to a population using visual observer data, including 8 encounters for the pelagic population and 4 encounters for each of the NWHI and MHI populations (Figure 2.2). Initial behaviors of individuals within encounters varied primarily between foraging, traveling, porpoising, and bow-riding, with no obvious dominant behavior. Photo-identification analyses found a total of 17 individuals resighted between the acoustic encounters, resulting in 1 pelagic animal resighted between P1 and P7, 10 NWHI animals resighted primarily between N1 and N4, and 6 MHI animals from M1 resighted in M2 and/or M4.

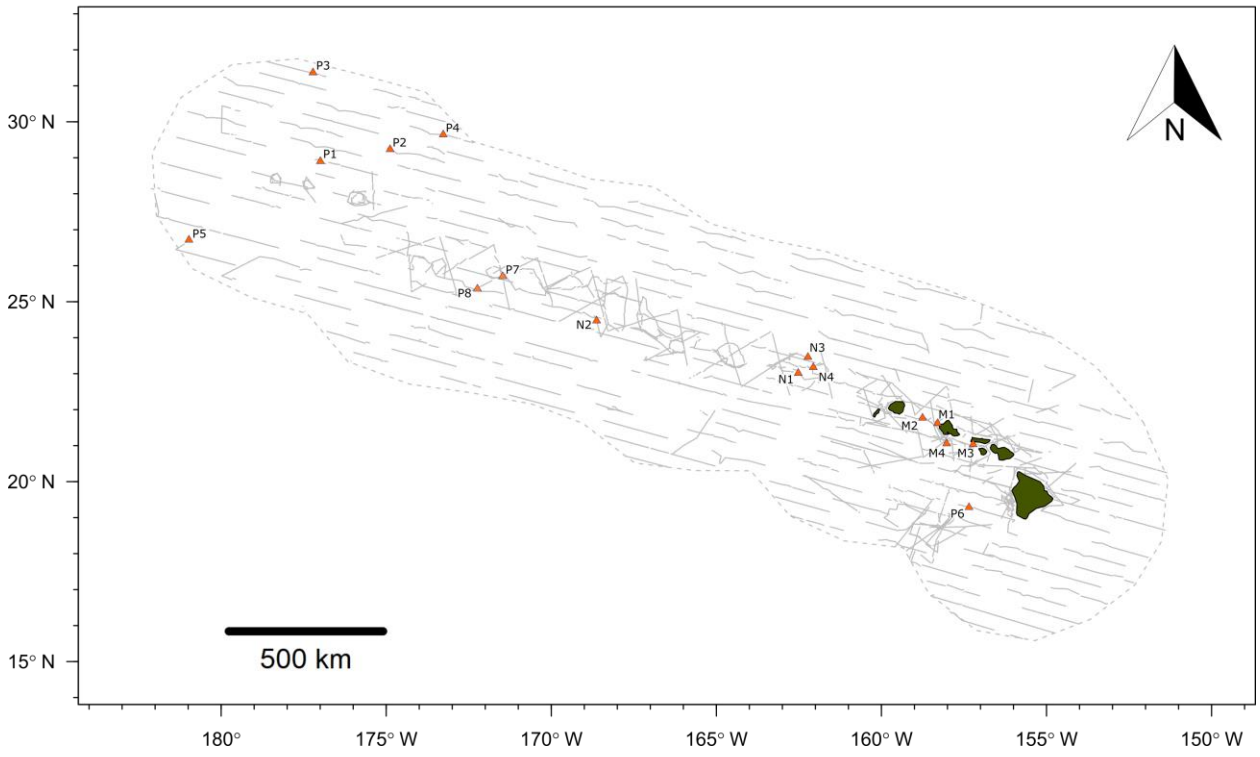

Figure 2.2. Map of false killer whale acoustic encounters identified to population based on photo-identification data, genetic samples, or satellite telemetry data. Gray dashed line indicates boundary of study area (Hawaiian Exclusive Economic Zone) and gray solid lines indicate transect lines from all line-transect surveys. ‘P’ denotes the pelagic population, ‘N’ denotes the Northwestern Hawaiian Island population, ‘M’ denotes the main Hawaiian Island population.

A total of 2400 whistles were manually extracted using ROCCA, including 1200 whistles for the pelagic population, 600 whistles for the NWHI population, and 600 whistles for the MHI population. Table 2.3 summarizes the metadata for each acoustic encounter. Four acoustic encounters were sampled from each population for each model iteration as that was the number of acoustic encounters available for the NWHI and MHI populations. Three acoustic encounters from each population (150 whistles each) were allocated to a training data set with one acoustic encounter allocated to the test data set. For the 100 models of RF_PNM, the total training data set included 135,000 whistles (150 whistles × 3 acoustic encounters × 3 populations × 100 model runs) and the total test data set included 45,000 whistles (150 whistles × 1 acoustic encounter × 3 populations × 100 model runs). The training data for each pairwise model totaled 90,000 whistles (150 whistles × 3 acoustic encounters × 2 populations × 100 model runs) with the test data totaling 30,000 whistles (150 whistles × 1 acoustic encounter × 2 populations × 100 model runs).

Table 2.3. Summary table listing information for each acoustic encounter, including population, acoustic encounter ID ('P' denotes the pelagic population, 'N' denotes the Northwestern Hawaiian Island population, 'M' denotes the main Hawaiian Island population), social cluster (when applicable; pers. comm. R. Baird), date, time (GMT), survey, group size (the geometric mean of observer best estimates), the acoustic and visual sighting survey IDs, and total duration of the recordings analyzed (s). The total number of whistles measured using ROCCA was equal for all acoustic encounters (n = 150).

Population	ID	Social Cluster	Date	GMT	Survey	Group Size	Acoustic ID	Sighting ID	Total Duration (s)	Initial Behavior
Pelagic	P1	NA	9/2/2010	2:39	HICEAS 2010	36	71	35	11795	travel
Pelagic	P2	NA	9/5/2010	17:23	HICEAS 2010	10.3	83	47	7278	porpoise, breach
Pelagic	P3	NA	9/7/2010	19:47	HICEAS 2010	32	98	61	9683	porpoise
Pelagic	P4	NA	9/10/2010	21:25	HICEAS 2010	18.3	116	74	15068	porpoise
Pelagic	P5	NA	11/10/2010	21:38	HICEAS 2010	51	325	241	7635	travel, forage
Pelagic	P6	NA	5/16/2012	22:59	PICEAS 2012	18	186	76	9925	travel
Pelagic	P7	NA	5/15/2013	0:55	PACES 2013	42	39	20	15484	travel
Pelagic	P8	NA	5/27/2013	1:35	PACES 2013	27	88	59	13184	mill, forage
NWHI	N1	NA	9/26/2010	1:12	HICEAS2010	52	33	86	9420	forage, breach
NWHI	N2	NA	10/8/2010	3:16	HICEAS 2010	13.8	224	140	13601	porpoise
NWHI	N3	NA	10/20/2010	2:29	HICEAS 2010	8.8	291	200	4448	travel
NWHI	N4	NA	10/22/2010	21:25	HICEAS 2010	20.4	299	206	5312	travel
MHI	M1	1, 3, 5	7/5/2016	1:45	HITEC 2016	48	10	18	7200	travel, breach
MHI	M2	2, 3, 5	10/8/2017	20:12	HICEAS 2017	NA	338	178	5200	rest
MHI	M3	4	10/9/2017	23:15	HICEAS 2017	15	214	86	7680	travel, forage
MHI	M4	3, 5	11/17/2017	18:31	HICEAS 2017	43	331	136	3540	travel, forage

The final combination of optimized parameter values for each model included the square root of total uncorrelated variables (~ 5) for *mtry* and 501–5001 decision trees for *ntree* for all configurations. The resulting accuracy rates for each optimized model are presented in Table 2.4. The highest accuracy rates across 100 models of RF_PNM ranged between 0.51 to 0.63, with a mean of 0.56. Both pairwise models resulted in higher accuracy rates. RF_PN ranged between 0.68 and 0.69, with a mean of 0.68 and RF_PM showed the highest accuracy rates of 0.68–0.75, with a mean of 0.72.

Table 2.4. Mean accuracy rates (with variances) of the training data for each model configuration. Accuracy rates are presented for individual populations across all models.

	Mean Accuracy Rates		
	RF_PNM	**RF_PN**	**RF_PM**
Pelagic	0.53 (0.002)	0.68 (0.001)	0.68 (0.001)
NWHI	0.51 (0.002)	0.69 (0.001)	---
MHI	0.63 (0.001)	---	0.75 (0.001)
Overall	0.56 (0.001)	0.68 (0.001)	0.72 (0.001)

Classification results of test data for all model configurations were organized into separate confusion matrices. RF_PNM resulted in a mean observed accuracy of 0.42 and κ = 0.15 when compared to the expected accuracy of 0.33. According to the suggested kappa coefficient scale, the classification results of the test data for RF_PNM are in 'slight' agreement with the true population of the test data. The confusion matrix (Table 2.5) also provides information about how the populations were misclassified - the pelagic whistles where mostly misclassified to the NWHI population, and the NWHI whistles were misclassified evenly between the pelagic and MHI population. The MHI whistles had the highest correct classification rate with misclassifications spread evenly between the pelagic and NWHI populations.

Table 2.6 shows separate confusion matrices for both pairwise models. RF_PN resulted in a mean observed accuracy of 0.56 and κ = 0.12 calculated using an expected accuracy of 0.5. The mean observed accuracy for RF_PM equaled 0.62 and κ = 0.24. The low kappa coefficient for RF_PN indicates low agreement between classification results of the test data with the true

population while the higher kappa coefficient for RF_PM suggests fair agreement. Correct classification rates of the pelagic population were similar between pairwise models but improved compared to RF_PNM results (by ~15%), which we expected since fewer populations were included in the pairwise models. The MHI population consistently showed the highest correct classification results for all model configurations while classification results for pelagic and NWHI whistles performed similarly throughout all models relative to the MHI population.

Table 2.5. Confusion matrix displaying classification results for test data (with variances) using the RF_PNM model. The proportion of whistles correctly classified are in bold. A total of 150 whistles were tested from three populations for 100 models (n = 45,000).

			PREDICTED POPULATION		
			Pelagic	NWHI	MHI
RF_PNM	**TRUE POPULATION**	Pelagic	**0.42** (0.008)	0.26 (0.009)	0.32 (0.01)
		NWHI	0.31 (0.007)	**0.36** (0.007)	0.33 (0.008)
		MHI	0.25 (0.004)	0.23 (0.011)	**0.52** (0.017)

Table 2.6. Confusion matrices displaying classification results for populations using the pairwise models, RF_PN and RF_PM. The proportion of whistles correctly classified are in bold. A total of 150 whistles were tested from two populations for the 100 models (n = 30,000).

			PREDICTED POPULATION	
RF_PN	**TRUE POPULATION**		Pelagic	NWHI
		Pelagic	**0.57** (0.009)	0.43
		NWHI	0.44	**0.56** (0.005)
RF_PM			Pelagic	MHI
		Pelagic	**0.58** (0.014)	0.42
		MHI	0.34	**0.66** (0.009)

This study also aimed to better understand the variability in whistle measurements within populations by classifying whistles to acoustic encounters instead of populations (Table 2.7). Since our data set included an unequal number of acoustic encounters per population (Table 2.3), we built separate RFs for each population. We selected the training and test whistle data using the same 75%/25% split and included equal proportions of whistles from each acoustic encounter. Pelagic whistles were classified to pelagic encounters with a mean observed accuracy of 0.31 ($\kappa = 0.21$) while whistles from the NWHI and MHI populations received higher mean accuracies of 0.49 ($\kappa = 0.32$) and 0.45 ($\kappa = 0.26$), respectively. These results suggest that the whistles from the MHI and NWHI acoustic encounters maintain certain time-frequency characteristics that allow them to be classified to the correct acoustic encounter more often than pelagic whistles.

Table 2.7. Mean observed accuracies and Kappa coefficients for acoustic encounter classification models. The total number of whistles included in the test data from all model iterations for each population are listed under *n*.

	Acoustic Encounter Classification			
Population	Mean Observed Accuracy	Kappa	Total Acoustic Encounters	*n*
Pelagic	0.31	0.21	8	29600
NWHI	0.46	0.32	4	14800
MHI	0.45	0.26	4	14800

Acoustic encounters were also classified to a population based on the majority classification of individual whistles for each model iteration to examine the variability of classification results among acoustic encounters within populations. Table 2.8 provides the percentages of correctly classified acoustic encounters for all models. Acoustic encounters of the MHI population were classified correctly more frequently than the pelagic and NWHI encounters. On average, 87% of MHI encounters were correctly classified across models, with the highest average score resulting from the RF_PM model (93%). The averages for the pelagic and NWHI acoustic encounters were lower (72% and 63%, respectively). Specific acoustic encounters, M1, N1, N2, and P7, showed the lowest scores in the RF-PNM model. Upon

inspection of how these encounters were misclassified, we found that M1 classified as NWHI 67% of the time (7% as MHI), 100% of the N1 encounters classified as MHI, while 70% of the N2 encounters classified as pelagic. P7 encounters were always classified as MHI. Classifications improved for most acoustic encounters using the pairwise models.

Table 2.8. Percentage of models in which acoustic encounters were correctly classified based on a majority of whistle classifications. The total number of times the model included a given acoustic encounter is listed under *n*. 'P' denotes the pelagic population, 'N' denotes the Northwestern Hawaiian Island population, 'M' denotes the main Hawaiian Island population.

Model	**RF_PNM**		**RF_PN**		**RF_PM**	
Acoustic Encounter ID	*n*	Percent Correctly Classified	*n*	Percent Correctly Classified	*n*	Percent Correctly Classified
P1	11	90.9	9	66.7	9	100
P2	12	75	4	75	4	100
P3	17	64.7	16	81.3	16	43.8
P4	12	66.7	14	42.9	14	100
P5	6	50	17	76.5	17	100
P6	12	83.3	13	69.2	13	100
P7	11	0	14	92.9	14	0
P8	19	73.7	13	100	13	76.9
N1	17	0	23	82.6	--	--
N2	27	29.6	28	64.3	--	--
N3	28	71.4	26	100	--	--
N4	28	71.4	23	87	--	--
M1	27	25.9	--	--	23	73.9
M2	20	100	--	--	28	100
M3	23	100	--	--	26	100
M4	30	100	--	--	23	100

The important variables from RF classification models of populations were ranked by MDA. Whistle variables with a negligible decline in accuracy when permuted received a lower

MDA while permuted variables causing a larger decline in accuracy were deemed more informative and received a higher measure of MDA. Whistle variables that ranked within the top 10 important variables (from approximately 26 uncorrelated variables depending on the model) were consolidated to assess which whistle variables consistently contributed to the most accurate RF models (Figure 2.3). Not all model configurations resulted in the same top 10 important variables with 14 variables occurring in the top 10 for all model configurations. Since RF models included different numbers of trees and different whistles, variable importance is not directly comparable. However, two variables (mean negative slope and third quarter frequency) consistently produced the highest median values of MDA for all model configurations. Other slope variables (mean slope, percentage of negative slope, and percentage of zero slope) also ranked within the top 10 important variables for 75–100% of all models for each configuration.

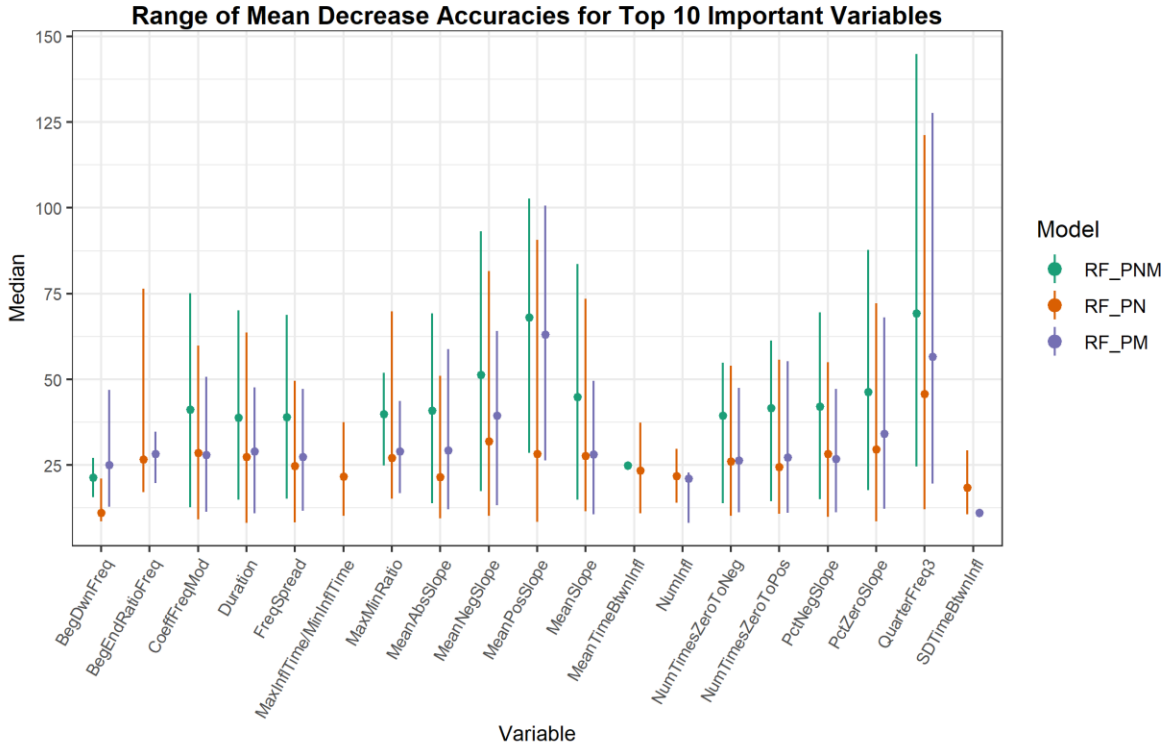

Figure 2.3. Range of mean decrease accuracies for whistle variables ranked as the 10 most important across all model iterations. Higher values of mean decrease in accuracy indicate whistle variables that are more important to classification. Whistle variables selected in the top 10 for only one model iteration are represented as a single dot.

Pairwise Kolmogorov-Smirnov tests examined whether the 14 whistle variables deemed most important for all model configurations were also significantly different between the populations. Results showed that six out of 14 important whistle variables differed significantly between all populations, including some slope variables, frequency spread, and the third quarter frequency (Figure 2.4).

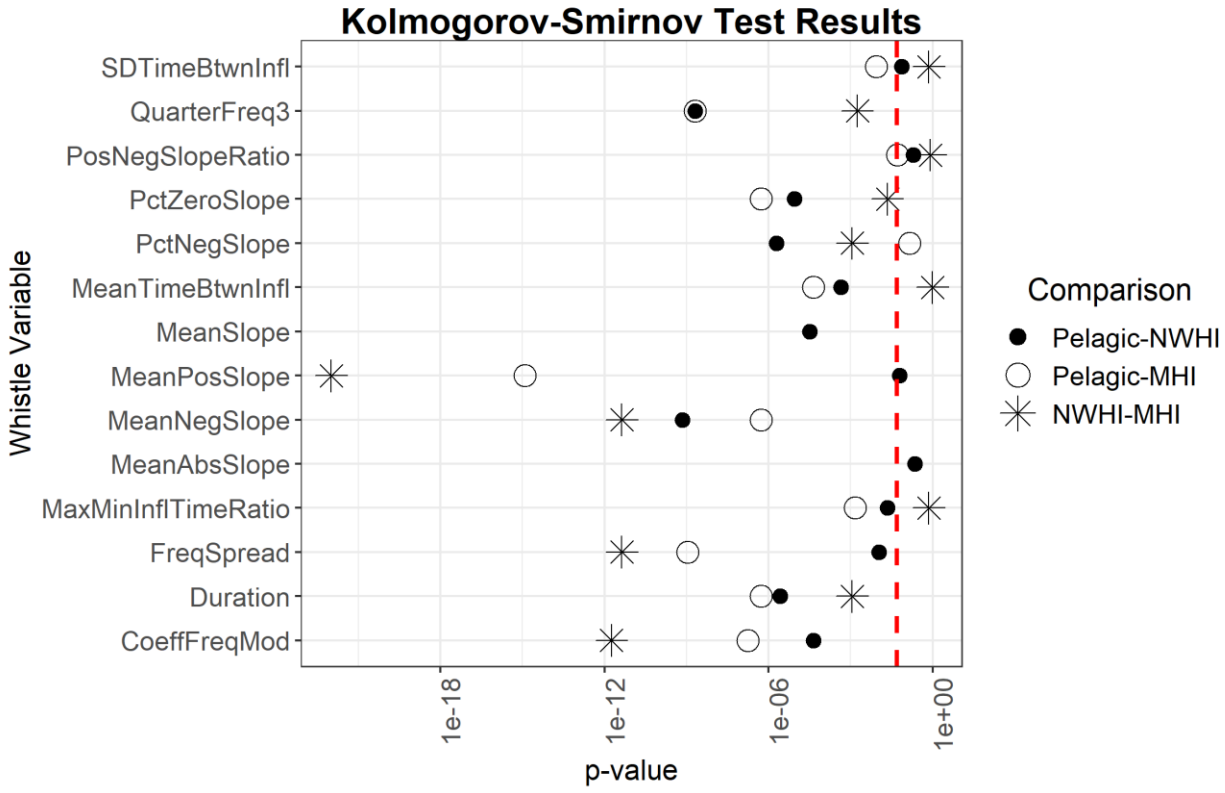

Figure 2.4. Results of Kolmogorov-Smirnov tests comparing uncorrelated important whistle variables between populations. Red dashed line represents $\alpha = 0.05$. Points to the left of the red dashed line indicate whistle variables that are significantly different for a given pairwise comparison of populations.

2.4 Discussion

The marine environment contains few barriers to the genetic dispersal of cetaceans, yet fine-scale genetic differentiation exists for these highly mobile species. For many cetacean species, measurable differences in their vocal repertoires are consistent with the genetic differentiation between geographically isolated populations and the intricate social structure within a population (Rendell *et al.*, 2012; Papale *et al.*, 2014; Van Cise *et al.*, 2018). This study

aimed to develop a whistle classifier to identify whistles from acoustic encounters of Hawaiian false killer whales to the population level. Identifying Hawaiian false killer whale populations using characteristics of their whistle repertoire could complement other population-specific data or provide population identity when other data are unavailable.

We applied the RF machine learning classification method to analyze whistle characteristics of the three false killer whale populations because of its high performance with diverse variables, including prior work differentiating dolphin species based on their whistle characteristics (Pal, 2005; Cutler *et al.*, 2007; Oswald, 2013; Keen *et al.*, 2014; Li *et al.*, 2016; Rankin *et al.*, 2017). Overall, RF classification models poorly differentiated the three populations as is evident from the low correct classification rates and low kappa coefficients for each model. The pelagic and NWHI whistles were correctly classified at similar rates in both RF_PNM and RF_PN models but whistles and acoustic encounters from the MHI population were consistently correctly classified at higher rates for all models.

Previous studies that examined geographic variation in whistle characteristics of allopatric populations found significant differences between several variables and achieved classification scores significantly higher than expected by chance (May-Collado and Wartzok, 2008; Azzolin *et al.*, 2013; Papale *et al.*, 2013). For this study, the populations are sympatric and overlap in part of their range. Our results indicated that most whistle variables are similar between these populations given that only 6 out of 50 whistle variables significantly differed between all populations (Figure 2.3). An additional RF was configured using only these six significantly different variables and resulted in even lower classification scores (0.40 overall accuracy, κ = 0.1) suggesting simplified models do not perform better and that a variety of variables should be included in this type of classification model for this species.

Despite the poor classification performance, our results provide insight into potential patterns of whistle characteristics between populations. While each RF model was built using balanced training and testing data, the total whistle data set included twice as many pelagic whistles and acoustic encounters than the NWHI and MHI populations. The pelagic whistle data presumably captured more variability due to behavioral states, group composition, and environment. This additional variability may be responsible for the lower classification scores of the pelagic whistles. Interestingly, while pairwise RF models improved classification scores for

all populations, classification results of pelagic whistles still performed similarly to the NWHI whistles despite the disproportionate number of whistles and acoustic encounters.

False killer whale whistles tend to be lower in frequency and less frequency-modulated than most delphinid whistles and have among the highest correct classification rates when other delphinid species are included in the classifier (Oswald *et al.*, 2007). However, these whistle characteristics may make it difficult to discern the subtle differences between populations using the time-frequency measurements commonly implemented in whistle classification analyses. Frequency-modulated calls, e.g. whistles, have been categorized into call types to identify geographically isolated populations of some odontocetes based on contour shape and time-frequency characteristics (Saulitis *et al.*, 2005; Van Cise *et al.*, 2017). No attempt was made to categorize whistle types for false killer whales since this study was interested in the overall classification of all whistles. A cursory look at the whistle data set shows there is potential to identify whistle categories, but it is unknown whether this would improve our ability to classify the three populations since whistle categories types may share the same magnitude of similarities as individual whistles.

Dolphin whistles are thought to act as a mechanism for group cohesion (Janik and Slater, 1998). and may differ depending on differences in the physical and social environments (May-Collado and Wartzok, 2008). Sympatric killer whale populations in the eastern North Pacific maintain social cohesion using dialects of stereotyped calls that are highly modulated in frequency and amplitude and vary between and within ecotypes (Ford, 1991; Thomsen *et al.*, 2002; Saulitis *et al.*, 2005; Riesch *et al.*, 2006; Riesch and Deecke, 2011). In contrast, the sympatric false killer whale populations in Hawaii produce less frequency-modulated whistles overall but can maintain social cohesion between subgroups that can span tens of kilometers (Bradford *et al.*, 2014; Baird, 2016). The overlapping ranges of the populations imply that they experience similar environments and perhaps optimize their whistle characteristics according to the same types of habitat features (such as bathymetry, bottom type, proximity to land or seamounts, and upwelling zones), which may explain the similar time-frequency measurements found in our data set.

Characteristics of vocal repertoires have been used as a proxy for defining geographically separate and/or ecologically distinct populations, as well as different social groupings within populations (Rendell and Whitehead, 2003; Saulitis *et al.*, 2005; Riesch and Deecke, 2011;

Rendell *et al.*, 2012; Gero and Whitehead, 2016). Social clusters have been recognized for the MHI population from social network analysis of photo-identification data where three main clusters and two additional smaller social clusters were identified (Baird *et al.*, 2012). Results from classifying whistles to an acoustic encounter instead of a population may reflect the finer-scale social structuring of the MHI population and suggest that social clusters may also be present in the NWHI population given the higher kappa coefficients for both populations (Table 2.7). Although photo-identification data are limited for the NWHI population, acoustic encounter classification results reveal that it may be of value to test whether social structuring exists for this island-associated population using the available association data (Baird, *et al.*, 2013).

Classification results of MHI whistles appeared to be influenced by the social clusters present during an acoustic encounter. When acoustic encounters were classified based on the majority of whistles for RF_PNM, M1 classified most frequently as 'NWHI' while M2, M3, and M4 always classified as 'MHI' (Table 2.8). Classification of M1 improved dramatically for RF_PM since the NWHI population was not included as a possible target variable. M1 was the only acoustic encounter containing individuals from Cluster 1. Differences in whistle characteristics between false killer whale social clusters have not been examined, nor can we with this data set. Some social clusters may have more highly variable whistles, and groups containing aggregations of several social clusters may use a different collection of whistles than those in single cluster groups (Van Cise *et al.*, 2018). Identifying variability in whistle characteristics among social clusters would require encounters with single cluster groups or accurate localization of vocalizing individuals matched with photographic data to confirm their identity within multi-cluster groups, data not currently available for Hawaiian false killer whale populations.

Several factors affect the vocal repertoire of any species, including behavior, social context, environmental factors, and even data collection methods. The challenge is capturing enough variability to build a successful classification model that can be applied under a variety of circumstances. Whistle quality may influence classification results if they are not representative of the species or population. This study included whistles of various quality to create a more flexible classifier for real-time and post-process classification since, often, there are not enough 'high quality' whistles available to confidently classify an encounter. Using various levels of whistle quality presumably captures a variety of individuals engaged in

different behaviors that may be located at various distances relative to the hydrophones and result in a more representative, and perhaps, successful classifier. Future studies may test this theory by building separate whistle classifiers based on discrete levels of whistle quality or behavioral states.

Investigating the acoustic classification of whistles for the Hawaiian false killer whale populations is an important step in furthering our understanding of this species for better management and conservation efforts. While overall whistle classification results from this study did not perform well, patterns emerged suggesting characteristics of the endangered MHI population's whistles are more distinguishable and that there may be fine-scale social structure in the NWHI population, similar to that seen in the MHI population. Additional whistle data for all populations may increase classification performance to differentiate the populations with more confidence and allow further investigation into social and population structure as well as how the populations remain demographically independent. Future analyses may also incorporate characteristics of echolocation clicks to improve classification, hybrid versions of important variables (Rankin *et al.*, 2017) or incorporate additional population or behavior variables (social cluster, group size, etc.) to better capture variability in whistle context and therefore whistle characteristics. Results from this study will inform future acoustic classification analyses for sympatric species that share similar traits in their acoustic repertoire and ecology.

CHAPTER 3
MODEL-BASED LOCALIZATION OF DEEP-DIVING CETACEANS USING TOWED LINE ARRAY ACOUSTIC DATA

Abstract

Passive acoustic monitoring is a standard method for studying cetacean populations to inform management and conservation decisions. Line-transect cetacean abundance surveys use towed line arrays of hydrophones to collect acoustic data for tracking and localizing vocalizing cetaceans. Localization provides perpendicular distance measurements from the array to the whales, which are essential for abundance estimation. Uncertainties in the acoustic data occur due to hydrophone movement, sound propagation effects, errors in the time of arrival differences, and whale depth, but are not accounted for by most two-dimensional localization methods. Consequently, location and distance estimates may be biased and create uncertainty in abundance estimates, especially for deep-diving cetaceans. Here, we apply a model-based localization approach to towed line array data that incorporates sounds propagation effects, accounts for sources of error, and localizes in three dimensions. We use simulations to examine the effects of various parameters on localization, and find that the true distance of the whale, the trajectory of the ship, and whale movement affect location estimates. We demonstrate the localization method using real acoustic data of two separate sperm whales. Results of the model-based method include three-dimensional estimates of distance and depth with position bounds for each whale. By incorporating sources of error and understanding the influences on data collection, this model-based approach provides a method to address and integrate the inherent uncertainties in the towed array data for more robust localization results.

3.1 Introduction

Passive acoustic monitoring (PAM) is commonly used to study the ecology and behavior of cetacean species using their vocalizations. The role of cetaceans as top predators and ecosystem sentinels (Moore, 2008; Bossart, 2011; Hazen *et al.*, 2019) makes it critical to obtain baseline data for these species to be able to detect changes in their distributions and abundance (Davis *et al.*, 2017; Gibb *et al.*, 2019). Over the past decade, advances in methods to detect and

classify cetacean sounds (Bittle and Duncan, 2013) have allowed for PAM data to be incorporated into an increasing number of studies that model species distributions and estimate abundance of cetacean populations (Marques *et al.*, 2009, 2013; Fleming *et al.*, 2018; Harris *et al.*, 2018). Passive acoustic data have also provided important information about cryptic and deep-diving cetacean species in the absence of other data types (e.g. visual observations, telemetry data) to inform conservation and management decisions (Carlén *et al.*, 2018; Hodge *et al.*, 2018; Hildebrand *et al.*, 2019).

Localization methods for PAM data vary depending on the application and design of the PAM system. Towed line arrays of hydrophones are an example of a mobile PAM system commonly used to track and localize vocalizing cetaceans during visual and acoustic line-transect surveys. The surveys are designed to estimate abundance of cetaceans based on distance sampling methods, which normally utilize distances from sighting data to derive the detection function (Buckland *et al.*, 2001). The detection function requires accurate measurements of distances for reliable abundance estimates.

The localization of PAM data collected with towed line arrays can also contribute distance estimates for cetaceans, including animals at depth missed by visual observers. A conventional localization method for towed line arrays includes target motion analysis (TMA). The perpendicular distances are measured from the array to the intersection of consecutive hyperbolic bearing lines calculated using the time difference of arrival (TDOA) of the signal between a pair of hydrophones (Lewis *et al.*, 2007; Rankin, Barlow and Oswald, 2008). In theory, this two-dimensional (2D) technique provides an opportunity for acoustic-based abundance estimation. However, it operates under assumptions that are frequently violated in practice, including the hydrophone positions are perfectly known, sound speed is constant, and the vocalizing whales are mostly stationary at the same depth as the array. The perpendicular distances estimated with 2D TMA do not account for the three-dimensional environment of the whales and the effects of depth when calculating distances. Additionally, errors associated with sources of uncertainty, such as inaccuracies in TDOA measurements, hydrophone movement, variation in sound speed profiles, or whale movement, are often not considered.

Deep-diving cetaceans, such as sperm whales and beaked whales, do not conform to the assumptions of 2D TMA since they primarily vocalize (echolocate) at depths hundreds of meters below the towed line array (Teloni *et al.*, 2008; Schorr *et al.*, 2014). This can result in

overestimated perpendicular distances, particularly for whales that are located deeper in the water column and closer to the ship. Accounting for the depth in location estimates of these deep-diving species may reduce bias in the detection functions and provide more reliable abundance estimates. While Barlow and Taylor (2005) found that the depths of sperm whales did not significantly affect abundance estimates when using a line array towed at 100 m depth, no error estimates were provided and it is unclear whether the same conclusions apply in all conditions (e.g. line arrays towed at shallower depths or in different ocean environments).

Other studies that localized deep divers using towed line array data incorporated surface reflections to overcome the uncertainty introduced by depth. Thode (2004) used surface reflections to simultaneously track dive profiles of sperm whales within close range. The method required slowly towing a wide-aperture tandem array consisting of two staggered line arrays (170-m maximum hydrophone spacing). The slow speeds (~3.7 km/h) allowed the array to sink deep enough to accurately identify the reflections of the long-duration, multipulsed echolocation clicks (≥ 10 ms; Møhl et al., 2003). DeAngelis *et al.* (2017) estimated the depths of beaked whales using surface reflections from PAM data collected with a single short-aperture line array (~30 m maximum hydrophone spacing) that was more maneuverable for towing at typical line-transect survey speeds (~18.5 km/h). Faster towing speeds resulted in an average array depth of 13 m, which was appropriate for identifying surface reflections of short-duration echolocation clicks (≤ 0.8 ms; Baumann-Pickering et al., 2013). Reflections are undeniably useful for estimating depths of diving whales (Zimmer *et al.*, 2008) but their presence relies heavily on the configuration of the PAM system and the vocal characteristics of the species making it difficult to accurately distinguish them in some data sets.

Model-based localization provides an approach to incorporate sound propagation effects, account for the depth of diving cetaceans and incorporate sources of uncertainty to provide error estimates. This technique was originally applied to track and localize diving whales using widely-spaced bottom-mounted hydrophone arrays (Tiemann *et al.*, 2004; Nosal and Frazer, 2006). Thode (2005) implemented a model-based approach using a towed tandem array to account for sound propagation effects while tracking and localizing sperm whales at close range. To our knowledge however, model-based methods have not previously been broadly applied to localize PAM data acquired from short-aperture towed line arrays. Instead, 2D TMA continues to be the common localization method for this type of PAM data, which is suitable for certain

species that are relatively stationary and detected at the same depth as the line array. However, assumptions are violated when localizing deep-diving species, and continuing to use 2D TMA perpetuates the use of potentially biased distance and location estimates without providing a method to quantify error.

Here we develop a semi-automated localization method that adapts a model-based approach to localize sperm whales using PAM data collected with a single short-aperture towed line array during line-transect surveys. Our method localizes in three dimensions, incorporates sources of uncertainties, accounts for sound propagation effects, and provides position bounds for stationary and moving whales. We demonstrate the method in a simulation study to examine several parameters that affect localization results. We then implement the method to localize two real acoustic encounters of sperm whales and discuss the benefits and limitations of adapting the model-based approach to towed line array data.

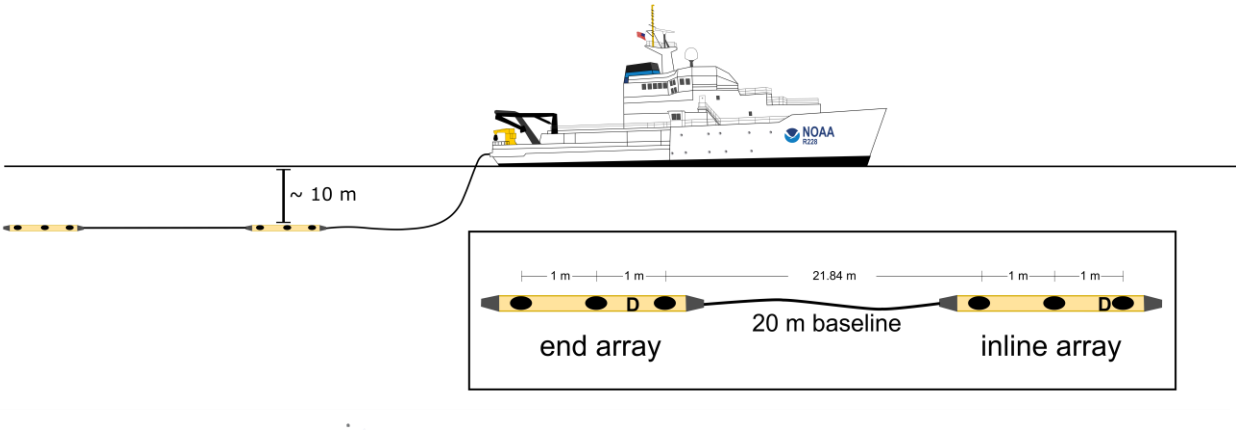

Figure 3.1. Diagram of the line array towed 300 m behind the NOAA research vessels, NOAA Ship Reuben Lasker, at approximately 10 m deep during a cetacean abundance line-transect survey in 2017. The line array consisted of two depth sensor (denoted with 'D') and two array nodes spaced 20 m apart, each housing three hydrophones (black dots) spaced approximately 1 m apart.

3.2 Theory

3.2.1 Ambiguity Volumes

Our method modifies the model-based localization methods that have been successfully used for fixed hydrophones (Tiemann *et al.*, 2004; Nosal and Frazer, 2007; Gebbie *et al.*, 2015) and applies them to acoustic data collected using mobile line arrays (Figure 3.1). Probabilistic indicators of source location, known as ambiguity volumes, are constructed by comparing measured and modeled TDOAs to estimate the location of the source (i.e. the location at which modeled TDOAs best match measured TDOAs is the estimated source location). Modeled TDOAs are generated using a sound propagation model to account for depth-dependent sound speed (Nosal, 2013).

For a hydrophone pair, modeled TDOAs are compared to the measured TDOAs to compute the ambiguity volumes, V, where V is given by:

$$V(\boldsymbol{x}) = \prod_j V_j(\boldsymbol{x}) = \prod_j e^{-\frac{1}{2\sigma_t^2}(\overline{\Delta t_j}(\boldsymbol{x}) - \Delta t_j)^2} \quad , \qquad \text{Eq. 3.1}$$

where $\boldsymbol{x} = (x, y, z)$ is the three-dimensional Cartesian coordinate of the candidate source locations, $\overline{\Delta t_j}(\boldsymbol{x})$ is the modeled TDOA at candidate source location $\boldsymbol{x}$, and Δt_j is the measured TDOA. The product in Eq. (1) is over detection number, where the index *j* corresponds to detections from different positions along the ship trackline that are associated with a single whale (or closely-spaced group of whales) (Figure 3.2) and V_j is the individual ambiguity volume corresponding to click *j*. This is a form of TMA whereby a wide baseline system is artificially created by moving a short baseline array though the environment. As V_j are multiplied, areas of high value are multiplied, areas of high value that overlap are reinforced resulting in a higher value of $V(\boldsymbol{x})$ while areas that do not overlap result in lower $V(\boldsymbol{x})$ values. The whale position is estimated at the position $\boldsymbol{x}$ which maximizes values of $V(\boldsymbol{x})$ across the entire space.

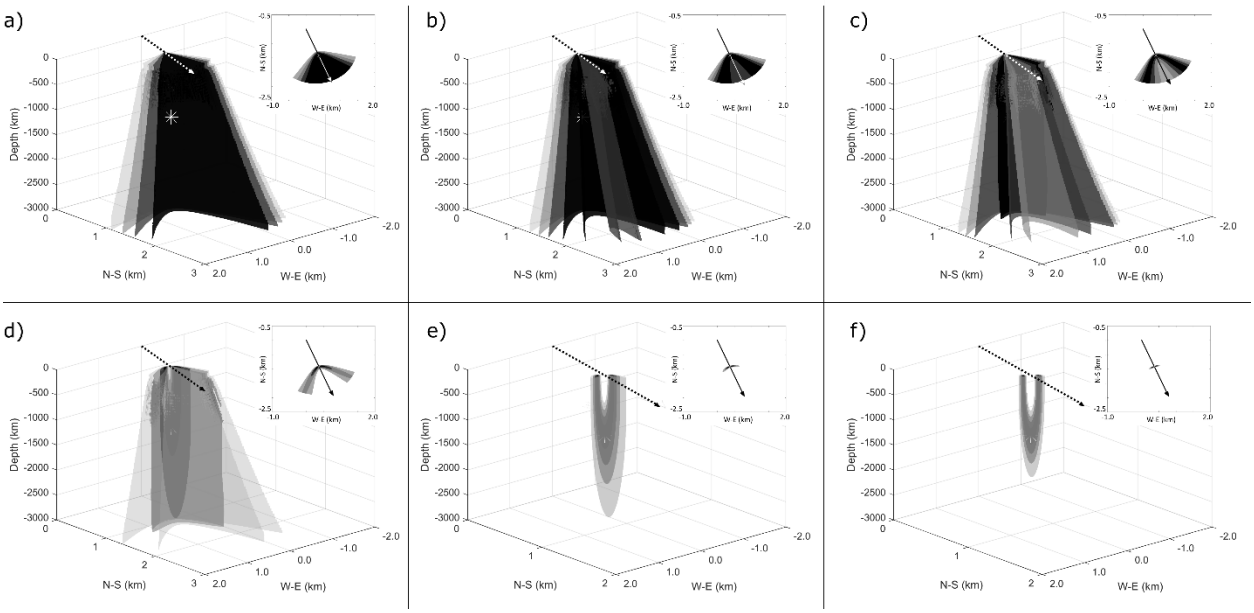

Figure 3.2. Cumulative ambiguity volumes (a-f) for detections of simulated echolocation clicks from a stationary whale located 1.2 km directly below the transect line (denoted by white asterisk). The product of all volumes results in a volume representing all possible location estimates for the whale (f). The color scale represents the ambiguity volume values ranging from 0 (white) as low probability to 1 (black) as high probability. The dotted lines (white or black) indicate the trackline traveling in the direction of the arrow.

The overall error is incorporated through sigma, σ_t, which includes errors in TDOA, model and sound speed profile, hydrophone position, and violated assumptions (such as whale movement). We computed conservative error estimates for each source of uncertainty and combined them via root sum of squares to calculate σ_t as:

$$\sigma_t = \sqrt{{\sigma_a}^2 + {\sigma_b}^2 + {\sigma_c}^2} \quad , \qquad \text{Eq. 3.2}$$

where σ_a is the standard deviation in the measured TDOAs, σ_b is the standard deviation due to uncertainty in hydrophone position (introduced by hydrophone movement), and σ_c is standard deviation due to sound speed uncertainty. For the simulations and data presented below we used σ_a = 0.001s, σ_b = 0.002s, and σ_c = 0.001s. σ_a was based on the peak width (at the noise floor) of the envelopes (computed via Hilbert transform) of the cross-correlation functions of sample of noisy echolocation clicks. σ_b was based on an estimated maximum 3 m hydrophone motion and an average sound speed of 1500 m/s. σ_c was estimated by executing the BELLHOP model

multiple times over a collection of typical sound speed profiles and then taking the maximum difference between the resulting TDOAs.

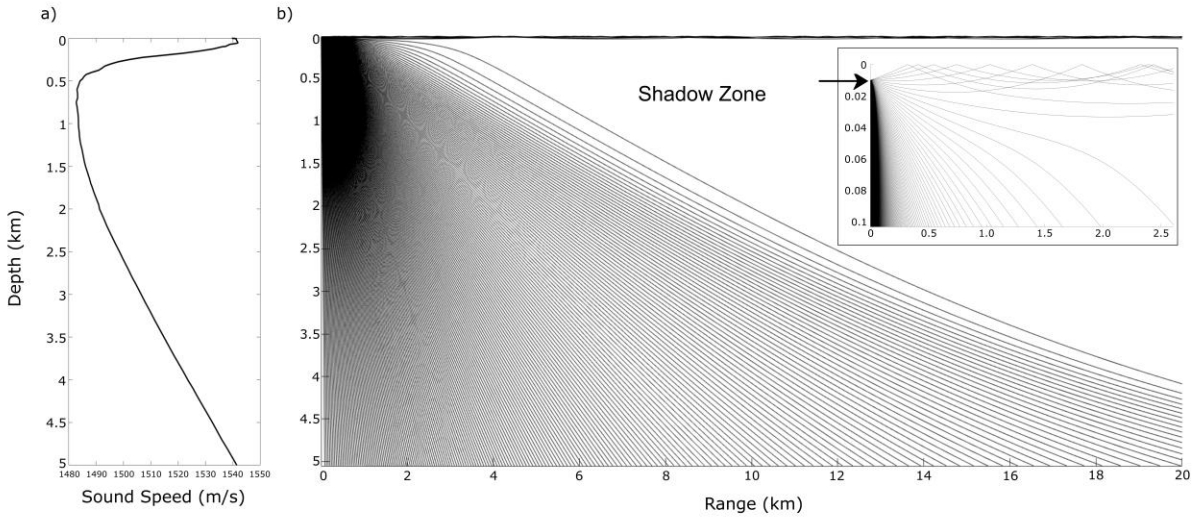

Figure 3.3. Sound speed profile (a) and ray traces (b) for the Hawaiian waters study area incorporated into the simulation study. The white space represents the shadow zone. Inset shows upper 100 m with a receiver at 10 m denoted with a black arrow. Note that in reality, the receiver (array) is at 10 m while the animal is at depth, but we apply the principle of reciprocity (i.e. the ray path is the same from source to receiver and vice versa) to simplify our modeling and illustration.

Position bounds are estimated by profiling the ambiguity volumes. The profiled ambiguity volume along the x-dimension is defined as:

$$VP(x) = \max_{y,z} V(\boldsymbol{x}) \qquad \text{Eq. 3.3}$$

Position bounds in x are defined by the x-positions that bracket the estimated whale position at which $VP(x)$ falls below a fixed threshold. Position bounds in y and z are estimated analogously. To estimate bounds on the whale's distance from the trackline, profiling of the ambiguity volume is applied relative to the perpendicular line that extends from the trackline and passes through the estimated whale location. A threshold of 0.8 resulted in conservative position bounds for this study.

3.2.2 Simulation Experiment

We demonstrate the application of the model-based localization approach in a simulation to estimate the location and distance of a foraging sperm whale detected at depth using a short-aperture towed line array. The position of a simulated whale was fixed at a known distance and depth relative to the array. A 15-minute encounter was simulated by generating 500 click times drawn from a standard uniform distribution on the interval (0s ,900s). The simulated line array was located at an average depth of 10 m while towed 300 m behind a ship traveling at 18.5 km/h. Hydrophone spacings within the array were equivalent to the towed line arrays used for line-transect cetacean surveys illustrated in Figure 3.1. All simulations used the Gaussian beam acoustic propagation model BELLHOP (Porter and Liu, 1994) passed through a representative sound speed profile of Hawaiian waters to create a look-up table of predicted arrival times for computing the acoustic ray paths (Figure 3.1). The representative sound speed profile combined averaged in situ data for depths up to 1 km collected during research surveys on September 2, 2017 and November 18, 2017 with historic data from the 2013 World Ocean Atlas (Boyer *et al.*, 2013) for depths below 1 km (Figure 3.1a). The click generation times, hydrophone positions, whale positions, and sound speed profile were used to simulate the TDOAs. Gaussian distributed white noise ($\mu = 0$, $\sigma = 0.012$) was added to the simulated TDOAs to mimic the noise in real towed array data.

We used a reduced set of simulated TDOAs by smoothing over 1-min increments. This resulted in one V_j per minute of encounter (15 total) and reduced the computing time while maintaining the overall pattern in the TDOAs. The spatial grid had horizontal and vertical spacing of 50 m, with depth dimension constrained to 3 km to represent an average bathymetry within the Hawaiian archipelago and account for the deepest measured dive depths of sperm whales (Teloni *et al.*, 2008).

Ambiguity volumes represent all possible locations of the detected whale, but the shape of this volume depends on the distance and depth of the whale, the ship trajectory, sound propagation effects and the overall uncertainty (σ_t). To evaluate the effects of these parameters on localization results, we included them in different combinations to simulate realistic scenarios based on line-transect survey design and sperm whale behavior (Table 3.1). Ship trajectory is an important parameter since location estimates for whales detected along a straight ship trajectory

are subject to left/right ambiguity, which can only be resolved by turning the ship. We included two types of ship trajectories, 'straight' or 'turn', to examine the effects on the ambiguity surfaces. For scenarios with a turn, we tested three turn angles (20°, 60°, 80°) representing a low, medium, and high degree of change in the direction of the ship during a survey. In addition, simulations included the whale to be stationary for the duration of the encounter or moving in one direction relative to the ship. In both cases, the whale's initial position was placed at a perpendicular distance and depth representative of the detection range of sperm whales using a towed line array (Barlow and Taylor, 2005; Teloni *et al.*, 2008).

Table 3.1. List of parameters included in combinations for the simulation study.

Ship Trajectory	**Turn Angles**	**Whale Perpendicular Distance (m)**	**Whale Depth (m)**	**Whale Behavior**
straight	NA	0 - 7000	400 – 2000	stationary, moving
turn	20, 60, 80	0 - 7000	400 – 2000	stationary, moving

It is particularly challenging to localize a stationary whale when it is detected directly below a ship traveling straight along the trackline (Figure 3.2, Figure 3.4). Two-dimensional TMA does not consider the depth of the whale and, therefore, automatically estimates it to be some distance from the trackline that is approximately equivalent to the whale's depth. A simulation of a whale located 1.1 km below the ship resulted in a U-shaped ambiguity volume where the whale could theoretically be located at any point within the volume (Figure 3.4.1a). The ambiguity volume was maximized ($V(\boldsymbol{x})$ = 0.99) at a distance of 0.25 km from the trackline (left/right ambiguous), and distance was bounded by [0, 1.1] km (Figure 3.4.1b). The maximum $V(\boldsymbol{x})$ occurred at a depth of 1.1 km with depth bounded by [0, 1.3] km (Figure 3.4.1c). Although the simulation provided an apparent "best" position (distance = 0.25 km and depth = 1.1 km), this is an artefact created by the limitations of the ship trajectory (straight trackline), the noise introduced to the system and the grid spacing used in the search. In reality for this scenario, there are infinitely many points along the U-shaped volume with $V(\boldsymbol{x})$'s near the maximum value. Consequently, the position cannot be further refined (beyond the U-shaped volume) given a straight trackline without the use of surface reflections or other information.

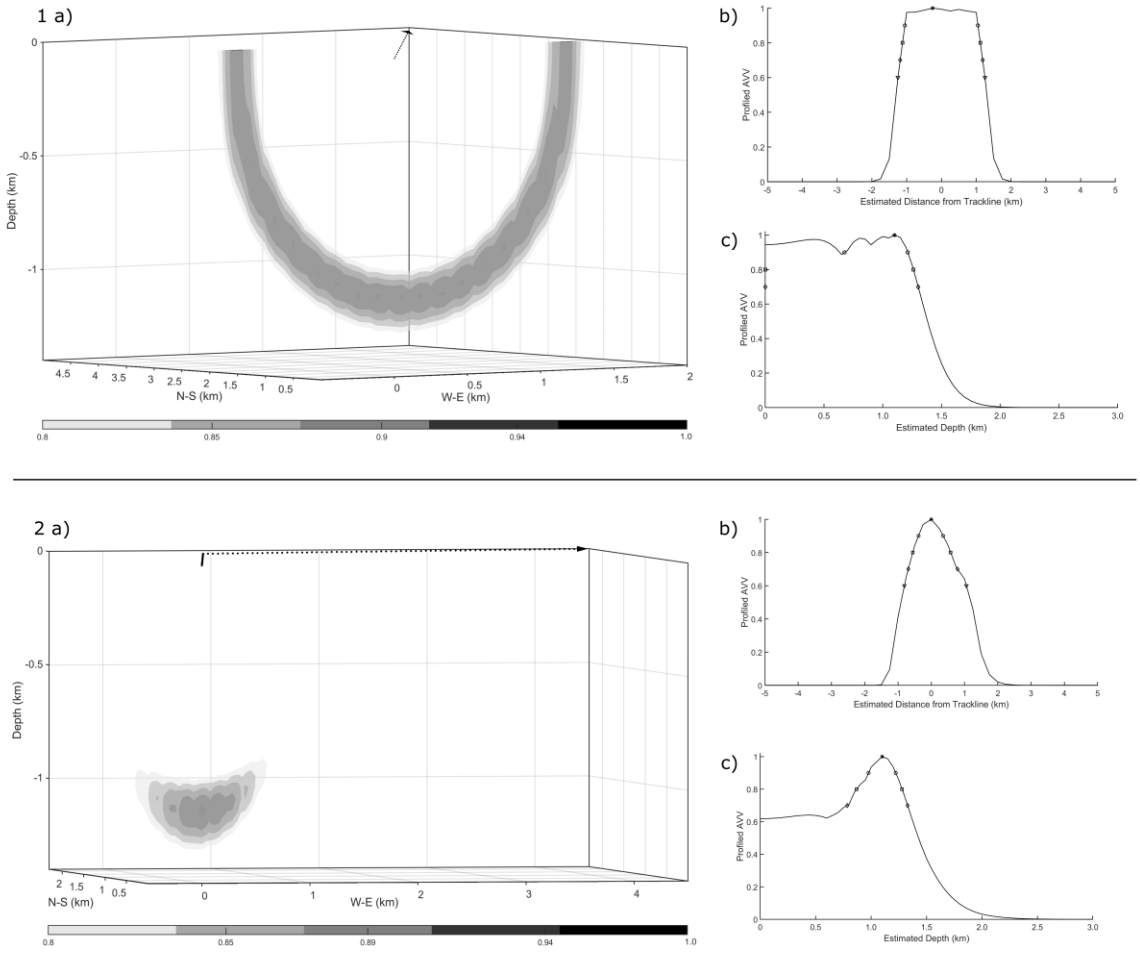

Figure 3.4. Simulations of a whale detected 1.1 km below a ship traveling straight along the trackline produced a U-shaped ambiguity volume(1a) resulting in a left/right ambiguous distance estimate of 0.25 km with distance bounds of [0, 1.1] km (1b) and a depth estimate of 1.1 km with a depth bound of [0, 1.3] km (1c). Implementing a 60° turn reduced the ambiguity volume (2a) resulting in a distance estimate of 0 km (2b) and depth estimate of 1.1 km (2c) with decreased position bounds of [0, 0.55] km and [0.87, 1.3] km, respectively. The gray scale represents the ambiguity volume values ranging from a fixed threshold of 0.8 (light gray) as low probability to 1 (black) as high probability of the whale's location (most "black" points are obscured "inside" the volume hence not visible here). The position bounds vary according to the fixed threshold value applied to profiled volume (b, c), denoted with symbols (downward triangle = 0.6, diamond = 0.7, square = 0.8, circle = 0.9). The black dotted lines indicate the ship's trackline traveling in the direction of the arrow (a).

The ambiguity and overall bounds on distance and depth estimates can be reduced if a turn is implemented during the encounter once the TDOAs reach 0 s, indicating the whale has passed 90° of the line array (Figure 3.4.2). For example, a 60° turn in the ship's trackline resulted in a more constrained ambiguity volume encompassing all possible whale locations with a best distance estimate below the trackline (0 km) at 1.1 km depth with distance bounded by [0, 0.56] km and depth bounded by [0.87, 1.3] km (Figure 3.4.2b & c). The resulting ambiguity volume provided a more precise location estimate for the whale by turning the ship, reducing both the possible distances and depths of the location estimate for a whale located directly below the trackline.

Turning the ship also improved the precision of localizations for stationary whales located farther from the trackline. For example, localizing a whale positioned 4 km away at 1.1 km depth under a straight trackline simulation created two cylindrical ambiguity volumes with an estimated distance of 3.5 [2.1, 4.7] km (left/right ambiguous) and depth of 2.4 [0, 3.0] km error (max $V(\boldsymbol{x})$ = 0.99; Fig 3.5.1). The 60° turn reduced the ambiguity volume entirely to one side and estimated that the whale was at a distance of 4 [3.8, 4.3] km and a depth of 0.7 km [0, 2.9] km (max $V(\boldsymbol{x})$ = 0.99; Fig 3.5.2). Overall, turning the ship reduced the volume of the ambiguity volume for whales closer and farther away from the track line in different ways. Changing the ship trajectory greatly decreased the three-dimensional ambiguity in distance estimates for whales detected below the trackline and resolved it completely for whales detected farther away. However, the bounds on depth remained large, especially for the farther whale. If they are available, surface reflections can be incorporated using the same framework and would further constrain depth estimates.

Simulations thus far have treated the whale as a stationary sound source. As with any TMA method, an important limiting assumption of this approach is that the whales are stationary relative to the array during the encounter. In reality, a whale is likely moving as it vocalizes while traveling, foraging, or socializing, causing a violation of assumptions behind the calculation of $V(\boldsymbol{x})$. $V_j(\boldsymbol{x})$ no longer overlap in space and so no longer reinforce each other at the animal position(s). We developed a strategy to incorporate the effects of whale movement by spatially dilating $V_j(\boldsymbol{x})$ before combining them in $V(\boldsymbol{x})$. This is a conservative approach resulting in larger position bounds that are more appropriate when the assumptions are violated.

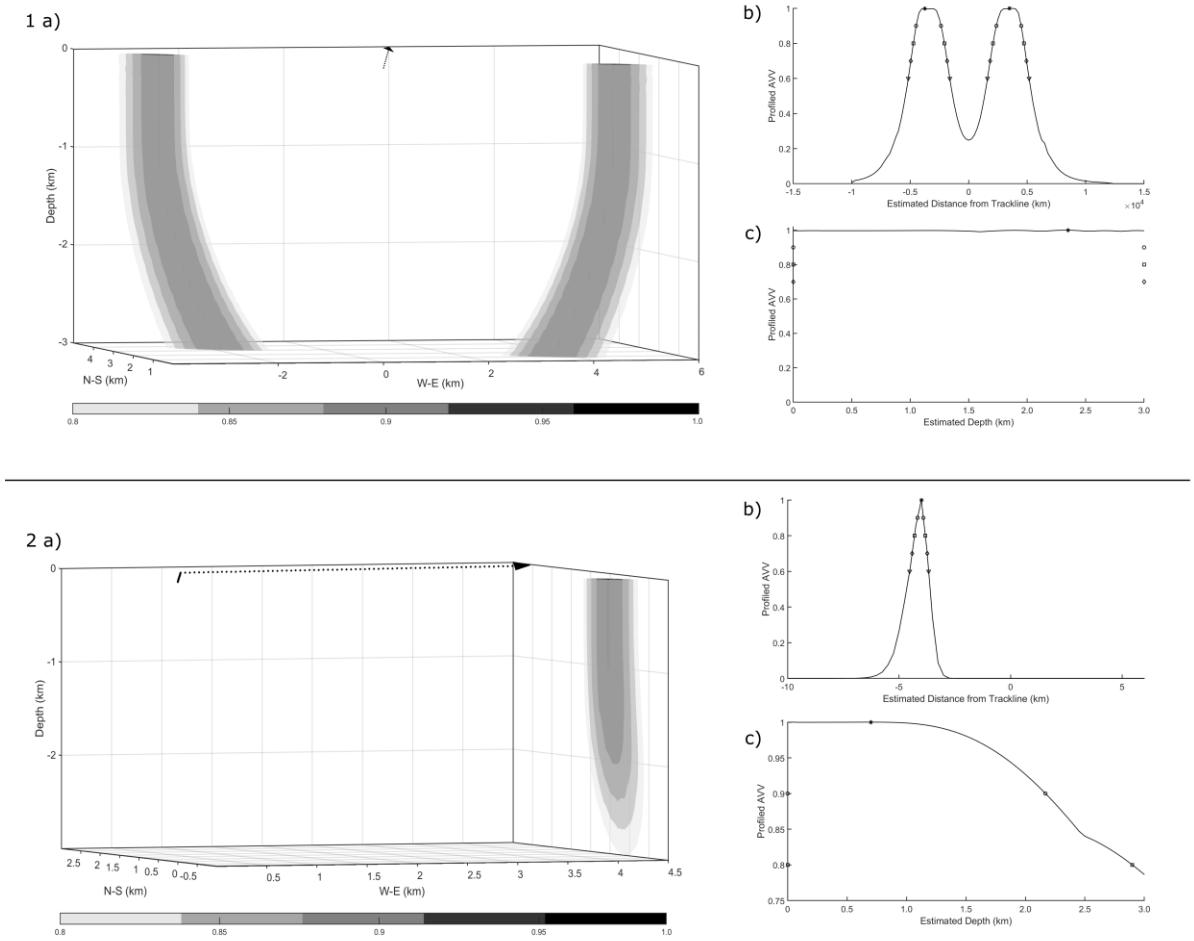

Figure 3.5. Simulations of a stationary whale located 4 km from the straight trackline produced separate cylindrical ambiguity volumes (1a) resulting in a left/right ambiguous distance estimate of 3.5 km with a distance bound of [2.1, 4.7] km (1b) and a depth estimate of 2.4 km depth bound of [0, 3.0] km (1c). Implementing a 60° turn reduced the ambiguity volume (2a) resulting in a distance estimate of 4 km (2b) and depth estimate of 0.7 km (2c) with decreased position bounds of [3.8, 4.3] km and [0, 2.9] km, respectively.

A local maximum dilation operator (Gonzalez *et al.*, 2009) was applied to each $V_j(\boldsymbol{x})$ to encompass the maximum possible distance the whale may have traveled in any direction during the encounter. The dilation of an ambiguity volume $V_j(\mathrm{x},\mathrm{y},\mathrm{z})$ was defined as:

$$\left(V_j \oplus B\right)(x,y,z) = max\left\{V_j(x-x',y-y',z-z') \middle| (x',y',z') \in D_B\right\} \quad , \qquad \text{Eq. 3.4}$$

where D_B is the domain of the "filter" volume B. $V_j \oplus B(\boldsymbol{x})$ is the maximum amplitude over all points in the neighborhood of $\boldsymbol{x}$; regions with higher amplitudes in V_j are enlarged in $V_j \oplus B$ proportionally to the size of B. The filter size and shape was an ellipsoid defined in proportion to averaged horizontal and vertical whale swim speeds of 0.5 m/s and 1.13 m/s, respectively (Wahlberg, 2002) multiplied by the maximum time between the each detection and the start or end of the encounter. Hence it dilated V_j according to the maximum possible swim distance for detection *j* within the encounter.

We simulated two 15-min encounters of separate diving whales with the same initial distances and depths as the whales in the previous examples but changed the whales' position at each time step to evaluate the performance of the localization algorithm for a moving whale. Thus, each click time was associated with a different three-dimensional whale position. The whale positions changed based on an average swim speed of 1.2 m/s (Wahlberg, 2002; Aoki *et al.*, 2007) in a constant direction of travel with a slowly varying vertical component to simulate a dive pattern. The directions of travel included towards or away from the array as well as in the same or opposite direction relative to the array. As in the stationary whale simulations, the moving whale simulations used a straight trackline and a trackline with a 60° turn. Successful localization was defined when the ambiguity surface encompassed the whale's position at TDOA = 0 s, i.e., the time when the whale was perpendicular to the array, to ensure a more precise distance estimate.

Table 3.2 summarizes the results of these moving whale simulations that incorporated the dilation filter. For whales initially located at 0 km, the true distance of the whale at TDOA = 0 s (90° to the array) was captured within the distance bounds of the ambiguity volumes for each direction of movement in both the straight and turn scenarios. The distance estimates that maximized the ambiguity volume varied based on the direction of movement, ranging between 0 and 1 km. The 'towards' and 'away' scenarios produced consistent results as it involved the whale moving either left or right of the trackline in a similar fashion. The minimum distance

bounds resulted from the turn scenario of a whale moving in the opposite direction as the array ([0, 0.9] km) and the maximum distance bounds occurred when the whale moved in the same direction along a straight trackline ([0, 2] km). Overall, the distance bounds of all turn scenarios were less than the straight scenarios given the reduction of the ambiguity volume. Resulting distance estimates and bounds for the moving whale with an initial distance of 4 km achieved similar success. Each ambiguity volume encompassed the true and estimated distances of the whale in every scenario with high maximum ambiguity values. Distance bounds were also much smaller for the turn scenarios with minimum distance bounds restricted to [2, 3.6] km for a diving whale moving towards the array. The largest distance bounds occurred during a straight scenario for a whale moving, again, in the same direction as the array, [1.9, 7.9] km. Depth estimates for all simulations included the true depth of the whale, however, they were deemed unreliable given the large depth bounds due to the limitations previously discussed.

Table 3.2. Localization results from different scenarios of a moving whale after incorporating the dilation filter to address the effects of whale movement on model-based estimates. Each simulation used $\delta = 0.0024$.

			Straight Scenario						Turn Scenario						
Initial Whale Distance (km)	**Whale Depth Range (km)**	**Whale Movement Relative to Array**	**Max *V(x)***	**True Whale Distance (km)**	**Distance Estimate (km)**	**Distance Bounds (km)**	**Depth Estimate (km)**	**Depth Bounds (km)**	**Max *V(x)***	**Turn (degrees)**	**True Whale Distance (km)**	**Distance Estimate (km)**	**Distance Bounds (km)**	**Depth Estimate (km)**	**Depth Bounds (km)**
0	1.1-1.4	towards	0.98	0.6	0.5	0-1.8	1.7	0-2.2	0.99	60	0.24	0	0-1.2	1.85	0-2.5
0	1.1-1.4	away	0.98	0.6	1.0	0-1.8	1.45	0-2.3	0.99	60	0.24	1.0	0.2-1.3	2.15	0-2.5
0	1.1-1.4	same	0.99	0	0.5	0-2.0	2.05	0-2.5	0.99	60	0	0	0-1.0	2.4	0-3.0
0	1.1-1.4	opposite	0.98	0	0.5	0-1.4	1.35	0-1.8	0.99	60	0	0.5	0-0.9	1.65	0-2.2
4	1.1-1.5	towards	0.99	3.4	4.0	0-5.1	1.55	0-3.0	0.99	60	2.3	3.0	2.0-3.6	2.65	0-3.0
4	1.1-1.5	away	1.0	4.6	4.75	1.0-6.4	2.1	0-3.0	1.0	60	4.2	6.0	3.7-7.1	2.5	0-3.0
4	1.1-1.5	same	1.0	4.0	6.0	1.9-7.9	1.9	0-3.0	1.0	60	4.0	6.0	3.6-6.9	2.75	0-3.0
4	1.1-1.5	opposite	0.99	4.0	3.75	0-4.68	0.95	0-3.0	0.99	60	4.0	4.0	2.5-4.5	2.9	0-3.0

3.3 Application to Real Acoustic Data

3.3.2 Data Description

Passive acoustic data were collected using a towed line array during a visual and acoustic line-transect cetacean survey conducted from July 6 to December 1, 2017 by the Pacific Islands Fisheries Science Center (PIFSC) and the Southwest Fisheries Science Center of the National Oceanic and Atmospheric Administration (NOAA) aboard the NOAA Ships *Oscar Elton Sette* and *Reuben Lasker* (Yano *et al.*, 2018). We tested the localization algorithm using two sperm whale encounters from the 2017 survey; one collected on October 2 at 03:12 GMT and the second on November 21 at 02:00 GMT (Table 3.3). The line arrays on both ships consisted two sub-arrays (inline and end array) separated by 20 m (Figure 3.1; Rankin et al., 2013). Each sub-array contained six hydrophones (HTI-96-MIN; 14-85 kHz ± 5 dB at -158 dB re 1 V/µPa) spaced approximately 1 m apart, custom-built pre-amps providing 37 dB (20-50 kHz ± 2dB) of gain and a 1500 Hz high-pass filter, and either a Keller (PA7FLE) or Honeywell (PX2EN1XX200PSCHX) depth sensor placed within the first meter of each array.

Continuous acoustic data were sampled at 500 kHz for each hydrophone channel using an analog-to-digital converter (DAQ; SA Instrumentation, Ltd.) and PAMGuard software (v. 2.00.10fa; Gillespie et al., 2008) while simultaneously collecting vessel GPS data. The acoustic data were monitored in real-time for vocalizing cetaceans during daylight hours. Sperm whale acoustic encounters were logged by trained acousticians who identified sperm whales aurally using headphones and visually with a spectrogram by their unique high-amplitude, low frequency broadband signals (Wahlberg, 2002; Møhl *et al.*, 2003).

Table 3.3. Two sperm whale acoustic encounters localized during a cetacean abundance line-transect survey in 2017 using the model-based approach for short-aperture towed line array data. Ship location is at the time of first detection.

NOAA Research Vessel	Acoustic Encounter ID	Ship Latitude	Ship Longitude	Start Time GMT	Duration (minutes)	Number of Detections
Reuben Lasker	A221	23.8276	-160.8906	10/18/2017 17:51	37	1082
Reuben Lasker	A352	23.7101	-160.4455	11/21/2017 2:00	61	167

3.3.3 Signal Analysis

Recordings of two of the sperm whale encounters from 2017 were reviewed to confirm the presence of echolocation clicks and the type of click. The whale detected on October 2, 2017 produced regular clicks, which have an interclick interval of 0.5 to 1 s and are associated with foraging (Whitehead, 2003). The whale detected on November 21, 2017 emitted slow clicks with an average interclick interval of 6 s, indicating a single male (Jaquet *et al.*, 2001). The click types offered information about the behavioral state of the sperm whale and provided context for the click detection results.

Acoustic data were downsampled from 500 kHz to 50 kHz prior to data analysis. We implemented a simple threshold detector to prioritize speed and robustness over optimal performance in the click detection phase. For each 1-min recording, the signal was filtered with a fourth-order, Butterworth bandpass filter using 2 kHz and 15 kHz as the lower and upper cutoff frequencies to reduce noise. The envelope of the entire filtered time series was computed for each channel using a Hilbert transform. Taking the maximum envelope across all channels increased the probability of detecting the directional sperm whale clicks (Møhl *et al.*, 2003). The detector threshold was empirically determined based on the acoustic data.

We used standard cross-correlation (Knapp and Carter, 1976) to measure TDOAS from the acoustic data. The TDOAs for all detections across all hydrophone pairs were estimated from cross-correlation peaks. The resulting TDOA sets were noisy, but scatterplots of TDOAs over detection time clearly showed the persistent TDOA tracks corresponding to sperm whale

echolocation clicks among detections of other sources. The persistent tracks were manually selected from scatterplots using a graphical data selection tool (*selectdata*, D'Errico 2007) (Figure 3.6). For localization, we selected the TDOAs from the two hydrophones with the largest separation that occurred along straight segments of the trackline since any TDOAs calculated during a turn would introduce more error than could be accounted for using this method. Selected TDOAs were smoothed and subsampled using 1-minute intervals over the duration of the acoustic encounter to reduce the noise in TDOA measurements and reduce the computational requirement by decreasing the number of volumes included in the product, $V(\boldsymbol{x})$ (Eq (1)).

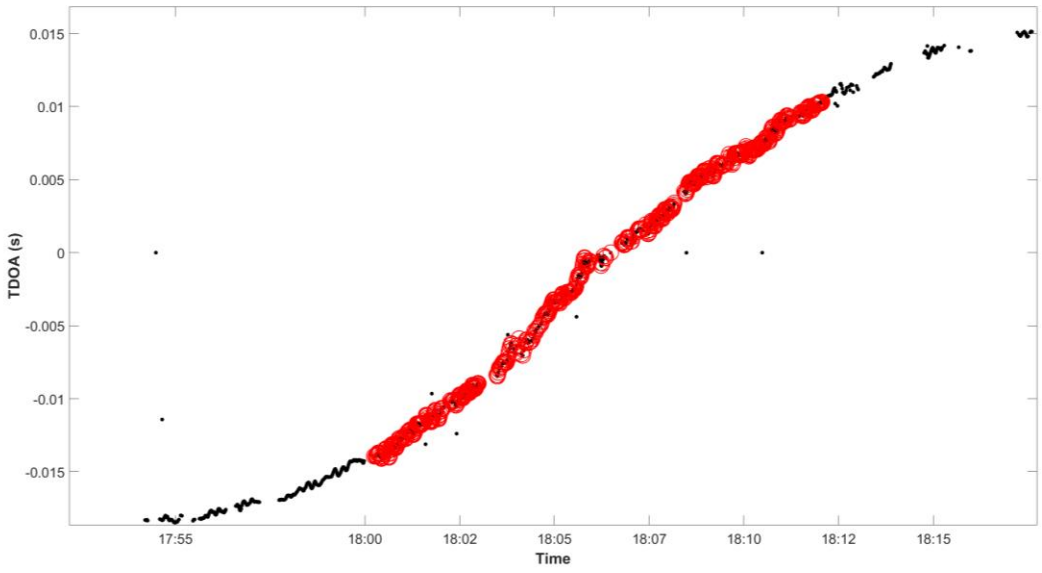

Figure 3.6. The TDOAs from click detections and noise (black dots) were manually subsetted to only include clicks within a shorter time window around TDOA = 0 s (red circles) to improve the accuracy of the localized position estimates.

Ambiguity volumes were generated using a grid that varied in extent according to the geographical range of the acoustic encounter. We used the same grid resolution as in the simulation; 50 m horizontal and vertical spacing, and a vertical limit of 3 km. Sound speed profiles were concatenated for the day of each encounter using the same methods as described in Section III. The same σ, and threshold values as the simulation study were incorporated along with the dilation filter to account for potential whale movement in the localization of each real acoustic sperm encounter.

3.3.4 Localization Results

Both encounters occurred entirely along straight segments of trackline and, therefore, resulted in location estimates with left/right ambiguity. We continued to use a fixed threshold of 0.8 to evaluate the position bounds from the ambiguity volumes for the real sperm whale data. Location estimates for the sperm whale encountered on October 18, 2017 resulted in a wide U-shaped ambiguity volume with an estimated distance of 2 [0, 3.3] km (max $V(\boldsymbol{x})$ = 0.99) and depth of 2.6 km [0, 3.0] km. This example showed a noticeable offset in the trackline that likely occurred due to normal variation in set and drift of the ship (Figure 3.7a). This offset did not appear to significantly affect the measurements from the ambiguity volume as this type of variation is accounted for within the position bounds. Figure 7b also demonstrates the effects of trackline variation on the 2D bearings, where a series of disjointed bearings is produced making it difficult to pinpoint a location and distance of the whale, and likely overestimating the results as well. During real-time operations, the point of convergence of 2D bearing lines estimated the whale to be located at a distance of 3.1 km. While the point estimate for distance is coincidentally included within the model-based position bounds, 2D TMA does not quantify the associated uncertainty related to depth and other error sources.

The TDOAs from the slow clicks of a whale detected on November 21, 2017 produced slightly asymmetrical columnar ambiguity volumes due to a slight offset in the trackline. The left/right ambiguous distances estimated the whale to be 7.3 [4.4, 10.5] km off the right side and 7.0 [3.8, 9.6] km off the left side at a depth of 2.4 km [0, 3.0] km (max $V(\boldsymbol{x})$ = 0.99; Figure 8). Distances estimates measured in real-time with 2D TMA placed the whale at 7.7 km, which is farther than the best estimated distance from the model-based approach but falls within the range of the position bounds. As in the previous example, the 2D TMA estimate does not provide error estimates.

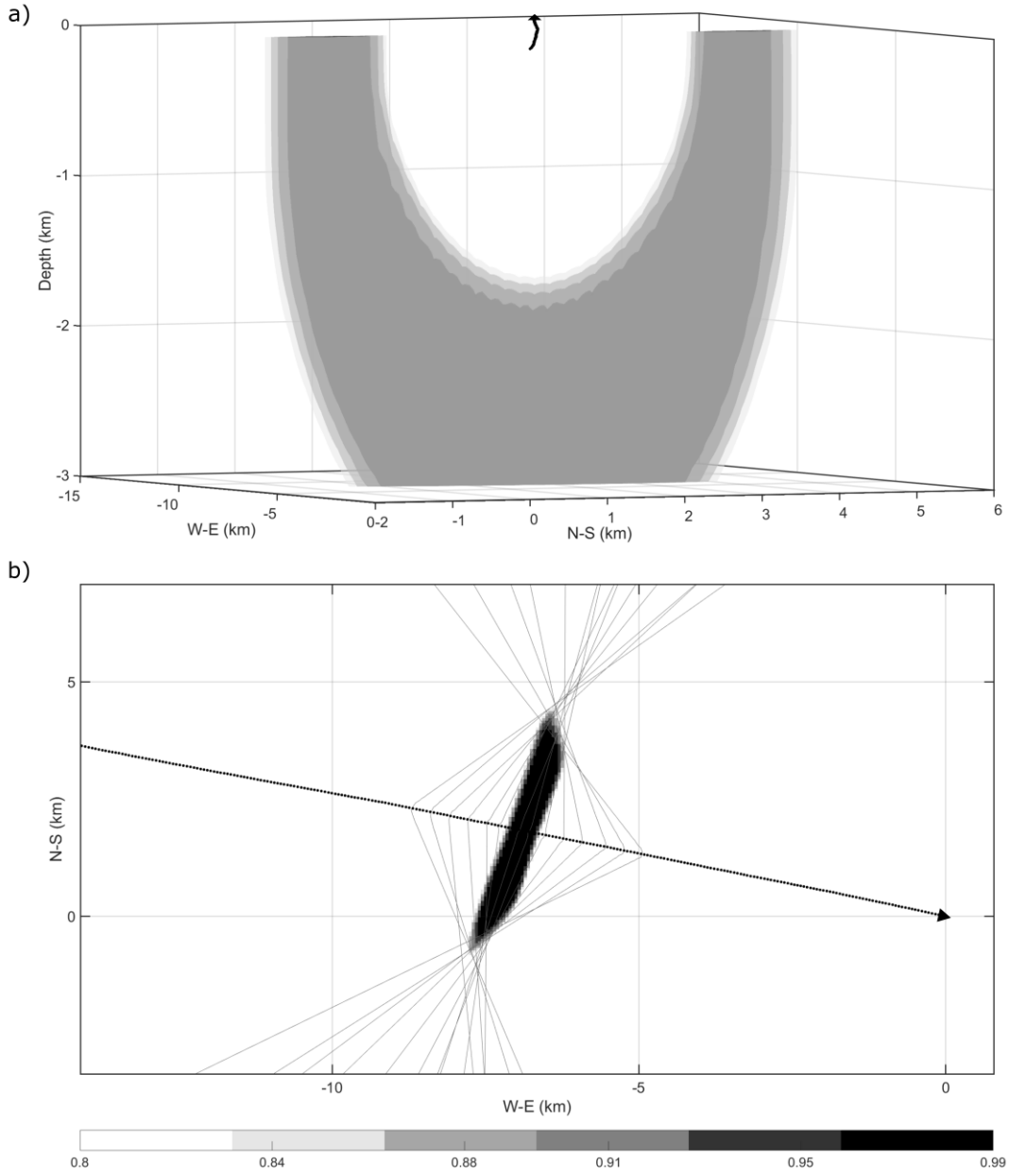

Figure 3.7. A sperm whale acoustically localized on October 18, 2017 produced a wide U-shaped ambiguity volume (a), representing all possible locations of the vocalizing animal and estimated the whale to be 2 km from the trackline and 2.6 km deep, with position bounds of [0, 3.3] km and [0, 3.0] km, respectively (max $V(\boldsymbol{x})$ = 0.99). The profiled ambiguity volume (b) is shown with gray lines to denote the 2D bearing lines generated using 2D TMA. The top-down view of the volume profiled over depth shows the difference between the 2D bearings and the 3D surface (b).

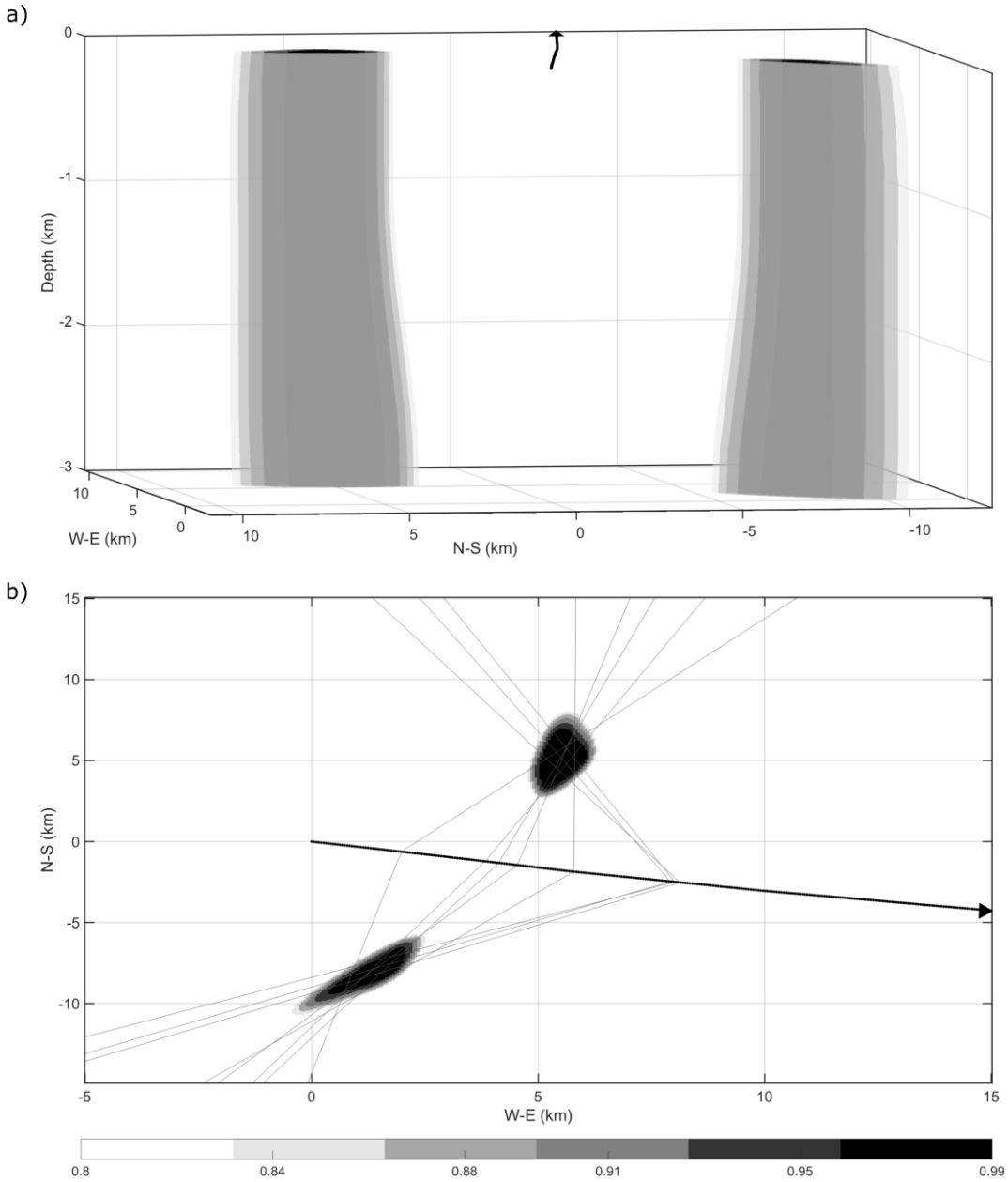

Figure 3.8. Ambiguity volumes for a sperm whale detected on November 21, 2017 estimated the whale to be 7.3 km off the right side ([4.4, 10.5] km position bounds) and 7.0 km off the left side ([3.8, 9.6] km position bounds) at a depth of 2.4 km ([0, 3.0] km position bounds; max $V(\boldsymbol{x})$ = 0.99). The profiled ambiguity volume (b) is shown with gray lines to denote the 2D bearing lines generated using 2D TMA. The top-down view of the volume shows the overlap between the 2D bearings and the 3D volumes (b).

3.4 Discussion

Estimating the location and distances of diving cetaceans is challenging using towed line array data due to various sources of error that introduce uncertainty and bias. We demonstrated a model-based approach for localizing deep-diving sperm whales using simulated and real acoustic data collected from a short-aperture towed line array. The method incorporated multiple error sources to calculate ambiguity volumes representing all possible locations of the whale based on TDOAs between the direct arrivals of echolocation clicks. The ambiguity volumes accounted for whale depth and provided position bounds on perpendicular distance and depth estimates.

The simulation experiment examined several parameters known to affect the localization of a diving sperm whale and found that the ambiguity volume's shape greatly depended on the distance, depth, ship trajectory and movement of the whale relative to the trackline. If detected along a straight ship trajectory, a stationary whale closer to the trackline generally resulted in a U-shaped ambiguity volume (Figure 4.1a). A stationary whale located farther away tended to produce two column-like volumes on either side of the trackline (Figure 5.1a). Turning the ship reduced the error in the distance estimates but did not always improve the error in depth. The uncertainty in depth for simulated and real data encounters was primarily attributed to the two-dimensional design of the towed line array. Despite the large depth bounds, the model-based localization method addressed this limitation by incorporating the uncertainty in depth into the position bounds of the location estimates.

Sound propagation is an important consideration in any localization method as it will affect the range at which sound can be detected depending on the depth of the hydrophones (Chapman, 2004; Tiemann *et al.*, 2004; Thode, 2005; Zimmer, 2013; von Benda-Beckmann *et al.*, 2018). The shadow zone, or the region where sound rays are refracted and fail to propagate in a direct path to the receiver, limits the detection range of a sound source and its extent depends on the oceanographic conditions of a study area (Figure 3.3). For example, in Hawaiian waters, it is unlikely that whales vocalizing at depths less than 0.4 km will be detected beyond approximately 2.5 km distance. While we do not explicitly test the effects of sound propagation in the simulation experiments, we account for them within the model-based localization framework.

Moving whale simulations resulted in larger position bounds from the dilated ambiguity volumes, which we found to be appropriate when the assumptions of a stationary source are violated. The advantage of the model-based approach is evident in its ability to incorporate and quantify the increase in uncertainty due to animal movement. The horizontal and vertical speeds used to parameterize the dilation filter conservatively represented all possible movement of a diving whale. The four directions of travel at a constant swim speed also depicted more dramatic examples of whale movement, which can be more static and variable depending on the whale's behavioral state (Whitehead, 2003). Nonetheless, despite the extreme simulated movement patterns, the true locations of the whales were successfully estimated within the more conservative position bounds.

The resolution and extent of the spatial grid used to generate the ambiguity volumes can also affect the localization results and depend greatly on the study area. The spatial resolution of the grid will affect the precision of the estimates and should be selected based on the specific needs of the application. Finer resolutions will provide more precise position bounds for estimates than coarser resolutions but are more computationally intensive. We chose a spatial grid with a horizontal and vertical spacing of 50 m because position bounds for distance estimates were smaller than coarser grid resolutions and similar to finer grid resolutions at a lower computational cost. Several factors should be considered when selecting the extent of the spatial grid (e.g., the detection range, the environment, animal behavior) to ensure estimates are relevant to the application as well. The extent of the grid assumes that it is physically impossible for the animals to be located beyond a certain range. For deep-diving cetaceans, the extent of the z dimension is an important consideration. While the depth limit was a realistic measure of bathymetry for our study area (3 km), it is also important to consider the available biological information about the species. For example, some of the predicted depths exceeded the deepest measured dive depth of any known sperm whale (1.9 km; Watwood et al., 2006). If the spatial grid were truncated to 2 km, the position bounds for distance and depth would be reduced for closer whales as the U-shaped volumes would be converted to columnar volumes. However, most depth position bounds would still span the vertical extent of the spatial grid without additional information. Likewise, depth position bounds for whales located farther away would be reduced to the full vertical extent of the truncated grid, but distance estimates would not be substantially different. In this application, we selected a conservative vertical extent of 3 km to

account for the possibility that sperm whales may exceed the deepest recorded dive and avoid over-constraining the grid, which would result in less precise estimates.

Our model-based localization method provides more informed distance estimates for deep-diving sperm whales compared to estimates from conventional 2D TMA methods. The semi-automated process we developed for calculating the ambiguity volumes contributes a method for incorporating errors and objectively localizing whales in three dimensions. The real acoustic encounter of the closer whale (Figure 3.7) highlighted the difference between subjectively choosing a location based on disjointed 2D bearings and automatically estimating them from the ambiguity volume. The 2D bearings are more likely to overestimate the distance of closer whales compared to whales located farther away (Figure 3.8), but in both instances, the estimates do not account for uncertainties when localizing whales at depth. The distance estimates (at max $V(\boldsymbol{x})$) may be utilized to compute a detection function for abundance estimation, but additional theoretical development is necessary to incorporate the distance bounds.

A major limitation in the current simulated and real acoustic data sets is the lack of surface reflections necessary to constrain the depth bounds. We chose to test the localization method using these acoustic data sets since similar data sets for sperm whales are common in the literature (Leaper *et al.*, 1992; Gillespie and Leaper, 1997; Barlow and Taylor, 2005; Lewis *et al.*, 2007; Yack *et al.*, 2016; Wild *et al.*, 2017). We now have a better understanding of the overall effects of the uncertainties on distance and depth estimates of sperm whales that may be useful for future surveys collecting towed line array data. The model-based framework can also be generalized to incorporate surface reflections when available from other deep-diving species detected on short-aperture line arrays. For example, the surface reflections from beaked whale species (Zimmer *et al.*, 2008; DeAngelis *et al.*, 2017) may be incorporated to achieve more precise distance and depth bounds for these species.

The simulation experiments and real-data examples only included localization results for single foraging whales. In tropical and subtropical oceans, sperm whales frequently congregate in social groups with multiple animals diving asynchronously to forage (Whitehead, 1996). The model-based localization approach is capable of iteratively localizing multiple animals within a group, but the overall distance estimate for the group may depend on the group's geographical spread. When visual observers estimate distances to large groups of dolphins spread over

hundreds of meters, the distance to the center of the groups are utilized in distance sampling methods. A similar approach could be applied in the case of localizing multiple deep-diving whales. Further simulation experiments are needed to test this theory and include appropriate parameters and errors to fully evaluate the capabilities of the model-based approach in this context.

Towed line array data will always be subject to uncertainties due to the array design and animal behavior. Developing this localization approach to quantify and incorporate these uncertainties can help identify data limitations and guide future PAM system design and data collection methods for more robust localization of deep-diving cetaceans.

CHAPTER 4
DISTRIBUTION PATTERNS DIFFER BETWEEN FORAGING AND NON-FORAGING SPERM WHALES IN HAWAIIAN WATERS

Abstract

Sperm whales (*Physeter macrocephalus*) are a globally distributed, endangered marine species typically observed in productive, deep oceanic waters away from emergent land masses. For a population occurring year-round throughout the Hawaiian Archipelago, we used observations from visual sighting and passive acoustic surveys to construct and compare species distribution models of foraging and non-foraging sperm whales. A total of 209 sperm whale encounters were collected during four annual NOAA marine mammal surveys (2010, 2013, 2016, and 2017) within the Hawaiian Exclusive Economic Zone. Using whale encounters as a predictive variable, we constructed five sperm whale distribution models using spatially-smoothed GAMs to compare the responses of different observational data (e.g., sighting, acoustic, and both combined) and behavioral group data (e.g., foraging and non-foraging using combined observations) fit to a suite of static and dynamic ocean environmental variables including depth, distance to land or seamounts, sea water temperatures, chlorophyll *a*, sea surface height, and eddy kinetic energy. Sperm whale click types were used to differentiate foraging and non-foraging sperm whale groups. Overall, higher densities of sperm whale groups were observed in the northwest region of the Archipelago and north of the Main Hawaiian Islands. The temperature at 584 m depth, surface chlorophyll a, and the standard deviation of sea surface height were explanatory variables for the distribution of foraging sperm whales but none of these variables were significant for non-foraging sperm whales. The behavioral information derived from the acoustic data helped to identify areas that are likely important sperm whale foraging habitat. Models with combined sighting and acoustic data used for behavioral group observations performed well suggesting these data types are complementary and the approach provides a novel ecological aspect to cetacean surveys and distribution analyses. This study contributes methods to incorporate sighting and acoustic data into species distribution models and provides new information about the Hawaiian sperm whale population to inform future research and conservation efforts for this endangered species.

4.1 Introduction

Species distribution models (SDMs) are commonly used to predict the spatial patterns of a species across their habitat by relating field observations of a species to environmental variables within a statistical framework. Such correlative models are used to gain a better understanding of the abiotic environmental conditions that influence the species' geographic range (Elith and Leathwick, 2009; Robinson *et al.*, 2017; Melo-Merino *et al.*, 2020). Insights gained from SDMs support efforts to design appropriate spatial management and conservation strategies.

Despite the challenges of collecting species occurrence data in the marine environment, many marine-based SDMs have been developed for a variety of marine taxa including plankton (e.g., Brun et al., 2016), corals (Franklin *et al.*, 2013), fish (e.g., Olden et al., 2002; Oyafuso et al., 2017), seabirds (e.g., Huettmann and Diamond, 2001; Fox et al., 2017), sharks (e.g., Brodie et al., 2018; Feitosa et al., 2020), and cetaceans (e.g., Fiedler et al., 2018; Virgili et al., 2019). Different types of observational data are incorporated into marine SDMs depending on the species and spatiotemporal scale of the sampling effort. For cetaceans, visual observations are primarily used but are limited to moments when animals emerge above the ocean surface. Technological advances have expanded observational data for many marine species to include satellite telemetry data (Abecassis *et al.*, 2012; Abrahms *et al.*, 2019), active acoustic data (Zhang *et al.*, 2009), and passive acoustic data (Carlén *et al.*, 2018; Fleming *et al.*, 2018) to increase the sample size and include more ecological information in the analysis.

Cetaceans are highly mobile marine predators that play important ecological roles across a wide range of marine habitats (Katona and Whitehead, 1988; Roman and McCarthy, 2010; Kaschner *et al.*, 2011; Roman *et al.*, 2014). Unfortunately, cetaceans face a number of threats throughout the world's oceans, which has resulted in the decline of numerous populations with many listed as threatened or endangered (Magera *et al.*, 2013; Avila *et al.*, 2018). Sperm whales (*Physeter macrocephalus*) are a cosmopolitan cetacean species and are listed globally as vulnerable by the IUCN (2019) with many sperm whale populations also listed as endangered. Developing a quantitative understanding of environmental factors influencing sperm whale distribution through the use of SDMs can help understand cetacean ecology and their role in the marine ecosystem as well as identify important habitats and areas which may overlap with

potentially harmful anthropogenic activities (Azzellino *et al.*, 2012; Redfern *et al.*, 2013; Roberts *et al.*, 2016).

Multiple studies have been conducted to understand sperm whale distribution patterns with respect to their environment (Jaquet and Whitehead, 1999; Jaquet and Gendron, 2002; Fiori *et al.*, 2014; Fiedler *et al.*, 2018). Sperm whales can forage at depths to nearly 2000 m and spend up to an hour submerged searching for cephalopod prey species (Clarke and Young, 1998; Watwood *et al.*, 2006; Teloni *et al.*, 2008). This foraging behavior increases the probability that the whales will be missed by visual observers during surveys. The unique characteristics of their echolocation clicks produced during foraging dives or socializing allows for passive acoustic monitoring methods to detect the whales tens of kilometers away from the acoustic receiver (Barlow and Taylor, 2005). Sperm whales produce clicks at different rates (interclick intervals), which are associated with different behaviors and demographics (Whitehead and Weilgart, 1990; Jaquet *et al.*, 2001; Marcoux *et al.*, 2006; Watwood *et al.*, 2006). Codas are repeated stereotyped sequences of clicks lasting approximately 3 s with highly variable group-specific interclick intervals (Rendell and Whitehead, 2004; Gero *et al.*, 2016; Oliveira *et al.*, 2016). Regular clicks and creaks are associated with foraging (Jaquet *et al.*, 2001; Miller *et al.*, 2004; Watwood *et al.*, 2006) while slow clicks are produced primarily by male sperm whales (Madsen *et al.*, 2002; Oliveira *et al.*, 2013). The acoustic data can be used as observations for sperm whale SDMs and account for groups that would otherwise be excluded from the analysis if not visually sighted (Backus and Schevill, 1966; Gannier and Praca, 2006; Pirotta *et al.*, 2011; Yack *et al.*, 2016; Diogou *et al.*, 2019).

Sperm whale populations in United States waters are listed as endangered under the U.S. Endangered Species Act. In the Hawaii Exclusive Economic Zone (EEZ), sperm whales are one of the most frequently encountered species during visual and acoustic line-transect cetacean surveys for abundance estimation (Bradford *et al.*, 2017; Yano *et al.*, 2018). To date, few studies have developed SDMs of sperm whales (and other cetacean species) in the Hawaii EEZ using line-transect sighting data (Becker *et al.*, 2012, In press.; Forney *et al.*, 2015). Sampling units were derived following methods in Becker (2010), which divided the survey effort into 5-km segments and assigned sighting data and environmental predictor values to each segment midpoint. Model results for sperm whales included distance to land and latitude as the important

predictor variables, predicting a broad pattern of increasing sperm whale density towards the northwestern region of the Hawaii EEZ.

An exploratory study conducted by Oleson *et al.* (2015) attempted to improve the sperm whale SDMs for the Hawaii EEZ by building models using the same methods as Forney *et al*. (2015) but incorporating passive acoustic data collected with towed line arrays of hydrophones. The study included data from a single 2010 survey to compare the predictive power and important variables resulting from SDMs that included only sighting data to SDMs built with only acoustic data. The acoustic-based models selected more dynamic environmental variables compared to the sighting-based models. However, the accuracy of the acoustic-based models was unclear due to the variability in predictions when modeling different subsets of the acoustic data. It was hypothesized that assigning all data to the segment midpoint for the sampling units may have incorrectly associated the local environmental data to sperm whales acoustically detected up to tens of kilometers from the trackline (Barlow and Taylor, 2005). Therefore, the authors suggested localizing the acoustic data to improve future modelling efforts for sperm whales using acoustic data.

Based on known aspects of sperm whale biology and ecology, we hypothesize that whales occur primarily in deep, productive offshore waters away from emergent land masses where they would encounter prey. To address this hypothesis, we evaluate the distribution patterns of sperm whales in Hawaiian waters using both passive acoustic and visual sighting data relative to static and dynamic environmental variables. We incorporate a novel localization method (from *Chapter 3*) to improve the accuracy of positional estimates and environmental information associated with acoustic data. Using the echolocation click characteristics from the passive acoustic data, we characterize whale groups as foraging and non-foraging to compare habitat characteristics and spatial distributions between the groups. This research contributes new information about the relationship between sperm whale distribution and environmental features of the Hawaiian EEZ, develops new techniques to incorporate sighting and acoustic data into SDMs, compares results between SDMs using different types of observational data, and leverages information from the acoustic data to examine the habitat preferences between foraging and non-foraging groups of sperm whales.

4.2 Methods

4.2.1 Data Collection

Observational data were collected within the Hawaii EEZ by the National Oceanic and Atmospheric Administration's (NOAA) Pacific Islands Fisheries Science Center (PIFSC) during cetacean and ecosystem assessment line-transect surveys conducted in 2010, 2013, 2016, and 2017. All surveys followed systematic line-transect sampling protocols described in detail in Yano et al. (2018). Briefly, three observers rotated through three positions searching for cetaceans during daylight hours. Observers along the port and starboard sides used 25×150 mounted binoculars while a center observer searched with 7×50 binoculars and unaided eyes. If animals were seen within 5.6 km of the trackline, observers would direct the ship to turn towards the group for species identification and group size estimates.

Continuous acoustic recordings were simultaneously collected using a towed line array of hydrophones. Array configuration varied between surveys, but all arrays contained 4 – 7 hydrophones capable of recording frequencies between at least 2 – 40 kHz. Detailed specifications of passive acoustic arrays and equipment are included in Table 4.1. Two acousticians aurally and visually monitored the real-time recordings during daylight hours. A suite of software enabled acousticians to detect and localize vocalizing cetacean groups using 2D target motion analysis (TMA) for all species (ISHMAEL, Mellinger, 2002; PAMGuard, Gillespie et al., 2008). Resulting location estimates were left/right ambiguous due to the linear array design and limitations of 2D TMA. The left/right ambiguity was resolved by turning the ship after localizing a group when possible. For each acoustic encounter, or acoustically detected cetacean group, acousticians documented the timestamp of the ship's trackline location upon first and last detection, the types of vocalizations recorded, the estimated perpendicular distances, and species classification when possible. Sperm whales were detected and classified based on their recognizable broadband, low frequency (2 – 15 kHz) echolocation clicks (Backus and Schevill, 1966).

Table 4.1. Details and specifications of the towed line arrays and equipment used for collecting passive acoustic monitoring data during four line-transect surveys.

	PIFSC/SWFSC 2010 (HICEAS)	**PIFSC 2013 (PACES)**	**PIFSC 2016 (HITEC)**	**PIFSC/SWFSC 2017 (HICEAS)**
NOAA ship & Dates	*McArthur II*: August 13 - December 1, 2010 *Oscar Elton Sette*: September 2 - October 29, 2010	*Oscar Elton Sette*: May 7 - June 5, 2013	*Oscar Elton Sette*: June 28 - July 27, 2016	*Reuben Lasker*: August 20 - December 1, 2017 *Oscar Elton Sette*: July 6 - October 10, 2017
Hydrophone	EDO EC65	APC 42-1021	HTI-96-MIN	HTI-96-MIN
Hydrophone flat response range	2-40 kHz	2-40 kHz	2-85 kHz	2-85 kHz
A/D converter	MOTU mK3	MOTU mK3	SA Instrumentation SAIL DAQ	SA Instrumentation SAIL DAQ
Sampling rate	192 kHz	192 kHz	500 kHz	500 kHz
Recorder bit depth/resolution	16-bit	16-bit	16-bit	16-bit
Pre-amplifier flat response range	>2 kHz	>2 kHz	>2 kHz	2-50 kHz
High pass filter	1.5 kHz	1.5 kHz	1.5 kHz	1.5 kHz

When sperm whales were visually sighted or acoustically detected, each team initiated a specific data collection protocol to reduce bias in visual abundance estimates and collect the necessary information for post-analyses of the acoustic data. Details about the visual and acoustic sperm whale protocols are found in Yano et al. (2018). Briefly, if whales were visually observed first within 5.6 km, at least 70 minutes were spent counting the number of animals within a group to account for asynchronous dive behavior. This step may have included slowing the ship and maneuvering towards the group to for better estimates. If sperm whales were first detected acoustically and were never visually observed, the whales were tracked and localized until they passed 90° of the towed array. If the whales were estimated at a perpendicular distance within 5.6 km from the trackline, the ship was directed towards the whales for group size estimates. Whale groups were not pursued beyond 5.6 km because such encounters are well-beyond the truncation distance for visual survey data (typically 5.5 km for sperm whales in Hawaii; Bradford *et al.*, 2017) and due to the time necessary to respond to groups at that distance (Buckland *et al.*, 2001; Thomas *et al.*, 2006).

4.2.2 Acoustic Data Processing

4.2.2.1 Sperm Whale Encounter Types

Model data sets included four types of sperm whale encounters: a visual sighting, a sighted acoustic encounter, a localized acoustic encounter, or a trackline acoustic encounter (Table 4.2). The encounter type determined the location of the sperm whale group used in the model data set and dictated how the data were processed. All acoustic encounters were validated for the presence of echolocation clicks by visually and aurally examining spectrograms of the acoustic data at the time of each encounter using Raven Pro (2048 FFT, Hann window, 50% overlap, version 1.5; Bioacoustics Research Program, 2017). The types of echolocation clicks detected during the encounter were determined aurally and by manually measuring the interclick interval from the spectrogram. We designated any acoustic encounters (i.e., sighted acoustic, localized acoustic, and trackline acoustic encounters) with regular clicks and creaks as "foraging" observations and all others as "non-foraging" observations.

Table 4.2. Description of sperm whale encounters included in the model data sets.

Encounter Type	Encounter Description	Encounter Location
Sighting	Detected visually only	At location of sighting
Sighted Acoustic	Detected visually and acoustically	At location of sighting
Localized Acoustic	Detected acoustically and localized	At location estimated from localization algorithm
Trackline Acoustic	Detected acoustically but not localized	At the ship's trackline location at time of detection

4.2.2.2 Localization Analysis

We reanalyzed acoustic encounters by applying the model-based localization algorithm presented in Chapter 3 and incorporated the re-estimated locations and distances of the localized sperm whale groups into the modeling data sets. When sperm whale groups could not be localized using the model-based approach presented in Chapter 3, we used the location of the ship at the time of first detection. Sightings and sighted acoustic encounters utilized the location from the visual observation data set and did not require additional data processing.

Many of the localized acoustic encounters included two location estimates, one for each side of the ship due to the left/right ambiguity caused by the linear array design and the collection of acoustic data along a straight trackline. Only one location estimate per localized acoustic encounter can be included in the model data sets. To select one location estimate, we compared the associated environmental variables measured on the left and right sides of the ship for each localized acoustic encounter to determine if they were significantly different. First, a correlation analysis revealed most environmental variables between the left and right sides were highly correlated for all encounters ($r \geq 0.7$), with the exception of slope and aspect (Figure 4.1). Next, we examined whether the differences in the environmental variables between the left and right sides were related to the mean estimated distance for each localized acoustic encounter. Whales detected at greater distances were expected to have larger differences in environmental variables compared to whales detected closer to the trackline. Simple linear regressions revealed low p-values for most relationships with low R^2 values and non-normally distributed, heteroscedastic residuals suggesting weak linear relationships between the environmental

variable differences and mean distances from the trackline (Figure 4.2). Hence, choosing the left or right side of the location estimates for localized acoustic encounters was appropriate.

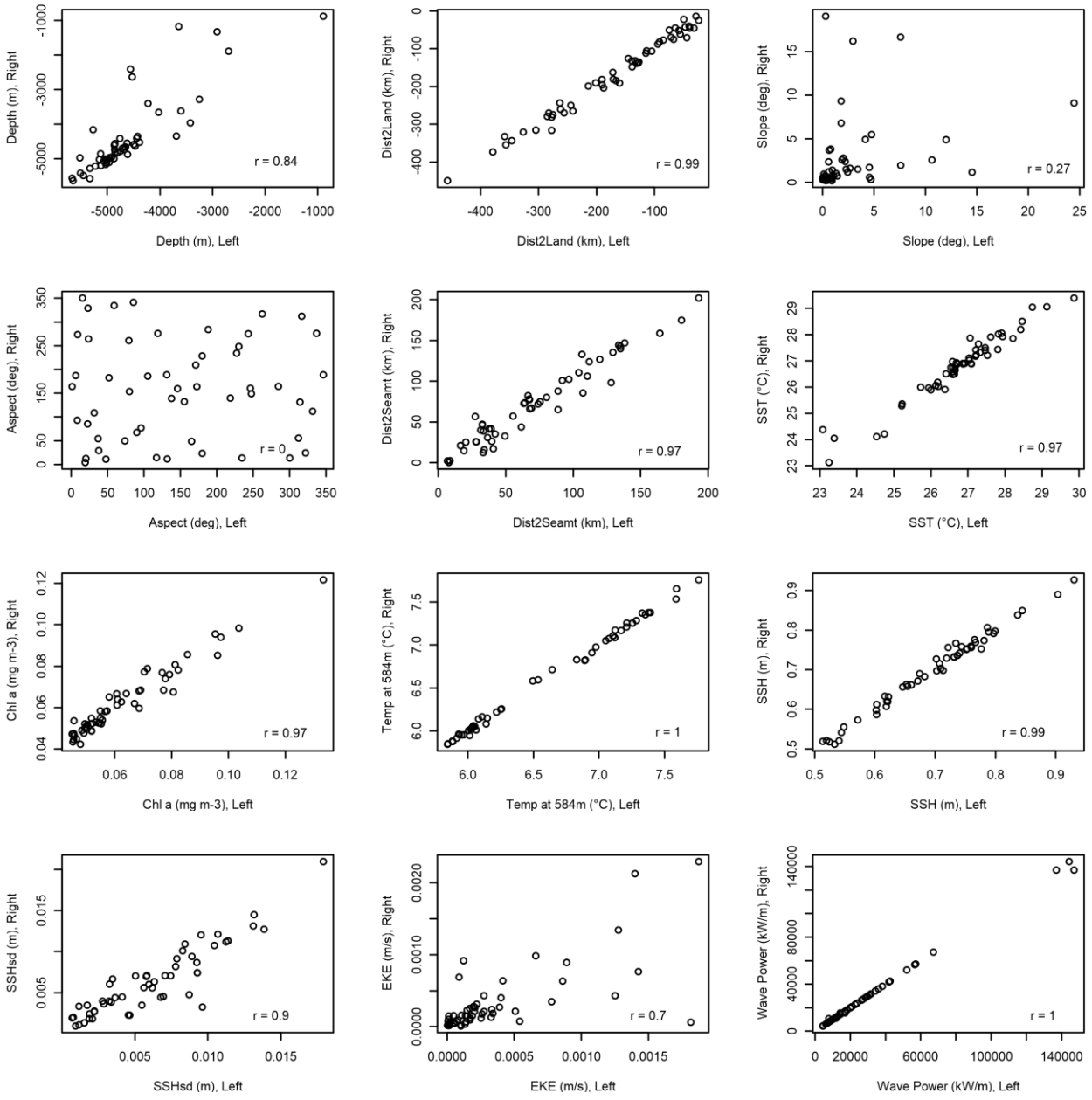

Figure 4.1. Correlation plots of environmental variables between the left and right location estimates from localized acoustic encounters.

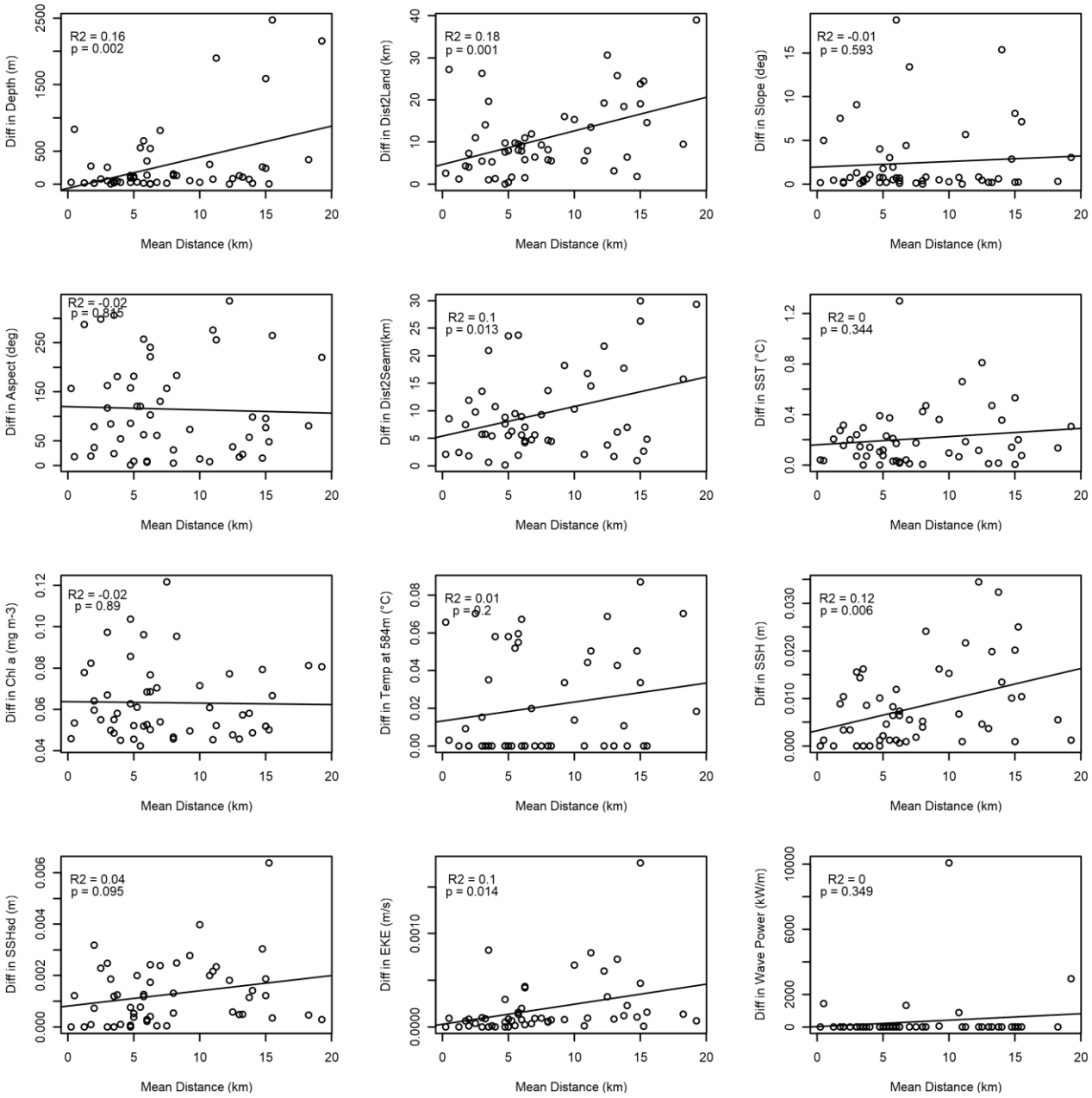

Figure 4.2. Linear regressions tested the relationship between the difference in environmental variables between the left and right side of the acoustic location estimates and the mean estimated distance of the encounter.

4.2.2.3 Trackline Acoustic Encounters

A portion of the overall acoustic encounters in this study could not be localized and were designated as trackline acoustic encounters, i.e., sperm whale groups that were validated but not localized. Localization was not possible if the whales stopped vocalizing or the ship turned towards another sighting before they passed 90° of the array. However, all acoustic encounters (including localized encounters) were associated with the ship's position on the trackline at the time of first detection, creating the potential for non-localized groups to be included in SDMs by linking their trackline location to environmental data. This also meant that each localized acoustic encounter had both an estimated location from the relocalization analysis as well as a trackline location at the time the group was detected. We compared environmental data between the trackline location and the localized location for the localized acoustic encounters using a Wilcoxon signed rank test to determine whether including trackline acoustic encounters was appropriate. If the test resulted in significant differences between the environmental data from each location, then the trackline acoustic encounters would not be included in the data set. Test results of the Wilcoxon signed rank test showed large p-values ($\alpha > 0.05$) indicating that the environmental variables between the estimated location and the trackline location of each localized acoustic encounter were not significantly different. Therefore, we included the trackline acoustic encounters within the data sets for the SDMs.

4.2.3 Model Configuration

SDMs were constructed to evaluate the overall spatial distribution patterns of sperm whale groups within the Hawaii EEZ as they relate to environmental variables. We developed and compared SDMs built using only sighting data (sighting-based), only acoustic data (acoustic-based model) with localized and trackline encounters, and using both sighting and acoustic data (combined model). Finally, behavioral information derived from the echolocations clicks were used to subset the acoustic dataset into foraging and non-foraging encounters to address our working hypothesis by comparing influential environmental variables and spatial patterns of foraging and non-foraging groups of whales. Foraging groups required the presence of regular clicks or creaks but could include all other click types during the encounter. Non-foraging groups included encounters with codas and slow clicks without regular clicks or creaks.

4.2.3.1 Survey Effort

All SDMs included data collected during times when observers were actively searching and listening for whales using visual and acoustic methods, respectively. Effort for the sighting-based model included data from times when the visual observer team was on effort regardless of the acoustics team's effort status. Effort for the acoustic-based model included data from times when the acoustics team was on effort regardless of the visual team's effort status. The data set for the combined model required both the visual and acoustics teams to be simultaneously on effort. Data sets for the foraging and non-foraging models were based on the combined model data set, but subsetted the sperm whale encounters according to the click type requirements.

Additionally, we considered the trajectory of the ship when building each data set since calculations for acoustic localization assumed the towed array to be straight in line with the ship. The ship turned during each survey for various reasons (e.g. approaching animals, avoiding rain, transiting to a new trackline). While turning, an unknown offset occurred between the towed array and ship that persisted for several minutes after the completion of the turn. The magnitude of the offset was unable to be measured causing any localization calculations computed during this time to be unreliable and, consequently, not incorporated into location or distance estimates of the group. Since the visual and acoustics teams often remained on effort when the ship turned for various reasons, all data sets only included data collected along straight segments of trackline to ensure the integrity of the location and distance estimates and allow for model comparisons. We used the *straightPath* function in the 'PAMmisc' R package (version 1.6.0; Sakai, 2020) to calculate all straight sections of trackline using the GPS and heading data of the ship. The method accounted for the normal variation in the ship's heading while identifying points along the trackline during turns. We configured the function to compare the ship's average heading from a 2-minute period with the average heading from the previous 8 minutes. A turn was indicated if the difference between the averaged headings exceeded a threshold of 20 degrees. All data points collected when the ship was turning were excluded from the data set.

4.2.3.2 Analytical Unit

We used the effort data along straight sections of trackline to compute the unit of the response variable, the number of sperm whale encounters per grid cell, for each model. The

number of individual whales was not able to be estimated from the localized and trackline acoustic encounters thus whale groups were used as the response variable for all models. A gridding method was developed using customized code written in the R programming language (version 4.0.2; R Core Team, 2020) to create grids with a 25 km by 25 km spatial resolution (i.e., 625 km^2 grid cells). The spatial resolution was selected according to previous sperm whale habitat studies (Jaquet, 1996; Jaquet and Whitehead, 1996), which found stronger correlations between sperm whale density and environmental variables at spatial scales greater than 593 km.

Effort and straight trackline data were utilized in the gridding process. The amount of effort for each grid cell was calculated in units of area (m^2) using an acoustic detection function, which described the relationship between the distance and detection probability of sperm whales (Figure 4.3). Since sperm whales were detected at farther distances using acoustic methods compared to visual observations, the detection function consisted of perpendicular distance estimates from the localized acoustic encounters to account for the maximum possible sperm whale detection range. We modeled the detection function using the 'Distance' R package (Miller *et al.*, 2019) to fit a half-normal model to a histogram of the acoustic distance estimates. The largest 3% of distances were removed to improve the fit of the half-normal model. Incorporating the detection function into effort calculations accounted for the proportion of area surveyed for each grid cell, which varied depending on the distance of the grid cell from the trackline. The centroids of each grid cell containing effort were extracted using the 'sf' R package (Pebesma, 2018). Sperm whale encounters within each grid cell were associated with the effort and environmental data computed at the grid cell centroid. Grids were computed separately for each model type (i.e., acoustic-based, combined) to include the appropriate sperm whale encounters and effort data. Separate grids were not computed for the foraging and non-foraging models since they were subsets of the combined model data set.

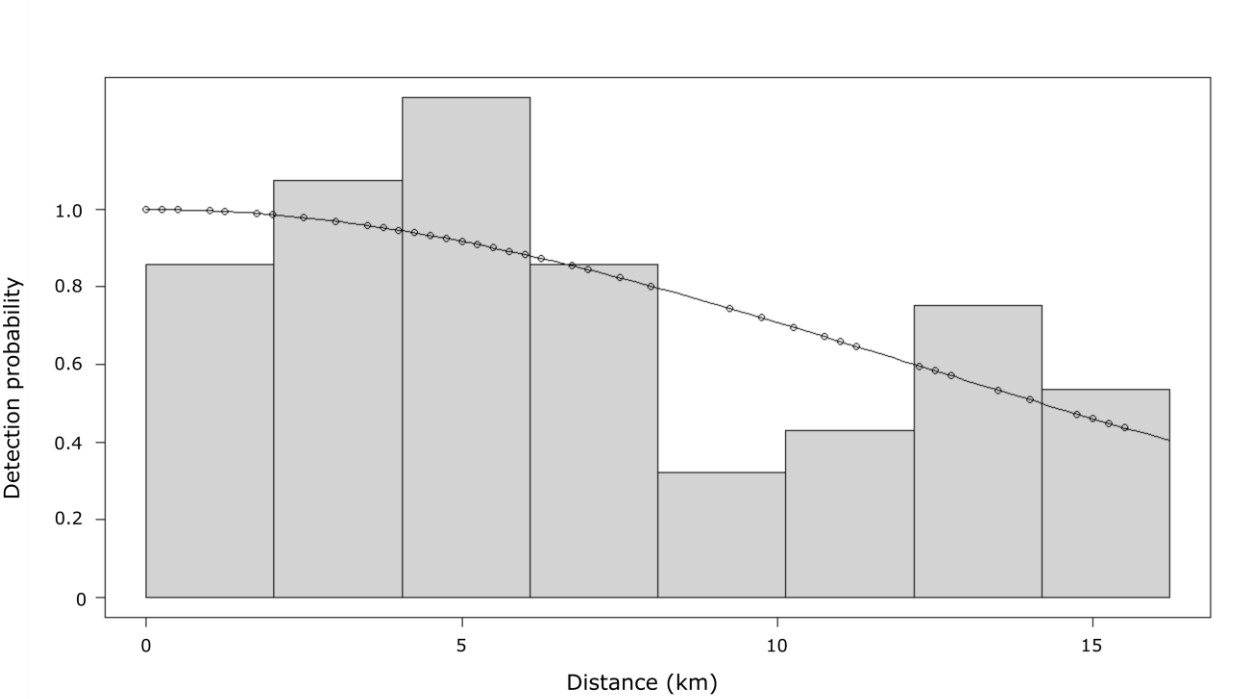

Figure 4.3. Half-normal distribution detection function modeling the detection probability of sperm whales as a function of the distances estimated from the localized acoustic encounters (black dots).

4.2.3.3 Environmental Variables

The environmental predictor variables associated with each grid centroid consisted of static bathymetric features and dynamic remotely sensed variables. The latter were included as indicators of mesoscale oceanographic processes to represent sperm whale habitat and proxies for prey distribution (Table 4.2). Static variables included seafloor depth, seafloor slope, seafloor aspect, distance to islands, and distance to seamounts. Seafloor bathymetric variables were obtained from the global bathymetry and topography 15 arcsecond data set, SRTM15+ (Tozer *et al.*, 2019). Since slope and aspect were highly uncorrelated between the left and right sides of localized acoustic encounters (Figure 4.1; r = 0.27, r = 0, respectively), they were excluded from the models.

Table 4.3. Candidate environmental variables included as predictors for species distribution models.

Environmental Variable	Unit	Resolution	Relevance	Data Source
Static				
Depth	m	15 arc-sec	Prey aggregations found in deeper water	SRTM15+ (https://topex.ucsd.edu/WWW_html/srtm15_plus.html)
Distance to shoreline	m	15 arc-sec	Proximity to land relates to areas of upwelling, enhanced primary production	GSHHG (https://www.soest.hawaii.edu/pwessel/gshhg/)
Distance to seamount	km		Interactions with currents influence prey aggregations and primary production	Global Seafloor Geomorphic Dataset (http://www.bluehabitats.org/?page_id=58)
Dynamic				
Chlorophyll-a	mg/m^3	0.04°, monthly	Proxy for prey availability	Aqua MODIS (https://oceancolor.gsfc.nasa.gov/data/aqua/)
Sea surface temperature (SST)	ºC	0.04°, monthly	Potentially associated with prey aggregations or enhanced productivity	
Standard Deviation of SST	ºC	0.04°, monthly		
Temperature at 584 m	ºC	0.33° Lat x 1° Lon, monthly	Depth of prey species	GODAS (https://psl.noaa.gov/data/gridded/data.godas.html)
Sea surface height (SSH)	m	0.08°, monthly	Variability over time and horizontal gradients of SSH indicate mesoscale oceanographic features associated with enhanced prey aggregations or primary production	GLORYS12V1 (https://resources.marine.copernicus.eu/?option=com_csw&task=results?option=com_csw&view=details&product_id=GLOBAL_REANALYSIS_PHY_001_030)
Standard Deviation of SSH	m	0.08°, monthly		
Eddy kinetic energy	m^2/s^2	0.08°, monthly	High EKE indicates stronger current velocities, influence prey aggregations and primary production	
Wave power	kW/m	0.45°, daily	Wave power accounts for wave height and period, indicator of energy movement through water, potentially associated with changes in primary production	WaveWatch III Global Wave Model (https://pae-paha.pacioos.hawaii.edu/erddap/griddap/ww3_global.html)

The distance to land was obtained from the Global Self-consistent, Hierarchical, High-resolution Geography Database (GSHHG; Wessel and Smith, 1996). This variable addressed the theory that sperm whales are typically found farther offshore, which is also related to depth and suitable prey habitat.

Seamounts are isolated topographic seafloor features taller than 100 m (Staudigel *et al.*, 2010) that aggregate lower trophic level communities, including cephalopods, a main prey item for sperm whales (Clarke *et al.*, 1993; Clarke, 1996; Clarke and Paliza, 2001; Pitcher *et al.*, 2007). Since many cetacean species are associated with seamounts (Kaschner, 2007; Wong and Whitehead, 2014) and roughly 600 seamounts exist within the Hawaiian archipelago, we included the distance to seamounts as a predictor variable. Locations of seamounts were extracted from the Seafloor Geomorphic Features Map (Harris *et al.*, 2014). Distances to seamounts were computed with the 'sp' and 'sf' R packages (Bivand *et al.*, 2013; Pebesma, 2018).

A two-dimensional spatial term (longitude x latitude) was included to explicitly account for geographic effects as well as spatial autocorrelation and integrates over the entire time period of all surveys (Miller *et al.*, 2013; Becker *et al.*, 2018). The inclusion of a spatial term may result in explaining the variation in the data not explained by the other environmental predictors, but it limits the transferability of the models to other study areas. A temporal term for year was also included as a predictor variable to account for any variation introduced by including data from surveys conducted in different years.

Remotely sensed dynamic variables included monthly sea surface temperature (SST) and chlorophyll-a from the Aqua Moderate Resolution Imaging Spectroradiometer (MODIS) data set. Chlorophyll-a was log-transformed to normalize the variance across the right-skewed observations (log(Chla)). Sea surface height (SSH), the standard deviation of SSH (SSHsd) and eddy kinetic energy (EKE) were obtained from the global ocean eddy-resolving physical reanalysis data set (GLORYS12V1) generated by the Copernicus Marine Environment Monitoring Service. The EKE is given by:

$$EKE = 1/2(U^2 + V^2) \ , \qquad \textit{Eq. 4.5}$$

where *U* and *V* are the zonal and meridional components of geostrophic currents, respectively. The SSH, SSHsd, and EKE act as mesoscale indicators of the ocean vertical structure and reflect gradients in ocean circulation and density structure that may influence the biological responses of lower trophic level organisms (Polovina and Howell, 2005). Wave power (WP) is given by:

$$WP = \frac{\rho g^2}{64\pi} H^2 t_p \ , \qquad Eq.\ 4.6$$

where ρ is the density of seawater (1024 kg/m^3) and g is the acceleration of gravity (9.8 m/s^2). Significant wave height, *H*, and peak wave period, t_p, were combined to represent a metric for the size and strength of waves. Monthly temperatures at 584 m were obtained from the Global Ocean Data Assimilation System (GODAS) provided by the NOAA Climate Prediction Center. We selected a depth of 584 m as the best approximate depth of prey habitat available from the resolution of the GODAS data set to be related to the presence of sperm whales. This depth corresponded with non-migrant squid species (e.g., *Histioteuthis hoylei*) that typically inhabit waters deeper than 400 m and are commonly found in stomach content analyses of sperm whales (Young, 1978; Clarke and Young, 1998; Watanabe *et al.*, 2006).

4.2.3.4 Model Parameterization

Generalized additive models are a statistical method commonly used in species distribution modeling for their flexibility in fitting complex, nonlinear species-habitat relationships. The data drive the relationships between the response and predictor variables without assuming a specific formula (Guisan *et al.*, 2002). To relate the number of sperm whale encounters per grid cell to environmental variables, we fitted GAMs using the 'mgcv' R package (v. 1.8-31; Wood, 2011) using a negative binomial distribution with a log-link function given the sparse encounter rate data and large numbers of zeros. Model data sets were partitioned into a training and test set with 70% and 30% of the data, respectively. Correlations among the predictor variables were found to be < |0.60|. The natural logarithm of effort was included as an offset variable to account for the variation in effort per grid cell.

Thin-plate regression splines were restricted to three degrees of freedom to avoid overfitting the non-linear trends and preserve the ecological interpretability of the relationships

(Forney, 2000; Ferguson *et al.*, 2006; Roberts *et al.*, 2016). Parameter estimates were optimized using restricted maximum likelihood (Wood, 2011). Model selection was conducted with automatic term selection, determined by the *p*-values of each predictor (Marra and Wood, 2011). Initial models were built with all potential environmental predictors. Non-significant ($\alpha = 0.05$) predictors were removed, and models were refit until only significant predictors remained.

4.2.3.5 Model Evaluation

SDMs were evaluated using a set of common evaluation metrics calculated on the trained models and the models fitted to the test datasets, including the percentage of explained deviance and the mean squared error (MSE). Partial effects plots were used to visualize the fitted smoothers and interpret the relationship of the selected environmental variables with the response variable. Selected predictor variables were compared between models to assess whether different types of data resulted in different model predictions.

4.3 Results

The post-processed acoustic data from the four surveys resulted in 209 total sperm whale encounters (11 sighted only, 67 sighted acoustic encounters, 58 localized acoustic encounters, and 73 trackline acoustic encounters) (Table 4.4). A total of 119 acoustic encounters were designated as a foraging group (44 sighted acoustic encounters, 40 localized acoustic encounters, and 35 trackline acoustic encounters) and 79 were designated as a non-foraging group (18 sighted acoustic encounters, 38 localized acoustic encounters, and 23 trackline acoustic encounters). Acoustic encounters that were not also sighted accounted for 63% of the total encounters. With four years of survey data included in the SDMs, year was not selected as a significant variable.

Table 4.4. Total encounters by type and survey year.

	Encounter Type				
Survey Year	**Sighted Only**	**Sighted-Acoustic**	**Localized-Acoustic**	**Trackline-Acoustic**	**Total Encounters**
2010	6	24	10	25	65
2013	2	17	4	4	27
2016	0	4	4	8	16
2017	3	22	40	36	101
Total					

4.3.1 Sighting-Based Models

The best-fit sighting-based models selected SST, SSHsd, and the spatial smoother as significant predictors (Figure 4.4). Sightings declined in warmer surface waters with the lowest number of sightings predicted when temperatures reached 30°C. The majority of sightings also occurred at the extremes of SSHsd. The 2D smoother of the spatial term using longitude and latitude depicted sperm whale sightings to gradually increase with latitude, with the majority occurring north of 25°N. The percentage of deviance explained for the sighting-based model was 16.2%, the highest of all models (Table 4.5). The sighting-based model also resulted in similar mean squared errors (MSE) for the training and test data sets, indicating minimal overfitting of the model.

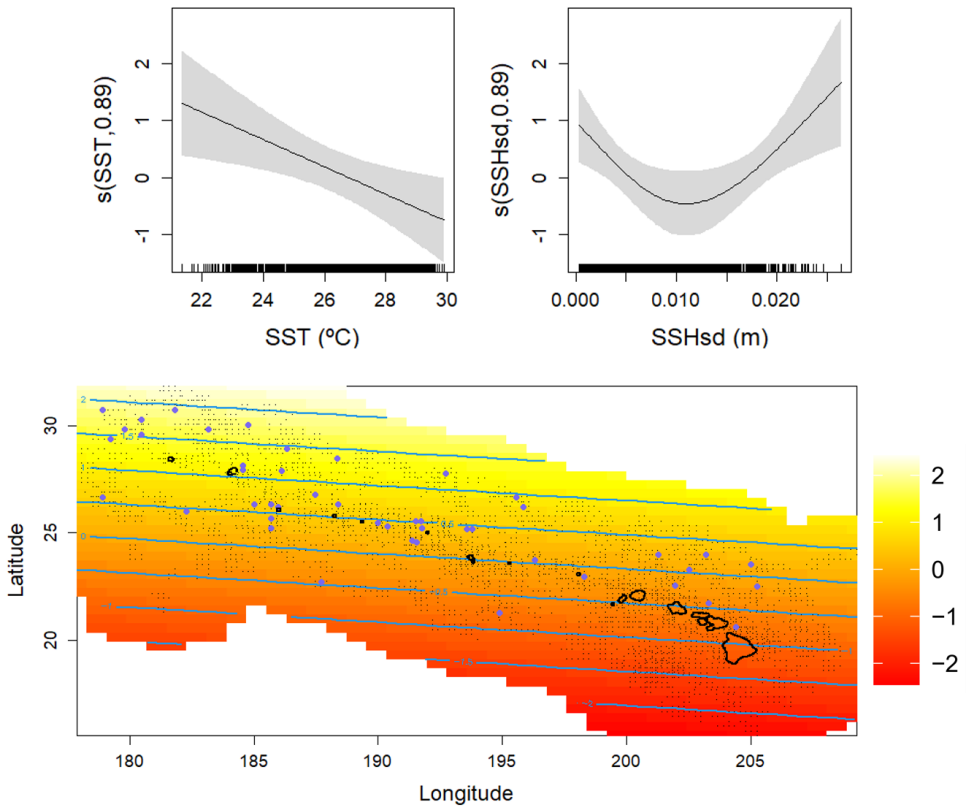

Figure 4.4. Environmental predictors selected for the sighting-based model included sea surface temperature (SST), standard deviation of sea surface height (SSHsd), and the 2D spatial term (Longitude, Latitude). Purple dots on the heat map of the spatial term represent all sighted sperm whales and the black dots indicate all data points included in the model. The blue contour lines represent predicted whale groups on the link scale and correspond with the color scale, increasing from red to yellow.

Table 4.5. Percentage of explained deviance, mean squared errors, total encounters, and selected environmental predictors for all models.

Model	% of Deviance Explained	MSE Train	MSE Test	Total Encounters	Environmental Predictors
Sighting-based	16.2	0.017	0.02	78	SST, SSHsd, LON:LAT
Acoustic-based	8.56	0.025	0.026	131	Depth, SSH, LON:LAT
Combined	12.62	0.041	0.05	209	Depth, SSHsd, LON:LAT
Foraging	16.04	0.03	0.029	119	Temp at 584m, SSHsd, log(Chla), LON:LAT
Non-Foraging	11.69	0.017	0.018	79	Depth, LON:LAT

4.3.2 Acoustic-Based Models

The best-fit acoustic-based models selected depth, SSH, and the spatial smoother as significant predictors (Figure 4.5). More acoustic encounters occurred in depths closer to 6000 m and shallower depths less than 1000 m with less occurring at depths between 3000-3500 m. Acoustic encounters also gradually declined with increasing SSH. The 2D smoother for the spatial term of the acoustic encounters showed sperm whales to be spatially distributed north of the Main Hawaiian Islands and north of the Northwestern Hawaiian Islands with fewer encounters south of all islands. The percentage of deviance explained was 8.56%, the lowest compared to other models. The acoustic-based model resulted in similar mean squared errors (MSE) for the training and test data sets, indicating minimal overfitting of the model.

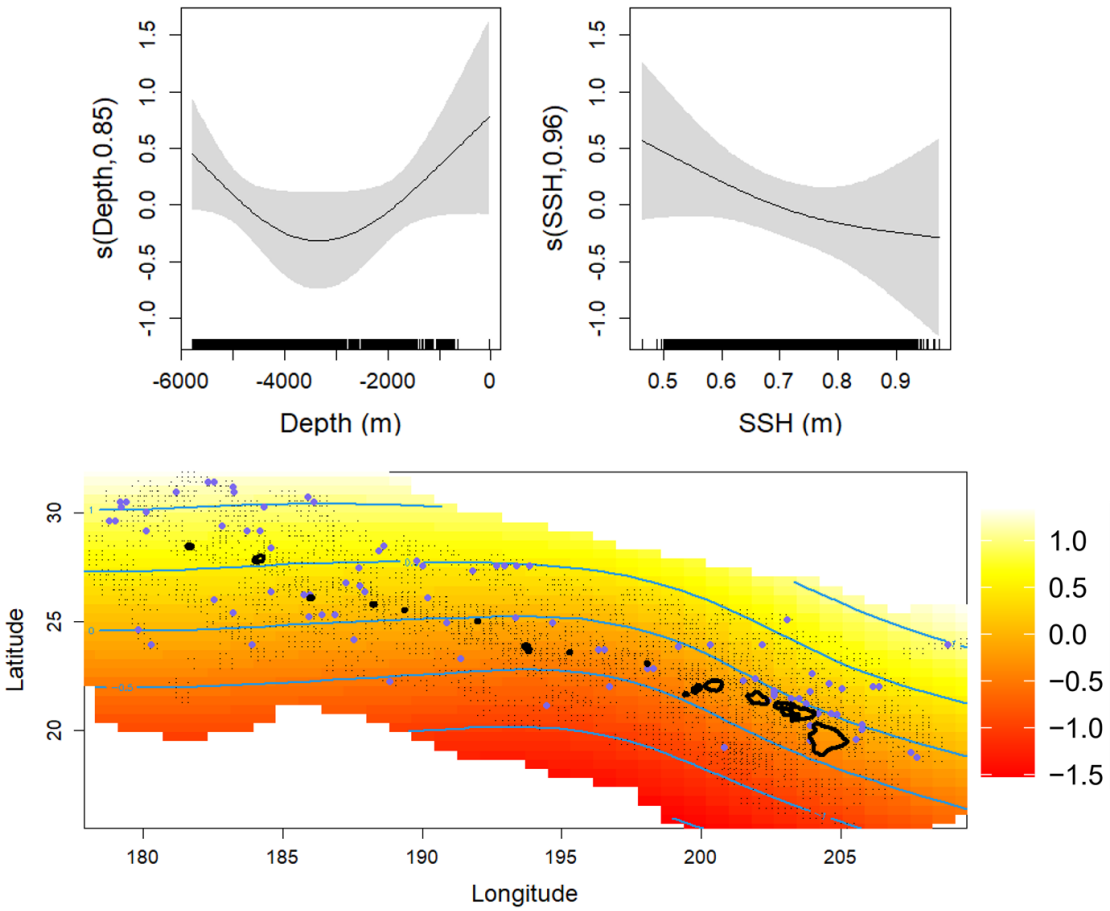

Figure 4.5. Environmental predictors selected for the acoustic-based model included depth, sea surface height (SSH) and the 2D spatial term (Longitude, Latitude). Purple dots on the heat map of the spatial term represent all sighted sperm whales and the black dots indicate all data points included in the model. The blue contour lines represent predicted whale groups on the link scale and correspond with the color scale, increasing from red to yellow.

4.3.3 Combined Models

The best-fit combined model selected depth, SSHsd, and the spatial term as significant environmental predictors. The simple smoother for depth resulted in a similar relationship as the acoustic-based model, with more sperm whales encountered in deeper and shallower depths compared to depths between 3000-3500 m. Sperm whale encounters gradually declined with increasing SSHsd until 0.01 m, where the encounter rate remained mostly stable. The spatial term for the combined data set showed an increase in sperm whale encounters within the Northwestern Hawaiian Islands region and north of the Main Hawaiian Islands. The fewest sperm whale encounters occurred south and east of French Frigate Shoals until the eastern edge

of the study area. The combined model resulted in a higher percentage of explained deviance (12.62%) compared to the acoustic-based model, but lower than the sighting-based model. The MSE of the models built with the training data was lower than the MSE of the predictions for the test data.

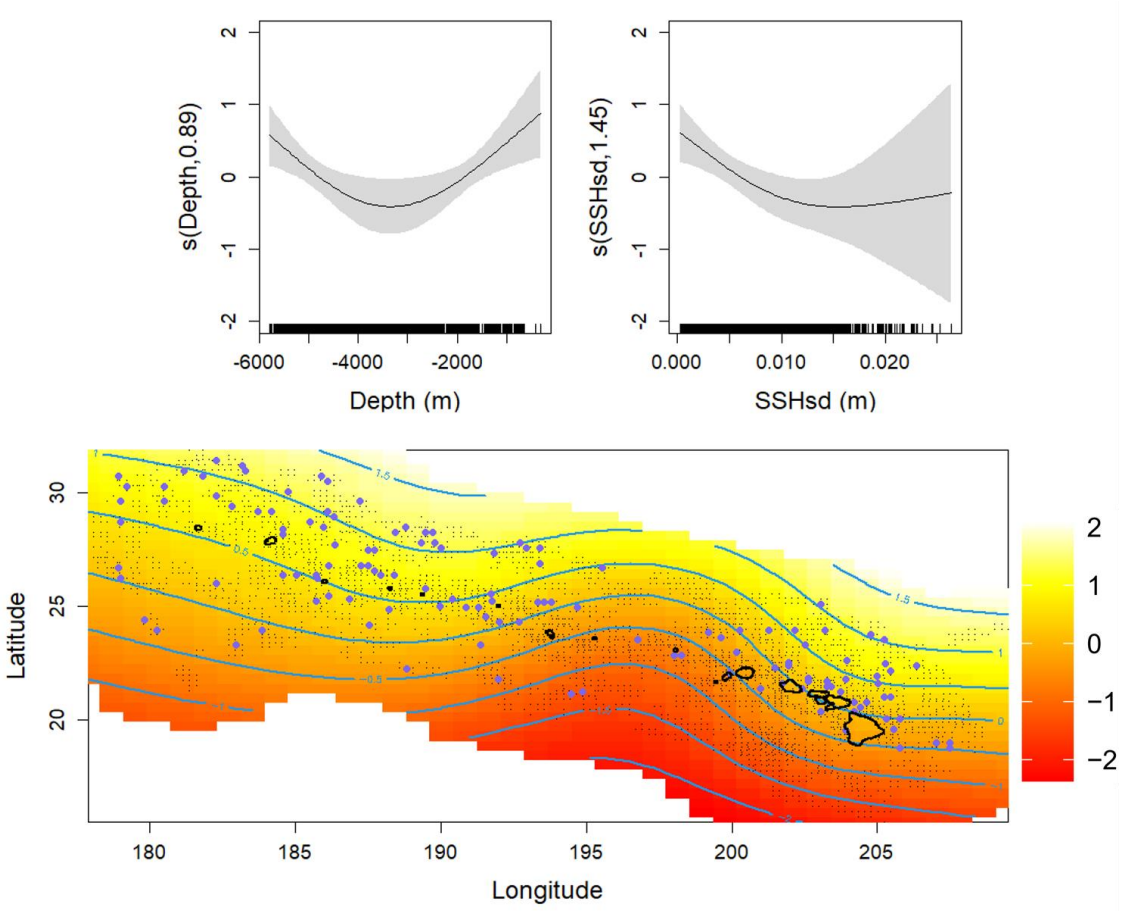

Figure 4.6. Environmental predictors selected for the combined model included depth, the standard deviation of sea surface height (SSHsd), and the 2D spatial term (Longitude, Latitude). Purple dots on the heat map of the spatial term represent all sighted sperm whales and the black dots indicate all data points included in the model. The blue contour lines represent predicted whale groups on the link scale and correspond with the color scale, increasing from red to yellow.

4.3.4 Foraging Models

The best-fit foraging model resulted in similar selected variables and relationships as the combined model except for selecting the natural log of chlorophyll concentration instead of depth (Figure 4.7). The relationship with temperature at 584 m depth showed more sperm whale

encounters occurring at the warmest and coolest temperatures with the less found in the intermediate temperatures between 6.5-7.0°C. Sperm whale encounters declined with increasing chlorophyll concentration. The 2D smoother for the spatial term showed a majority of foraging sperm whale groups to be spatially distributed between Laysan Island and Pearl and Hermes Atoll with another cluster of foraging groups associated with the area north of the Main Hawaiian Islands. The foraging model resulted in an explained deviance of 16% and similar MSE between the training and test data sets.

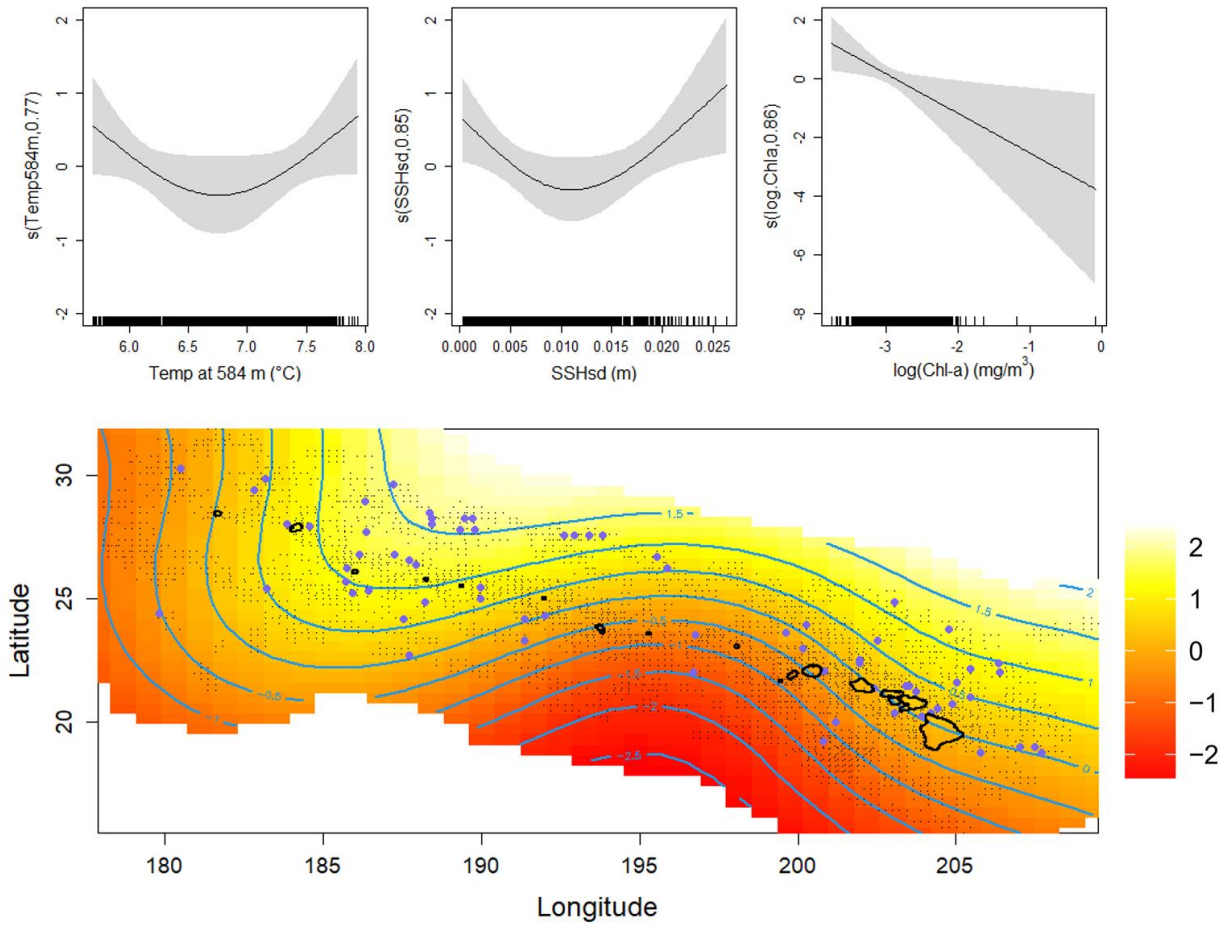

Figure 4.7. Environmental predictors selected for the foraging model included temperature at 584 m, the standard deviation of sea surface height (SSHsd), log of chlorophyll-a concentration (log(Chl-a)), and the 2D spatial term (Longitude, Latitude). Purple dots on the heat map of the spatial term represent all sighted sperm whales and the black dots indicate all data points included in the model. The blue contour lines represent predicted whale groups on the link scale and correspond with the color scale, increasing from red to yellow.

4.3.5 Non-Foraging Models

The best-fit model for non-foraging sperm whales included the spatial term and depth as significant predictors (Figure 4.8). The non-foraging groups were predicted to be at the extreme depth values, a similar relationship as the acoustic-based and combined models. The spatial term, while considered significant, depicted a relatively uniform spatial distribution of the non-foraging groups across the study area. Models yielded 11.69% for the percentage of deviance explained with similar MSE between training and test data sets.

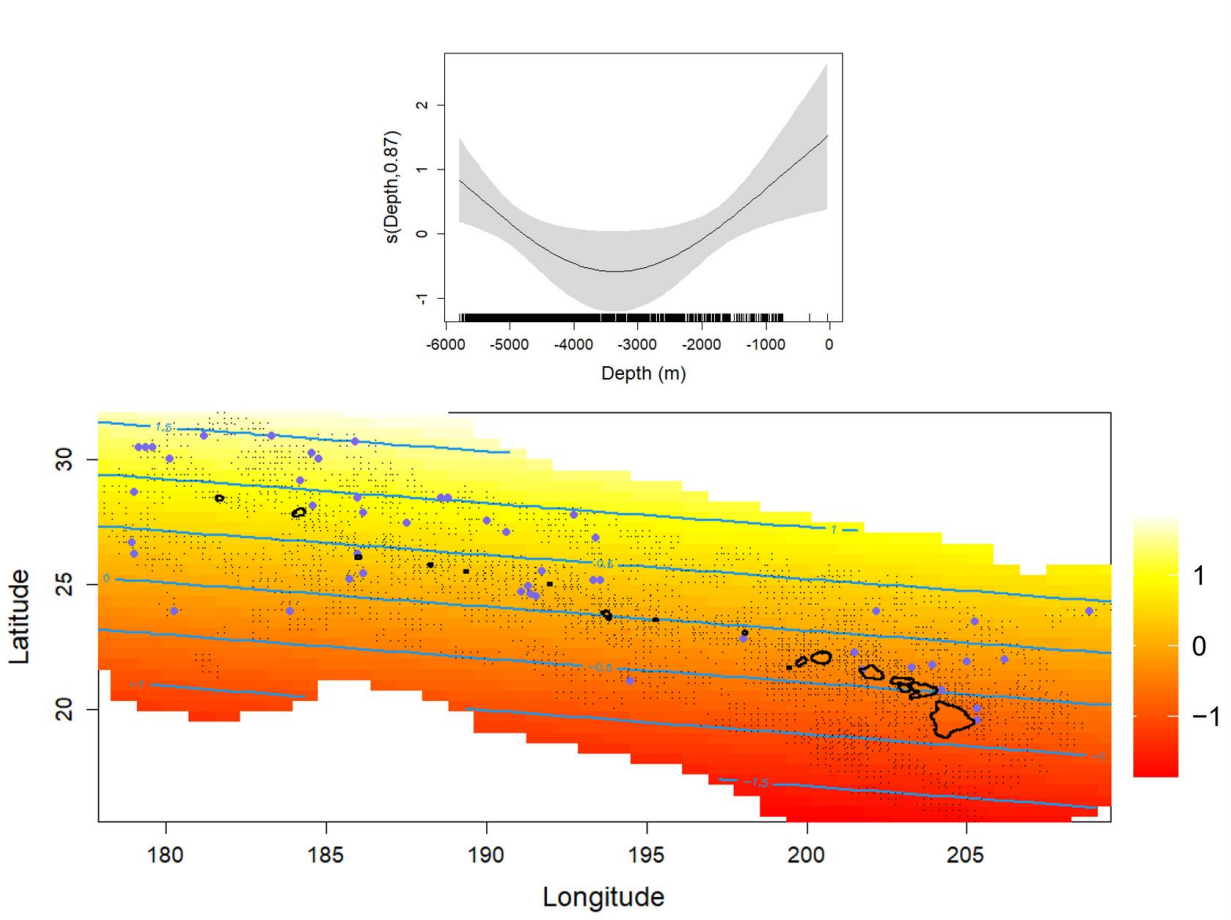

Figure 4.8. Environmental predictors selected for the non-foraging model included depth and the 2D spatial term (Longitude, Latitude). Purple dots on the heat map of the spatial term represent all sighted sperm whales and the black dots indicate all data points included in the model. The blue contour lines represent predicted whale groups on the link scale and correspond with the color scale, increasing from red to yellow.

4.4 Discussion

Our results demonstrate that distribution patterns differed between foraging and non-foraging sperm whales in Hawaiian waters. The foraging whales were associated with the temperature at 584 m, standard deviation of SSH, and chlorophyll concentration. The temperature at 584 m depth was included in the SDMs as an environmental variable to account for subsurface conditions at an average depth representing sperm whale prey habitat (Clarke and Young, 1998; Watanabe *et al.*, 2006). Warmer temperatures occurred to the west of French Frigate Shoals and continued further towards the Northwestern Hawaiian Islands (NWHI). Cooler temperatures at depth occurred towards the east near the Main Hawaiian Islands. This temperature gradient at depth is a persistent characteristic of the North Pacific Subtropical Gyre between depths of ~250-600 m predicted by GODAS (Wang *et al.*, 2000; Saha *et al.*, 2006) that is reflected in the correlations between densities of foraging sperm whales and the upper and lower ranges of temperature at 584 m. While this is an important predictor in the SDM for foraging sperm whales, further data collection and analysis is required to determine if a biological explanation exists for this relationship.

The Hawaii EEZ study area is influenced by the surrounding oceanographic features of the North Pacific Subtropical Gyre. The northern end of the Northwestern Hawaiian Islands (NWHI) is adjacent to broad frontal zones that promote primary production, which attracts higher trophic level organisms (Seki *et al.*, 2002). The northwesterly flow of the North Hawaiian Ridge Current along the north side of the main Hawaiian Islands (MHI) (Qiu *et al.*, 1997) may contribute to localized areas of upwelling with enhanced primary production creating patchy aggregations of squids and other sperm whale prey. Since the model data sets span four years, it is not possible to attribute a specific physical process to the overall distribution of sperm whales. However, examples of foraging sperm whale groups that are spatially and temporally associated with extreme values of temperature at 584 m and the standard deviation of SSH indicate that it is likely that mesoscale physical features are concurrent with the presence of sperm whale groups (Woodworth *et al.*, 2012). Eddies and fronts are examples of mesoscale physical processes that enhance nutrient concentrations in the euphotic zone, which in turn enhance primary production, and presumably benefit sperm whale prey communities. These oceanographic features are typical in the study region and occur throughout the year (Qiu, 1999; Firing and Merrifield, 2004).

Two separate groups of foraging sperm whales observed in the NWHI at the end of July 2017 were associated with lower Temp584 along with a relatively high standard deviation of Temp584 compared to the surrounding area (Figure 4.9). The latter variable was not included in the model, but used in this example to demonstrate how the gradient in subsurface temperatures promote areas of enhanced productivity that may result in larger aggregations of mesopelagic organisms and provide areas of higher concentrations of sperm whale prey (Mann and Lazier, 2006; Robinson *et al.*, 2012; Scales *et al.*, 2014). Further data collection and analyses are required to quantify potential subsurface frontal regions and their relationship with foraging sperm whales.

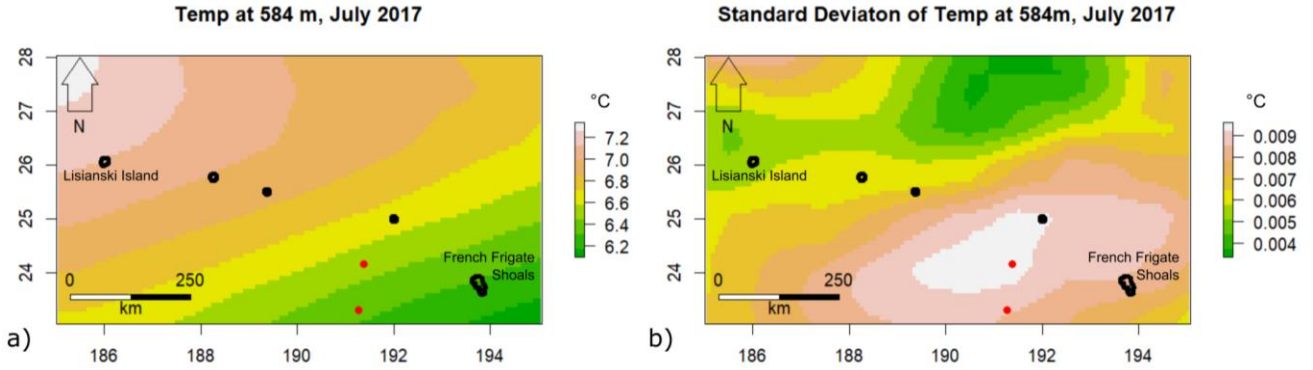

Figure 4.9. Two groups of foraging sperm whales (red dots) observed west of French Frigate Shoals occurred in areas with lower temperatures at 584 m depth that corresponded with relatively high standard deviations.

Foraging sperm whale groups north of Maui and Oahu were observed between September 18-20, 2010 in a region with high SSHsd, which is an indicator of the presence of eddies (Figure 4.10; Polovina and Howell, 2005). The SSH associated with the sperm whale encounters offers evidence that the sperm whales coincided with the edges of anticyclonic (areas of higher SSH) and cyclonic eddies (areas of lower SSH). These mesoscale features uplift isopycnals which results in cold, nutrient-rich waters being transported into the euphotic zone creating patchy areas of increased primary production that may accumulate higher amounts of prey biomass for sperm whales.

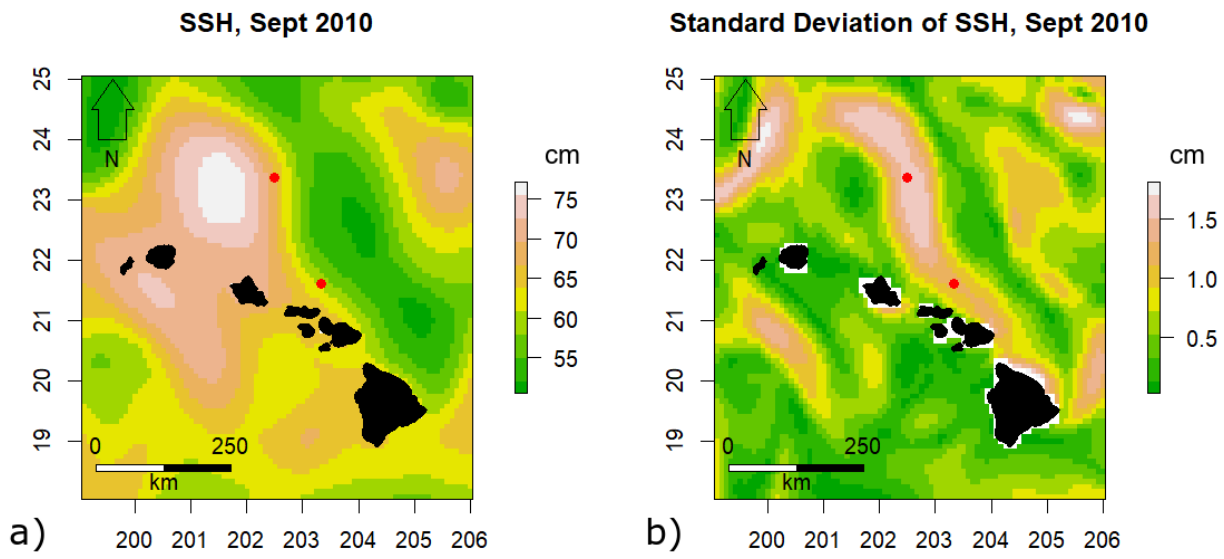

Figure 4.10. Two groups of foraging sperm whales (red dots) observed in September 2010 were associated with a higher standard deviation of SSH north of the Main Hawaiian Islands.

Obtaining an accurate representation of a pelagic, highly mobile, deep-diving species is a challenging objective. For sperm whales, we incorporated different types of observational data to accommodate their surface and diving behavior along with ecologically relevant environmental predictors to best represent their habitat. The distribution of sperm whales for the sighting-based SDM predicted a latitudinal increase in groups, which is a similar pattern to a sperm whale SDM developed by Forney *et al.* (2015) using only sighting data. More complex spatial patterns resulting from the acoustic-based and combined SDMs predicted sperm whales to occur in higher densities in specific areas of the NWHI and MHI, which were similar to more recent cetacean SDMs for the Hawaii EEZ from Becker *et al.* (In press) that also only included sighting data. Overall, the addition of acoustic encounters did not result in substantial differences in SDMs. However, the acoustic behavioral information did allow for the distribution of foraging and non-foraging sperm whales to be examined to get closer to explaining sperm whale distribution patterns in a more direct ecological and biological context that cannot be confirmed using only sighting data.

All models that selected depth as a significant variable resulted in a similar relationship predicting fewer whales at intermediate depths (3000-3500 m). This depth range possibly represents less suitable conditions for prey habitat. Shallower depths may be associated with areas closer to the islands or seamounts with enhanced communities of micronekton that provide

more foraging opportunities for larger cephalopod species that are preyed upon by sperm whales (Clarke and Young, 1998; Benoit-Bird *et al.*, 2008; Choy *et al.*, 2016). Deeper depths may represent areas suitable for larger mesopelagic or bathypelagic squid prey species associated with the deep scattering layer (Hazen and Johnston, 2010).

In general, the spatial term accounted for spatial autocorrelation in the SDMs and explained the variation not accounted for by the environmental predictors. It proved useful for visualizing and comparing the geographic patterns of sperm whale distribution between the different types of encounters. The combined model included all encounters, which contributed more information to the models and increased the complexity of the contours in the spatial term compared to the sighting-based and acoustic-based models. The spatial contours of the acoustic-based model showed a similar pattern in distribution in that fewer whales were predicted south of the island chain. The sighting-based model showed an increasing latitudinal gradient of sperm whale encounters towards the northwest region with less variation in the spatial contours. For comparison, SDMs built with only the spatial term resulted in approximately 0.7-5% less deviance explained than the SDMs presented here. This indicates that the spatial term alone is finding a similar pattern, but the environmental predictors still explain additional variation within the data.

Sighting-based and acoustic-based SDMs differed in the selected environmental variables and in the spatial patterns predicted by the spatial term. Differences in the number of sperm whale encounters included in the SDMs may contribute to differences in the spatial patterns. More acoustic encounters (n = 131) likely provided more geographic information resulting in more complex spatial patterns compared to the sighting-based SDM (n = 78). Both SDMs selected an SSH variable, but the acoustic-based SDM was also best explained by depth while the SDM based on sightings was explained by SST. The reason for this difference between SDMs is unclear but could be attributed to differences in sample size and behavioral states associated with each encounter type. Combining all encounter types into one SDM also selected an SSH variable as a significant environmental predictor. While SSH variables are indicators of eddies and have been associated with higher concentrations of several high trophic level pelagic species (Seki *et al.*, 2002; Polovina *et al.*, 2006; Woodworth *et al.*, 2012), only the results of the acoustic-based SDM were consistent with previous studies predicting more sperm whale groups to occur in more productive areas. We assume that more productive areas are related to higher

prey density, which attracts foraging animals. However, the sighting-based and combined SDMs that associated higher density of sperm whale groups in areas of lower SSHsd and may be capturing a portion of the population exhibiting behaviors unrelated to foraging, such as travel or reproduction.

This analysis is a step towards developing a better understanding of sperm whale distribution in the Hawaiian Archipelago and provides an approach for incorporating behavioral information into SDMs for sperm whales. A better ecological understanding of this population may be gained through dedicated surveys in areas of higher sperm whale density focused on prey sampling and in situ oceanographic measurements that include subsurface measurements more related to their foraging habitat at depth. Deploying archival tags to track dive patterns and record acoustic behavior or satellite telemetry tags to track movement patterns would also provide valuable biological insight and help assess the geographic range of this population. Future line-transect cetacean surveys should continue to collect visual and acoustic data of sperm whales to incorporate all available information in SDMs to improve our understanding of their distribution patterns.

CHAPTER 5 CONCLUSION

In this dissertation, I developed innovative methods for analyzing acoustic data to derive this critical information for two endangered cetacean populations in the Hawaiian Archipelago. Most research conducted on these populations relies on visual observation data to study their distribution and estimate abundance (Baird *et al.*, 2013; Forney *et al.*, 2015; Bradford *et al.*, 2017). Here, I expanded upon this work to further our understanding of these species and pose questions about each population that could only be addressed using passive acoustic data.

In Chapter 2, I investigated the use of whistle characteristics as a method for classifying three sympatric populations of false killer whales to the population level. Classification results from Random Forest models indicated that whistles characteristics were too similar to confidently distinguish between the populations. Overall, it is not surprising that the whistle characteristics were similar given the fact that the populations occupy similar habitat, likely forage for the same prey species, and overlap in their broader distributions (Riesch and Deecke, 2011). However, the mechanisms maintaining the separation between the false killer whale populations remain unexplained. Results from the whistle classification models suggested that unique patterns may exist within in the whistle characteristics of the endangered MHI and NWHI populations. It is possible that the animals use distinct features of their vocalizations as one way to discriminate between individuals of a population, but these features were not captured within the whistle measurements included in the Random Forest classification models. Further analyses are required to examine alternative classification models that include different vocalization metrics and consider the effects of behavioral context on vocalization characteristics for future acoustic classification models of the sympatric false killer whale populations (Henderson *et al.*, 2012; Rankin *et al.*, 2017).

In Chapter 3, I developed a model-based localization method for towed line array acoustic data to estimate the location of deep-diving sperm whales in their three-dimensional habitat. The method improved upon conventional target motion analysis by incorporating sources of error, environmental conditions, and animal depth into localization results (Hastie *et al.*, 2003; Barlow and Taylor, 2005; Wild *et al.*, 2017). Using examples from simulated and real data of diving sperm whales, we tested different localization scenarios to better understand the effects of depth, distance, whale movement, and ship trajectory on location and distance estimates. The

three-dimensional locations of diving sperm whales also included position bounds to provide a range of possible locations and distances of the whale relative to the towed array. While incorporating the distances with error estimates into abundance estimation requires further analytical development, this study provided important information about the factors influencing the localization of deep-diving cetaceans. Acquiring more robust location estimates from acoustic data offers additional information about the species and their habitat and increases the reliability of the data for subsequent analyses. Future work may apply this localization method to other deep-diving species, such as beaked whales and *Kogia* spp., and incorporate surface reflections to refine the depth estimates from the model-based localization approach.

In Chapter 4, I developed SDMs to study the relationship between sperm whales and their physical environment to gain insight about their ecology and distribution. SDMs related the number of sperm whale groups to environmental data using observations collected with visual and PAM methods during four surveys. Since most SDMs only include sighting data, a proportion of the population occurring below the surface are typically excluded from the analysis. We compared SDMs that incorporated the locations of visually and acoustically detected sperm whale groups to evaluate differences in the resulting spatial patterns and environmental variables that best predicted their distributions. Overall, we found that the acoustic data contributed more information to the SDMs resulting in more complex spatial distribution patterns that corresponded with gradients in environmental variables, including temperature at depth and sea surface height.

Since sperm whale echolocation clicks differ depending on behavior, we used the type of echolocation clicks associated with foraging behavior to develop SDMs for foraging and non-foraging groups. The spatial patterns resulting from the behavioral models may indicate more suitable foraging areas, but it is difficult to definitively designate foraging habitat since it is likely influenced by physical oceanographic features that change over time (Hazen and Johnston, 2010; Woodworth *et al.*, 2012). While limitations in the acoustic data did not allow for predicting animal density using SDMs, we gained more ecological insight about the spatial distributions using the behavioral information from the acoustic data. As new developments in PAM data collection and analytical methods become available, future work should continue to include acoustic data in SDMs for cetaceans when possible for a more complete representation of their populations.

Cetacean populations worldwide are adjusting to a rapidly changing environment and increased anthropogenic impacts that come with our growing human population. Passive acoustic monitoring is one tool that has undergone vast technological improvements over the past decade that allow for all known cetacean vocalizations to be recorded. However, the steps required between collecting acoustic data and incorporating acoustic data into population assessments are not trivial. Several features of an acoustic data set often limit its direct applicability to more complex analyses including the inability to estimate the number of animals, the lack of information for location estimates, or the inconsistent vocalization behavior of individual animals (Marques *et al.,* 2013). The work performed in this dissertation contributed analytical methods to advance the use of acoustic data for assessing the endangered populations of false killer whales and sperm whales, which can also be applied to other cetacean species. Using acoustic data in combination with sighting data, satellite telemetry data, genetics, and tag data provides valuable information for more complete population assessments (Sveegaard *et al.*, 2015; Mikkelsen *et al.,* 2016; Silva *et al.,* 2016). It is important to have multiple tools to gather baseline information about cetacean species for management and conservation efforts that appropriately account for their ecological requirements. Since acoustic data provides unique information about cetaceans not necessarily available from other data types, the continued advancement of acoustic data analyses is essential for a comprehensive understanding of these species.

REFERENCES

Abecassis, M., Dewar, H., Hawn, D. and Polovina, J. (2012) 'Modeling swordfish daytime vertical habitat in the North Pacific Ocean from pop-up archival tags', *Marine Ecology Progess Series*, 452, pp. 219–236. doi:10.3354/meps09583.

Abecassis, M., Polovina, J. J., Baird, R. W., Copeland, A., Drazen, J. C., Domokos, R., Oleson, E., Jia, Y., Schorr, G. S., Webster, D. L. and Andrews, R. D. (2015) 'Characterizing a foraging hotspot for short-finned pilot whales and blainville's beaked whales located off the west side of Hawai'i island by using tagging and oceanographic data', *PLoS ONE*, 10(11). doi:10.1371/journal.pone.0142628.

Abrahms, B., Welch, H., Brodie, S., Jacox, M. G., Palacios, D. M., Becker, E. A., Bograd, S. J., Irvine, L. M., Mate, B. R. and Hazen, E. L. (2019) 'Dynamic ensemble models to predict distributions and anthropogenic risk exposure for highly mobile species', *Biodiversity Research*, (25), pp. 1182–1193. doi:10.1111/ddi.12940.

Alexander, R. D. (1962) 'Evolutionary change in cricket acoustical communication', *Society of the Study of Evolution*, 16(4), pp. 443–467.

Aniceto, A. S., Biuw, M., Lindstrøm, U., Solbø, S. A., Broms, F. and Carroll, J. (2018) 'Monitoring marine mammals using unmanned aerial vehicles: Quantifying detection certainty', *Ecosphere*, 9(3). doi:10.1002/ecs2.2122.

Aoki, K., Amano, M., Sugiyama, N., Muramoto, H., Suzuki, M., Yoshioka, M., Mori, K., Tokuda, D. and Miyazaki, N. (2007) 'Measurement of swimming speed in sperm whales', in *International Symposium on Underwater Technology, UT 2007 - International Workshop on Scientific Use of Submarine Cables and Related Technologies 2007*, pp. 467–471.

Au, W. W. L. and Hastings, M. C. (2008) *Principles of marine bioacoustics*. Springer.

Avila, I. C., Kaschner, K. and Dormann, C. F. (2018) 'Current global risks to marine mammals : Taking stock of the threats', *Biological Conservation*. Elsevier, 221(August 2017), pp. 44–58. doi:10.1016/j.biocon.2018.02.021.

Azzellino, A., Panigada, S., Lanfredi, C., Zanardelli, M., Airoldi, S. and Notarbartolo di Sciara, G. (2012) 'Predictive habitat models for managing marine areas: Spatial and temporal distribution of marine mammals within the Pelagos Sanctuary (Northwestern Mediterranean

sea)', *Ocean and Coastal Management*. Elsevier Ltd, 67, pp. 63–74. doi:10.1016/j.ocecoaman.2012.05.024.

Azzolin, M., Gannier, A., Lammers, M. O., Oswald, J. N., Papale, E., Buscaino, G., Buffa, G., Mazzola, S. and Giacoma, C. (2014) 'Combining whistle acoustic parameters to discriminate Mediterranean odontocetes during passive acoustic monitoring.', *The Journal of the Acoustical Society of America*, 135(1), pp. 502–12. doi:10.1121/1.4845275.

Azzolin, M., Papale, E., Lammers, M. O., Gannier, A. and Giacoma, C. (2013) 'Geographic variation of whistles of the striped dolphin (*Stenella coeruleoalba*) within the Mediterranean Sea.', *The Journal of the Acoustical Society of America*, 134(1), pp. 694–705. doi:10.1121/1.4808329.

Bachman, M. J., Keller, J. M., West, K. L. and Jensen, B. A. (2014) 'Persistent organic pollutant concentrations in blubber of 16 species of cetaceans stranded in the Paci fi c Islands from 1997 through 2011', *Science of the Total Environment, The*. Elsevier B.V., 488–489, pp. 115–123. doi:10.1016/j.scitotenv.2014.04.073.

Backus, R. H. and Schevill, W. E. (1966) *Physeter clicks, Whales, dolphins and porpoises*. University of California Press.

Baird, R. W. (2009) 'A review of false killer whales in Hawaiian waters: biology, status, and risk factors', *Report prepared for the U.S. Marine Mammal Commission*, p. 40.

Baird, R. W. (2016) 'The lives of Hawaii's dolphins and whales: natural history and conservation', *University of Hawai'i Press, Honolulu, HI*.

Baird, R. W. and Gorgone, A. M. (2005) 'False killer whale dorsal fin disfigurements as a possible indicator of long-line fishery interactions in Hawaiian waters', *Pacific Science*, 59(4), pp. 593–601. doi:10.1353/psc.2005.0042.

Baird, R. W., Gorgone, A. M., McSweeney, D. J., Webster, D. L., Salden, D. R., Deakos, M. H., Ligon, A. D., Schorr, G. S., Barlow, J. and Mahaffy, S. D. (2008) 'False killer whales (Pseudorca crassidens) around the main Hawaiian Islands: Long-term site fidelity, inter-island movements, and association patterns', *Marine Mammal Science*, 24(3), pp. 591–612. doi:10.1111/j.1748-7692.2008.00200.x.

Baird, R. W., Hanson, M. B., Schorr, G. S., Webster, D. L., McSweeney, D. J., Gorgone, A. M., Mahaffy, S. D., Holzer, D. M., Oleson, E. M. and Andrews, R. D. (2012) 'Range and primary habitats of Hawaiian insular false killer whales: informing determination of critical habitat',

Endangered Species Research, 18(1), pp. 47–61. doi:10.3354/esr00435.

Baird, R. W., Mahaffy, S. D., Gorgone, A. M., Cullins, T., Mcsweeney, D. J., Oleson, E. M., Bradford, A. L., Barlow, J. and Webster, D. L. (2014) 'False killer whales and fisheries interactions in Hawaiian waters: Evidence for sex bias and variation among populations and social groups', *Marine Mammal Science*, 31(2), pp. 579–590. doi:10.1111/mms.12177.

Baird, R. W., Oleson, E. M., Barlow, J., Ligon, A. D., Gorgone, A. M. and Mahaffy, S. D. (2013) 'Evidence of an island-associated population of false killer whales (Pseudorca crassidens) in the Northwestern Hawaiian Islands', *Pacific Science*, 67(4), pp. 513–521. doi:10.2984/67.4.2.

Baird, R. W., Schorr, G. S., Webster, D. L., Mahaffy, S. D., McSweeney, D. J., Hanson, M. B. and Andrews, R. D. (2011) 'Open-ocean movements of a satellite-tagged Blainville's beaked whale (Mesoplodon densirostris): Evidence for an offshore population in Hawai'i?', *Aquatic Mammals*, 37(4), pp. 506–511. doi:10.1578/AM.37.4.2011.506.

Baird, R. W., Schorr, G. S., Webster, D. L., McSweeney, D. J., Hanson, M. B. and Andrews, R. D. (2010) 'Movements and habitat use of satellite-tagged false killer whales around the main Hawaiian Islands', *Endangered Species Research*, 10(1), pp. 107–121. doi:10.3354/esr00258.

Baird, R. W., Webster, D. L., Aschettino, J. M., Schorr, G. S. and McSweeney, D. J. (2013) 'Odontocete cetaceans around the main Hawaiian Islands: Habitat use and relative abundance from small-boat sighting surveys', *Aquatic Mammals*, 39(3), pp. 253–269. doi:10.1578/AM.39.3.2013.253.

Barkley, Y., Oswald, J. N., Carretta, J. V, Rankin, S., Rudd, A. and Lammers, M. O. (2011) 'Comparison of Real-Time and Post- Cruise Acoustic Species Identification of Dolphin Whistles Using ROCCA (Real-Time Odontocete Call Classification Algorithm)', *NOAA Technical Memorandum*, (NMFS-SWFSC-473), p. 29.

Barlow, J. (1999) 'Trackline detection probability for long-diving whales', in *Marine Mammals Survey and Assessement Methods*. Aa Balkema Rotterdam, pp. 209–221.

Barlow, J. (2006) 'Cetacean abundance in Hawaiian waters estimated from a summer/fall survey in 2002', *Marine Mammal Science*, 22(2), pp. 446–464. doi:10.1111/j.1748-7692.2006.00032.x.

Barlow, J. (2015) 'Inferring trackline detection probabilities, g(0), for cetaceans from apparent densities in different survey conditions', *Marine Mammal Science*, 31(3), pp. 923–943.

doi:10.1111/mms.12205.

Barlow, J., Gerrodette, T. and Forcada, J. (2001) ‘Factors affecting perpendicular sighting distances on shipboard line-transect surveys for cetaceans’, *Journal of Cetacean Research and Management*, 3(2), pp. 201–212.

Barlow, J. and Rankin, S. (2007) ‘False killer whale abundance and density: Preliminary estimates for the PICEAS study area south of Hawaii and new estimates for the U.S. EEZ around Hawaii’, *Administrative Report LJ-07-02*.

Barlow, J. and Taylor, B. L. (2005) ‘Estimates of Sperm Whale Abundance in the Northeastern Temperate Pacific From a Combined Acoustic and Visual Survey’, *Marine Mammal Science*, 21(3), pp. 429–445. doi:10.1111/j.1748-7692.2005.tb01242.x.

Baum, J. K. and Worm, B. (2009) ‘Cascading top-down effects of changing oceanic predator abundances’, *Journal of Animal Ecology*, 78(4), pp. 699–714. doi:10.1111/j.1365-2656.2009.01531.x.

Baumann-Pickering, S., McDonald, M. A., Simonis, A. E., Berga, A. S., Merkens, K. P. B., Oleson, E. M., Roch, M. A., Wiggins, S. M., Rankin, S., Yack, T. M. and Hildebrand, J. A. (2013) ‘Species-specific beaked whale echolocation signals’, *The Journal of the Acoustical Society of America*, 134(3), pp. 2293–301. doi:10.1121/1.4817832.

Baumann-Pickering, S., Simonis, A. E., Oleson, E. M., Baird, R. W., Roch, M. A. and Wiggins, S. M. (2015) ‘False killer whale and short-finned pilot whale acoustic identification’, *Endangered Species Research*, 28(2), pp. 97–108. doi:10.3354/esr00685.

Bayless, A. R., Oleson, E. M., Baumann-Pickering, S., Simonis, A. E., Marchetti, J., Martin, S. and Wiggins, S. M. (2017) ‘Acoustically monitoring the Hawai‘i longline fishery for interactions with false killer whales’, *Fisheries Research*. Elsevier B.V., 190, pp. 122–131. doi:10.1016/j.fishres.2017.02.006.

Bazúa-Durán, C. and Au, W. W. L. (2004) ‘Geographic variations in the whistles of spinner dolphins (*Stenella longirostris*) of the Main Hawai‘ian Islands’, *The Journal of the Acoustical Society of America*, 116(6), pp. 3757–3769. doi:10.1121/1.1785672.

Becker, E. A., Forney, K. A., Ferguson, M. C., Foley, D. G., Smith, R. C., Barlow, J. and Redfern, J. V. (2010) ‘Comparing California current cetacean-habitat models developed using in situ and remotely sensed sea surface temperature data’, *Marine Ecology Progress Series*, 413, pp. 163–183. doi:10.3354/meps08696.

Becker, E. A., Forney, K. A., Foley, D. G. and Barlow, J. (2012) 'Density and spatial distribution patterns of cetaceans in the Central North Pacific based on habitat models', *NOAA Technical Memorandum*, (NOAA-TM-NMFS-SWFSC-490).

Becker, E. A., Forney, K. A., Oleson, E. M., Bradford, A. L., Moore, J. E. and Barlow, J. P. (no date) 'Habitat-based density estimates for cetaceans within the waters of the U.S. Exclusive Economic Zone around the Hawaiian Archipelago', *NOAA Technical Memorandum*, NOAA-TM-NM, p. 38.

Becker, E. A., Forney, K. A., Redfern, J. V., Barlow, J., Jacox, M. G., Roberts, J. J. and Palacios, D. M. (2018) 'Predicting cetacean abundance and distribution in a changing climate', *Diversity and Distributions*, 25(4), pp. 626–643. doi:10.1111/ddi.12867.

Benoit-Bird, K. J. and Au, W. W. L. (2003) 'Prey dynamics affect foraging by a pelagic predator (*Stella longirostris*) over a range of spatial and temporal scales', *Behavioral Ecology and Sociobiology*, 53, pp. 364–373. doi:10.1007/s00265-003-0585-4.

Benoit-Bird, K. J., Zirbel, M. J. and McManus, M. A. (2008) 'Diel variation of zooplankton distributions in Hawaiian waters favors horizontal diel migration by midwater micronekton', *Marine Ecology Progress Series*, 367, pp. 109–123. doi:10.3354/meps07571.

'Bioacoustics Research Program. Raven Pro: Interactive Sound Analysis Software (Version 1.5)' (2017). Ithaca, NY: The Cornell Lab of Ornithology.

Bittle, M. and Duncan, A. (2013) 'A review of current marine mammal detection and classification algorithms for use in automated passive acoustic monitoring', in *Proceedings of Acoustics*, p. 8.

Bivand, R. S., Pebesma, E. and Gomez-Rubio, V. (2013) *Applied spatial data analysis with R*. Second. Springer, NY. https://asdar-book.org/.

Bossart, G. D. (2011) 'Marine mammals as sentinel species for oceans and human health', *Veterinary Pathology*, 48(3), pp. 676–690. doi:10.1177/0300985810388525.

Bowen, W. D. (1997) 'Role of marine mammals in aquatic ecosystems', *Marine Ecology Progress Series*, 158(1), pp. 267–274. doi:Doi 10.3354/Meps158267.

Boyer, T. P., Antonov, J. I., Baranova, O. K., Coleman, C., Garcia, H. E., Grodsky, A., Johnson, D. R., Locarnini, R. A., Mishonov, A. V., O'Brien, T. D., Paver, C. R., Reagan, J. R., Seidov, D., Smolyar, I. V. and Zweng, M. M. (2013) 'World Ocean Database 2013, NOAA Atlas NESDIS 72'. Edited by S. Levitus and A. Mishonov. Silver Spring, MD, p. 209.

doi:doi.org/10.7289/V5NZ85MT.

Bradford, A. L., Baird, R. W., Mahaffy, S. D., Gorgone, A. M., Mcsweeney, D. J., Cullins, T., Webster, D. L. and Zerbini, A. N. (2018) 'Abundance estimates for management of endangered false killer whales in the main Hawaiian Islands', *Endangered Species Research*, 36, pp. 297–313. doi:doi.org/10.3354/esr00903 ENDANGERED.

Bradford, A. L. and Forney, K. A. (2014) 'Injury determinations for cetaceans observed interacting with Hawaii and American Samoa longline fisheries during 2007-2011', *NOAA Technical Memorandum*, (NMFS-PIFSC-41), pp. 1–30. doi:10.7289/V5JM27KJ.

Bradford, A. L., Forney, K. A., Oleson, E. M. and Barlow, J. (2012) 'Line-transect Abundance Estimates of False Killer Whales (*Pseudorca crassidens*) in the Pelagic Region of the Hawaiian Exclusive Economic Zone and in the Insular Waters of the Northwestern Hawaiian Islands', *Administrative Report H-12-02*, p. 31.

Bradford, A. L., Forney, K. A., Oleson, E. M. and Barlow, J. (2014) 'Accounting for subgroup structure in line-transect abundance estimates of false killer whales (Pseudorca crassidens) in Hawaiian waters', *PLoS ONE*. Public Library of Science, 9(2), pp. 1–11. doi:10.1371/journal.pone.0090464.

Bradford, A. L., Forney, K. A., Oleson, E. M. and Barlow, J. (2017) 'Abundance estimates of cetaceans from a line-transect survey within the U.S. Hawaiian Islands Exclusive Economic Zone', *Fishery Bulletin*, 115(2), pp. 129–142. doi:10.7755/FB.115.2.1.

Bradford, A. L. and Lyman, E. (2019) *Injury Determinations for Humpback Whales and Other Cetaceans Reported to NOAA Response Networks in the Hawaiian Islands during 2007-2012*, *NOAA Technical Memorandum*. doi:10.7289/V5TX3CB1.

Bradford, A. L., Oleson, E. M., Baird, R. W., Boggs, C. H., Forney, K. A. and Young, N. C. (2015) 'Revised stock boundaries for false killer whales (*Pseudorca crassidens*) in Hawaiian waters', *NOAA Technical Memorandum*, (NMFS-PIFSC-47), p. 28. doi:10.7289/V5DF6P6J.

Breiman, L. (2001) 'Random Forests', *Machine Learning*, 45(1), pp. 5–32. doi:10.1017/CBO9781107415324.004.

Brodie, S., Jacox, M. G., Bograd, S. J., Welch, H., Dewar, H., Scales, K. L., Maxwell, S. M., Briscoe, D. M., Edwards, C. A., Crowder, L. B., Lewison, R. L. and Hazen, E. L. (2018) 'Integrating dynamic subsurface habitat metrics into species distribution models', *Frontiers in Marine Science*, 5, pp. 1–13. doi:10.3389/fmars.2018.00219.

Brough, T. (1969) ‘The dispersal of starlings from woodland roosts and the use of bio-acoustics’, *Journal of Applied Ecology*. JSTOR, 6(3), pp. 403–410.

Brun, P., Kiørboe, T., Licandro, P. and Payne, M. R. (2016) ‘The predictive skill of species distribution models for plankton in a changing climate’, *Global Change Biology*, 22(9), pp. 3170–3181. doi:10.1111/gcb.13274.

Buckland, S. T. (2004) *Advanced distance sampling*. Oxford University Press.

Buckland, S. T., Anderson, D. R., Burnham, K. P., Laake, J. L., Borchers, D. L. and Thomas, L. (2001) *Introduction to distance sampling estimating abundance of biological populations.* New York: Oxford University Press.

Carlén, I., Thomas, L., Carlström, J., Amundin, M., Teilmann, J., Tregenza, N., Tougaard, J., Koblitz, J. C., Sveegaard, S., Wennerberg, D., Loisa, O., Dähne, M., Brundiers, K., Kosecka, M., Kyhn, L. A., Ljungqvist, C. T., Pawliczka, I., Koza, R., Arciszewski, B., Galatius, A., Jabbusch, M., Laaksonlaita, J., Niemi, J., Lyytinen, S., Gallus, A., Benke, H., Blankett, P., Skóra, K. E. and Acevedo-Gutiérrez, A. (2018) ‘Basin-scale distribution of harbour porpoises in the Baltic Sea provides basis for effective conservation actions’, *Biological Conservation*, 226, pp. 42–53. doi:10.1016/j.biocon.2018.06.031.

Carretta, J. V, Forney, K. A., Oleson, E. M., Weller, D. W., Lang, A. R., Baker, J., Muto, M. M., Hanson, B., Orr, A. J., Huber, H., Lowry, M. S., Barlow, J., Moore, J. E., Lynch, D., Carswell, L. and Brownell Jr., R. L. (2020) ‘U.S. Pacific marine mammal stock assessments: 2019.’, *NOAA Technical Memorandum*, (NMFS-SWFSC-629). doi:10.7289/V5/TM-SWFSC-577.

Catchpole, C. K. and Slater, P. J. B. (2008) *Bird Song - Biological themes and variations*. Second, *Cambridge University Press*. Second. http://www.publish.csiro.au/?paper=MU952208b.

Chapman, D. M. F. (2004) ‘You can’t get there from here: Shallow water sound propagation and whale localization’, *Canadian Acoustics*, 32(2), pp. 167–171.

Charif, R. A. and Clark, C. W. (2009) ‘Acoustic monitoring of large whales in deep waters north and west of the British Isles: 1996-2005’, *Cornell Lab of Ornithology*, 08(07), p. 40. doi:10.1578/AM.35.3.2009.313.

Chivers, S. J., Baird, R. W., Martien, K. M., Taylor, B., Archer, L. E., Gorgone, A. M., Hancock, B. L., Hedrick, N. M., Mattila, D. K., McSweeney, D. J., Oleson, E. M., Palmer, C. L., Pease, V., Robertson, K. M., Robbins, J., Salinas, J. C., Schorr, G. S., Schultz, M., Theileking, J. L.

and Webster, D. L. (2010) ‘Evidence of genetic differentiation for Hawaii insular false killer whales (*Pseudorca crassidens*)’, *NOAA Technical Memorandum*, (NMFS-SWFSC-458), p. 44. doi:10.7289/V5/TM-SWFSC-549.

Choy, C. A., Wabnitz, C. C. C. C., Weijerman, M., Woodworth-Jefcoats, P. A. and Polovina, J. J. (2016) ‘Finding the way to the top: How the composition of oceanic mid-trophic micronekton groups determines apex predator biomass in the central North Pacific’, *Marine Ecology Progress Series*, 549, pp. 9–25. doi:10.3354/meps11680.

Citta, J. J., Richard, P., Lowry, L. F., O’Corry-Crowe, G., Marcoux, M., Suydam, R., Quakenbush, L. T., Hobbs, R. C., Litovka, D. I., Frost, K. J., Gray, T., Orr, J., Tinker, B., Aderman, H. and Druckenmiller, M. L. (2017) ‘Satellite telemetry reveals population specific winter ranges of beluga whales in the Bering Sea’, *Marine Mammal Science*, 33(1), pp. 236–250. doi:10.1111/mms.12357.

Clarke, M. R. (1996) ‘Cephalopods as Prey. III. Cetaceans’, *Philosophical Transactions of the Royal Society of London B: Biological Sciences*. The Royal Society, 351(1343), pp. 1053–1065. doi:10.1098/rstb.1996.0093.

Clarke, M. R., Martins, H. R. and Pascoe, P. (1993) ‘The Diet of Sperm Whales (Physeter macrocephalus Linnaeus 1758) off the Azores’, *Philosophical Transactions: Biological Sciences*, 339(1287), pp. 67–82.

Clarke, M. and Young, R. (1998) ‘Description and Analysis of Cephalopod Beaks from Stomachs of Six Species of Odontocete Cetaceans Stranded on Hawaiian Shores’, *Journal of the Marine Biological Association of the United Kingdom*. University of Hawaii at Manoa Library, 78(02), pp. 623–641. doi:10.1017/S0025315400041667.

Clarke, R. and Paliza, A. (2001) ‘The food of sperm whales in the Southeast Pacific’, *Marine Mammal Science*, 17(2), pp. 427–429. doi:10.1111/j.1748-7692.2001.tb01287.x.

Cohen, J. (1960) ‘A coefficient of agreement for nominal scales’, *Educational and Psychological Measurement*, (1), pp. 37–46.

Cutler, A., Cutler, D. R. and Stevens, J. R. (2012) ‘Ensemble Machine Learning’, *Random Forests*, (January), pp. 225–250. doi:10.1007/978-1-4419-9326-7.

Cutler, D. R., Edwards, Jr., T. C., Beard, K. H., Cutler, A., Hess, K. T., Gibson, J. and Lawler, J. J. (2007) ‘Random Forests for Classification in Ecology’, *Ecological Society of America*, 88(11), pp. 2783–2792.

Davis, G. E., Baumgartner, M. F., Bonnell, J. M., Bell, J., Berchok, C., Bort Thornton, J., Brault, S., Buchanan, G., Charif, R. A., Cholewiak, D., Clark, C. W., Corkeron, P., Delarue, J., Dudzinski, K., Hatch, L., Hildebrand, J., Hodge, L., Klinck, H., Kraus, S., Martin, B., Mellinger, D. K., Moors-Murphy, H., Nieukirk, S., Nowacek, D. P., Parks, S., Read, A. J., Rice, A. N., Risch, D., Širović, A., Soldevilla, M., Stafford, K., Stanistreet, J. E., Summers, E., Todd, S., Warde, A. and Van Parijs, S. M. (2017) 'Long-term passive acoustic recordings track the changing distribution of North Atlantic right whales (*Eubalaena glacialis*) from 2004 to 2014', *Scientific Reports*, 7(1), pp. 1–12. doi:10.1038/s41598-017-13359-3.

DeAngelis, A. I., Valtierra, R., Van Parijs, S. M., Cholewiak, D., Parijs, S. M. Van, Cholewiak, D., Van Parijs, S. M. and Cholewiak, D. (2017) 'Using multipath reflections to obtain dive depths of beaked whales from a towed hydrophone array', *Journal of Acoustical Society of America*, 142(2), pp. 1078–1087. doi:10.1121/1.4998709.

Deecke, V. B., Barrett-Lennard, L. G., Spong, P. and Ford, J. K. B. (2010) 'The structure of stereotyped calls reflects kinship and social affiliation in resident killer whales (*Orcinus orca*)', *Naturwissenschaften*, 97(5), pp. 513–518. doi:10.1007/s00114-010-0657-z.

Delarue, J., Todd, S. K., Van Parijs, S. M. and Di Iorio, L. (2009) 'Geographic variation in Northwest Atlantic fin whale (*Balaenoptera physalus*) song: Implications for stock structure assessment', *The Journal of the Acoustical Society of America*, 125(3), pp. 1774–1782. doi:10.1121/1.3068454.

DeSalle, R. and Amato, G. (2004) 'The expansion of conservation genetics', *Nature Reviews Genetics*, 5(9), pp. 702–712. doi:10.1038/nrg1425.

Diogou, N., Palacios, D. M., Nystuen, J. A., Papathanassiou, E., Katsanevakis, S. and Klinck, H. (2019) 'Sperm whale (*Physeter macrocephalus*) acoustic ecology at Ocean Station PAPA in the Gulf of Alaska – Part 2: Oceanographic drivers of interannual variability', *Deep-Sea Research Part I: Oceanographic Research Papers*. Elsevier Ltd, 150(May), p. 103044. doi:10.1016/j.dsr.2019.05.004.

Doty, M. S. and Oguri, M. (1956) 'The Island Mass Effect', *ICES Journal of Marine Science*, 22(1), pp. 33–37. doi:10.1093/icesjms/22.1.33.

Durban, J. W., Elston, D. A., Ellifrit, D. K., Dickson, E., Hammond, P. S. and Thompson, P. M. (2005) 'Multisite Mark-Recapture for Cetaceans: Population Estimates With Bayesian Model Averaging', *Marine Mammal Science*, 21(1), pp. 80–92. doi:10.1111/j.1748-

7692.2005.tb01209.x.

Edds-Walton, P. L. (2012) ‘Acoustic communication signals of mysticete whales’, *Bioacoustics*, 8(1–2), pp. 47–60. doi:10.1080/09524622.1997.9753353.

Efron, B. and Tibshirani, R. (1997) ‘Improvements on Cross-Validation: The .632+ Bootstrap Method’, *Journal of the American Statistical Association*, 92(438), pp. 548–560.

Elith, J. and Leathwick, J. R. (2009) ‘Species Distribution Models: Ecological explanation and prediction across space and time’, *Annual Review of Ecology, Evolution, and Systematics*, 40, pp. 677–697. doi:10.1146/annurev.ecolsys.l.

Estes, J. A., Heithaus, M., McCauley, D. J., Rasher, D. B. and Worm, B. (2016) ‘Megafaunalimpacts on structure and function of ocean ecosystems’, in *Annual Review of Environment and Resources*, pp. 83–116.

Estes, J. A., Terborgh, J., Brashares, J. S., Power, M. E., Berger, J., Bond, W. J., Carpenter, S. R., Essington, T. E., Holt, R. D., Jackson, J. B. C., Marquis, R. J., Oskanen, L., Oskanen, T., Paine, R. T., Pikitch, E. K., Ripple, W. J., Sandin, S. A., Scheffer, M., Schoener, T. W., Shurin, J. B., Sinclair, A. R. E., Soule, M. E., Virtanen, R. and Wardle, D. A. (2011) ‘Trophic downgrading of planet Earth.’, *Science*, 333(6040), pp. 301–306. doi:10.1126/science.1205106.

Estes, J. A., Tinker, M. T., Williams, T. M. and Doak, D. F. (1998) ‘Killer whale predation on sea otters linking oceanic and nearshore ecosystems’, *Science*, 282(1998), pp. 473–476. doi:10.1126/science.282.5388.473.

Evans, K. and Hindell, M. A. (2004) ‘The diet of sperm whales (*Physeter macrocephalus*) in southern Australian waters’, *ICES Journal of Marine Science*, 61(8), pp. 1313–1329. doi:10.1016/j.icesjms.2004.07.026.

Evans, P. G. H. and Hammond, P. S. (2004) ‘Monitoring cetaceans in European waters’, *Mammal Review*, 34(1–2), pp. 131–156. doi:10.1046/j.0305-1838.2003.00027.x.

Feitosa, L. M., Martins, L. P., de Souza Junior, L. A. and Lessa, R. P. (2020) ‘Potential distribution and population trends of the smalltail shark Carcharhinus porosus inferred from species distribution models and historical catch data’, *Aquatic Conservation: Marine and Freshwater Ecosystems*, 30(5), pp. 882–891. doi:10.1002/aqc.3293.

Ferguson, M. C., Barlow, J., Reilly, S. B. and Gerrodette, T. (2006) ‘Predicting Cuvier’s (*Ziphius cavirostris*) and Mesoplodon beaked whale population density from habitat characteristics in

the eastern tropical Pacific Ocean', *Journal of Cetacean Research and Management*, 7(3), pp. 287–299.

Fiedler, P. C., Redfern, J. V., Forney, K. A., Palacios, D. M., Sheredy, C., Rasmussen, K., García-Godos, I., Santillán, L., Tetley, M. J., Félix, F. and Ballance, L. T. (2018) 'Prediction of large whale distributions: A comparison of presence-absence and presence-only modeling techniques', *Frontiers in Marine Science*, 5, pp. 1–15. doi:10.3389/fmars.2018.00419.

Fiori, C., Giancardo, L., Aïssi, M., Alessi, J. and Vassallo, P. (2014) 'Geostatistical modelling of spatial distribution of sperm whales in the Pelagos Sanctuary based on sparse count data and heterogeneous observations', *Aquatic Conservation: Marine and Freshwater Ecosystems*, 24(Suppl. 1), pp. 41–49. doi:10.1002/aqc.2428.

Firing, Y. L. and Merrifield, M. A. (2004) 'Extreme sea level events at Hawaii : Influence of mesoscale eddies', *Geophysical Research Letters*, 31, pp. 1–4. doi:10.1029/2004GL021539.

Fleming, A. H., Yack, T., Redfern, J. V., Becker, E. A., Moore, T. J. and Barlow, J. (2018) 'Combining acoustic and visual detections in habitat models of Dall's porpoise', *Ecological Modelling*, 384, pp. 198–208. doi:10.1016/j.ecolmodel.2018.06.014.

Ford, J. K. B. (1991) 'Vocal traditions among resident killer whales (*Orcinus orca*) in coastal waters of British Columbia', *Canadian Journal of Zoology*, 69(6), pp. 1454–1483. doi:10.1139/z91-206.

Forney, K. A. (2000) 'Environmental models of cetacean abundance: Reducing uncertainty in population trends', *Conservation Biology*, 14(5), pp. 1271–1286.

Forney, K. A., Becker, E. A., Foley, D. G., Barlow, J. and Oleson, E. M. (2015) 'Habitat-based models of cetacean density and distribution in the central North Pacific', *Endangered Species Research*, 27(1), pp. 1–20. doi:10.3354/esr00632.

Forney, K. A., Kobayashi, D. R., Johnston, D. W., Marchetti, J. A. and Marsik, M. G. (2011) 'What's the catch? Patterns of cetacean bycatch and depredation in Hawaii-based pelagic longline fisheries', *Marine Ecology*, 32(3), pp. 380–391. doi:10.1111/j.1439-0485.2011.00454.x.

Foskolos, I., Koutouzi, N., Polychronidis, L., Alexiadou, P. and Frantzis, A. (2020) 'A taste for squid: the diet of sperm whales stranded in Greece, Eastern Mediterranean', *Deep-Sea Research Part I: Oceanographic Research Papers*. Elsevier Ltd, 155, p. 103164. doi:10.1016/j.dsr.2019.103164.

Fox, C., Huettmann, F., Harvey, G., Morgan, K., Robinson, J., Williams, R. and Paquet, P. (2017) 'Predictions from machine learning ensembles: marine bird distribution and density on Canada's Pacific coast', *Marine Ecology Progress Series*, 566, pp. 199–216. doi:10.3354/meps12030.

Franklin, E. C., Jokiel, P. L. and Donahue, M. J. (2013) 'Predictive modeling of coral distribution and abundance in the Hawaiian Islands', *Marine Ecology Progress Series*, 481, pp. 121–132. doi:10.3354/meps10252.

Gannier, A., Fuchs, S., Quèbre, P., Oswald, J. N., Quebre, P. and Oswald, J. N. (2010) 'Performance of a contour-based classification method for whistles of Mediterranean delphinids', *Applied Acoustics*, 71(11), pp. 1063–1069. doi:10.1016/j.apacoust.2010.05.019.

Gannier, A. and Praca, E. (2006) 'SST fronts and the summer sperm whale distribution in the north-west Mediterranean Sea', *Journal of the Marine Biological Association of the United Kingdom*, 87(1), pp. 187–193. doi:10.1017/s0025315407054689.

Gannon, D. P. (2008) 'Passive Acoustic Techniques in Fisheries Science: A Review and Prospectus', *Transactions of the American Fisheries Society*, 137(2), pp. 638–656. doi:10.1577/T04-142.1.

García, S., Fernández, A., Luengo, J. and Herrera, F. (2009) 'A study of statistical techniques and performance measures for genetics-based machine learning: Accuracy and interpretability', *Soft Computing*, 13(10), pp. 959–977. doi:10.1007/s00500-008-0392-y.

Garzón, M. B., Blazek, R., Neteler, M., Dios, R. S. de, Ollero, H. S. and Furlanello, C. (2006) 'Predicting habitat suitability with machine learning models: The potential area of *Pinus sylvestris* L. in the Iberian Peninsula', *Ecological Modelling*, 197(3–4), pp. 383–393. doi:10.1016/j.ecolmodel.2006.03.015.

Gebbie, J., Siderius, M. and Allen, J. S. (2015) 'A two-hydrophone range and bearing localization algorithm with performance analysis', *The Journal of the Acoustical Society of America*, 137(3), pp. 1586–97. doi:10.1121/1.4906835.

Gerhardt, H. C. (1994) 'The evolution of vocalization in frogs and toads', *Annual Review of Ecology and Systematics*, 25(1), pp. 293–324. doi:10.1146/annurev.es.25.110194.001453.

Gero, S. and Whitehead, H. (2016) 'Critical decline of the eastern Caribbean sperm whale population', *PLoS ONE*, 11(10), pp. 1–11. doi:10.1371/journal.pone.0162019.

Gero, S., Whitehead, H. and Rendell, L. (2016) 'Individual , unit and vocal clan level identity

cues in sperm whale codas', *Royal Society Open Science*, 3, pp. 1–12. doi:10.1098/rsos.150372.

Gibb, R., Browning, E., Glover-Kapfer, P. and Jones, K. E. (2019) 'Emerging opportunities and challenges for passive acoustics in ecological assessment and monitoring', *Methods in Ecology and Evolution*, 10(2), pp. 169–185. doi:10.1111/2041-210X.13101.

Gillespie, D. and Leaper, R. (1997) 'An acoustic survey for sperm whales in the Southern Ocean Sanctuary conducted from the RSV Aurora Australis', *Reports of the International Whaling Commission*, 47, pp. 897–907.

Gillespie, D., Mellinger, D. K., Gordon, J., McLaren, D., Redmond, P., McHugh, R., Trinder, P. W., Deng, X. Y. and Thode, A. (2008) 'PAMGUARD: Semiautomated, open source software for real-time acoustic detection and localisation of cetaceans', *The Journal of the Acoustical Society of America*, 30(5), pp. 54–62.

Gilman, E., Brothers, N. and McPherson, G. (2006) 'A review of cetacean interactions with longline gear', *Journal of Cetacean Res. Management*, 8(2), pp. 215–223.

Gonzalez, R. C., Woods, R. E. and Eddins, S. L. (2009) 'Digital image processing using Matlab'. Gatesmark Publishing.

Gove, J. M., McManus, M. A., Neuheimer, A. B., Polovina, J. J., Drazen, J. C., Smith, C. R., Merrifield, M. A., Friedlander, A. M., Ehses, J. S., Young, C., Dillon, A. K. and Williams, G. J. (2015) 'Near-island biological hotspots in barren ocean basins', *Nature Communications*. Nature Publishing Group, 7, pp. 1–34. doi:10.1038/ncomms10581.

Gregorutti, B., Michel, B. and Saint-Pierre, P. (2017) 'Correlation and variable importance in random forests', *Statistics and Computing*, 27(3), pp. 659–678. doi:10.1007/s11222-016-9646-1.

Guisan, A., Edwards, T. C. and Hastie, T. (2002) 'Generalized linear and generalized additive models in studies of species distributions : Setting the scene', *Ecological Modelling*, 157, pp. 89–100. doi:10.1016/S0304-3800(02)00204-1.

Harris, D. V., Miksis-Olds, J. L., Vernon, J. A. and Thomas, L. (2018) 'Fin whale density and distribution estimation using acoustic bearings derived from sparse arrays', *The Journal of the Acoustical Society of America*, 143(5), pp. 2980–2993. doi:10.1121/1.5031111.

Harris, P. T., Macmillan-Lawler, M., Rupp, J. and Baker, E. K. (2014) 'Geomorphology of the oceans', *Marine Geology*. Elsevier B.V., 352, pp. 4–24. doi:10.1016/j.margeo.2014.01.011.

Hastie, G. D., Swift, R. J., Gordon, J., Slesser, G. and Turrell, W. R. (2003) 'Sperm whale distribution and seasonal density in the Faroe Shetland Channel', *Journal of Cetacean Research and Management*, 5(3), pp. 247–252.

Hazen, E. L., Abrahms, B., Brodie, S., Carroll, G., Jacox, M. G., Savoca, M. S., Scales, K. L., Sydeman, W. J. and Bograd, S. J. (2019) 'Marine top predators as climate and ecosystem sentinels', *Frontiers in Ecology and the Environment*, pp. 565–574. doi:10.1002/fee.2125.

Hazen, E. L. and Johnston, D. W. (2010) 'Meridional patterns in the deep scattering layers and top predator distribution in the central equatorial Pacific', *Fisheries Oceanography*, 19(6), pp. 427–433. doi:10.1111/j.1365-2419.2010.00561.x.

Heithaus, M. R., Frid, A., Wirsing, A. J. and Worm, B. (2008) 'Predicting ecological consequences of marine top predator declines', *Trends in Ecology & Evolution*, 23(4), pp. 202–210. doi:10.1016/j.tree.2008.01.003.

Henderson, E. E., Hildebrand, J. A., Smith, M. H. and Falcone, E. A. (2012) 'The behavioral context of common dolphin (*Delphinus* sp.) vocalizations', *Marine Mammal Science*, 28(3), pp. 439–460. doi:10.1111/j.1748-7692.2011.00498.x.

Hildebrand, J. A. (2005) 'Impacts of Anthropogenic Sound', in Reynolds III, J. E., Perrin, W. F., Reeves, R. R., Montgomery, S., and Ragen, T. J. (eds) *Marine Mammal Research: Conservation beyond Crisis*. Baltimore, Maryland: The Johns Hopkins University Press, pp. 101–124.

Hildebrand, J. A., Frasier, K. E., Baumann-Pickering, S., Wiggins, S. M., Merkens, K. P., Garrison, L. P., Soldevilla, M. S. and McDonald, M. A. (2019) 'Assessing seasonality and density from passive acoustic monitoring of signals presumed to be from pygmy and dwarf sperm whales in the Gulf of Mexico', *Frontiers in Marine Science*, 6, pp. 1–17. doi:10.3389/fmars.2019.00066.

Hodge, L. E. W., Baumann-Pickering, S., Hildebrand, J. A., Bell, J. T., Cummings, E. W., Foley, H. J., McAlarney, R. J., McLellan, W. A., Pabst, D. A., Swaim, Z. T., Waples, D. M. and Read, A. J. (2018) 'Heard but not seen: Occurrence of *Kogia* spp. along the western North Atlantic shelf break', *Marine Mammal Science*, 34(4), pp. 1141–1153. doi:10.1111/mms.12498.

Hoelzel, A. R. (1992) 'Conservation genetics of whales and dolphins', *Molecular Ecology*, 1(2), pp. 119–125. doi:10.1111/j.1365-294X.1992.tb00163.x.

Huettmann, F. and Diamond, A. W. (2001) 'Seabird colony locations and environmental

determination of seabird distribution: A spatially explicit breeding seabird model for the northwest atlantic', *Ecological Modelling*, 141(1–3), pp. 261–298. doi:10.1016/S0304-3800(01)00278-2.

Huetz, C. and Aubin, T. (2012) 'Bioacoustics approaches to locate and identify animals in terrestrial environments', in *Sensors for ecology*, pp. 83–96. http://www.cb.u-psud.fr/pdf/Sensors_Aubin.pdf.

Irvine, L., Palacios, D. M., Urbán, J. and Mate, B. (2017) 'Sperm whale dive behavior characteristics derived from intermediate-duration archival tag data', *Ecology and Evolution*, 7(19), pp. 7822–7837. doi:10.1002/ece3.3322.

Janik, V. M. and Sayigh, L. S. (2013) 'Communication in bottlenose dolphins: 50 years of signature whistle research', *Journal of Comparative Physiology A: Neuroethology, Sensory, Neural, and Behavioral Physiology*, 199(6), pp. 479–489. doi:10.1007/s00359-013-0817-7.

Janik, V. M. and Slater, P. J. B. (1998) 'Context-specific use suggests that bottlenose dolphin signature whistles are cohesion calls', *Animal Behaviour*, 56(4), pp. 829–838. doi:10.1006/anbe.1998.0881.

Jaquet, N. (1996) 'How spatial and temporal scales influence understanding of Sperm Whale distribution: A review', *Mammal Review*, 26(1), pp. 51–65. doi:10.1111/j.1365-2907.1996.tb00146.x.

Jaquet, N., Dawson, S. and Douglas, L. (2001) 'Vocal behavior of male sperm whales: Why do they click?', *Journal of the Acoustical Society of America*, 109(5 Part 1), pp. 2254–2259. doi:10.1121/1.1360718.

Jaquet, N. and Gendron, D. (2002) 'Distribution and relative abundance of sperm whales in relation to key environmental features, squid landings and the distribution of other cetacean species in the Gulf of California, Mexico', *Marine Biology*, 141(3), pp. 591–601. doi:10.1007/s00227-002-0839-0.

Jaquet, N. and Whitehead, H. (1996) 'Scale-dependent correlation of sperm whale distribution with environmental features and productivity in the South Pacific', *Marine Ecology Progress Series*, 135(1–3), pp. 1–9. doi:10.3354/meps135001.

Jaquet, N. and Whitehead, H. (1999) 'Movements, distribution and feeding success of sperm whales in the Pacific Ocean, over scales of days and tens of kilometers', *Aquatic Mammals*, 25(1), pp. 1–13.

Kaschner, K. (2007) ‘Air-breathing visitors to seamounts. Section A: Marine mammals’, *Seamounts: Ecology, Fisheries and Conservation*, (June).

Kaschner, K., Tittensor, D. P., Ready, J., Gerrodette, T. and Worm, B. (2011) ‘Current and future patterns of global marine mammal biodiversity’, *PLoS ONE*, 6(5). doi:10.1371/journal.pone.0019653.

Katona, S. and Whitehead, H. (1988) ‘Are Cetacea ecologically important?’, *Oceanography and Marine Biology Annual Review*, 26, pp. 553–568.

Keen, S., Ross, J. C., Griffiths, E. T., Lanzone, M. and Farnsworth, A. (2014) ‘A comparison of similarity-based approaches in the classification of flight calls of four species of North American wood-warblers (*Parulidae*)’, *Ecological Informatics*, 21, pp. 25–33. doi:10.1016/j.ecoinf.2014.01.001.

Kinzey, D., Gerrodette, T., Barlow, J., Dizon, A., Perryman, W. and Olson, P. (2000) ‘Marine Mammal Data Collected during a Survey in the Eastern Tropical Pacific Ocean Aboard the NOAA Ships McArthur and David Starr Jordan, July 28-December 9, 1999’, *NOAA Technical Memorandum*, (NMFS-SWFSC-293), p. 89.

Kiszka, J. J., Heithaus, M. R. and Wirsing, A. J. (2015) ‘Behavioural drivers of the ecological roles and importance of marine mammals’, *Marine Ecology Progress Series*, 523, pp. 267–281. doi:10.3354/meps11180.

Knapp, C. and Carter, G. (1976) ‘The generalized correlation method for estimation of time delay’, *IEEE transactions on acoustics, speech, and signal processing*. IEEE, 24(4), pp. 320–327.

Landis, R. J. and Koch, G. G. (1977) ‘The Measurement of Observer Agreement for Categorical Data’, *Biometrics*, 33(1), pp. 159–174.

Leaper, R., Chappell, J. and Gordon, J. (1992) *The development of practical techniques for surveying sperm whale populations acoustically*. University of Oxford, Department of Zoology, Wildlife Conservation Research Unit.

Leaper, R., Gillespie, D. and Papastavrou, V. (2000) ‘Results of passive acoustic surveys for odontocetes in the Southern Ocean’, *Journal of Cetacean Research and Management*. INTERNATIONAL WHALING COMMISSION, 2(3), pp. 187–196.

Lewis, T., Gillespie, D., Lacey, C., Matthews, J., Danbolt, M., Leaper, R., McLanaghan, R. and Moscrop, A. (2007) ‘Sperm whale abundance estimates from acoustic surveys of the Ionian

Sea and Straits of Sicily in 2003', *Journal of the Marine Biological Association of the UK*, 87(01), p. 353. doi:10.1017/S0025315407054896.

Li, J., Tran, M. and Siwabessy, J. (2016) 'Selecting optimal random forest predictive models: A case study on predicting the spatial distribution of seabed hardness', *PLoS ONE*, 11(2), p. 29. doi:10.1371/journal.pone.0149089.

Liaw, A. and Wiener, M. (2002) 'Classification and Regression by randomForest', *R News*, 2(3), pp. 18–22.

Lieberman, P. (1968) 'On the acoustic analysis of primate vocalizations', *Behavior Research Methods & Instrumentation*. Springer, 1(5), pp. 169–174.

Loftus-Hills, J. J. and Littlejohn, M. J. (1971) 'Mating call sound intensities of anuran amphibians', *The Journal of the Acoustical Society of America*. Acoustical Society of America, 49(4B), pp. 1327–1329.

Madsen, P. T., Wahlberg, M. and Møhl, B. (2002) 'Male sperm whale (*Physeter macrocephalus*) acoustics in a high-latitude habitat: Implications for echolocation and communication', *Behavioral Ecology and Sociobiology*, 53(1), pp. 31–41.

Magera, A. M., Mills Flemming, J. E., Kaschner, K., Christensen, L. B. and Lotze, H. K. (2013) 'Recovery trends in marine mammal populations', *PLoS ONE*, 8(10), p. e77908. doi:10.1371/journal.pone.0077908.

Mann, K. H. and Lazier, J. R. N. (2006) *Dynamics of Marine Ecosystems: Biological-Physical Interactions in the Oceans*. Third, *Blackwell Publishing*. Third. Blackwell Publishing Ltd.

Marcoux, M., Whitehead, H. and Rendell, L. (2006) 'Coda vocalizations recorded in breeding areas are almost entirely produced by mature female sperm whales (Physeter macrocephalus)', *Canadian Journal of Zoology*, 84, pp. 609–614. doi:10.1139/Z06-035.

Marques, T. A., Thomas, L., Martin, S. W., Mellinger, D. K., Ward, J. A., Moretti, D. J., Harris, D. and Tyack, P. L. (2013) 'Estimating animal population density using passive acoustics', *Biological Reviews*, 88(2), pp. 287–309. doi:10.1111/brv.12001.

Marques, T. A., Thomas, L., Ward, J., DiMarzio, N. and Tyack, P. L. (2009) 'Estimating cetacean population density using fixed passive acoustic sensors: an example with Blainville's beaked whales.', *The Journal of the Acoustical Society of America*, 125(4), pp. 1982–1994. doi:10.1121/1.3089590.

Marra, G. and Wood, S. N. (2011) 'Practical variable selection for generalized additive models',

Computational Statistics & Data Analysis. Elsevier, 55(7), pp. 2372–2387.

Martien, K. K., Chivers, S. J., Baird, R. W., Archer, F. I., Gorgone, A. M., Hancock-Hanser, B. L., Mattila, D., McSweeney, D. J., Oleson, E. M., Palmer, C., Pease, V. L., Robertson, K. M., Schorr, G. S., Schultz, M. B., Webster, D. L. and Taylor, B. L. (2014) 'Nuclear and Mitochondrial Patterns of Population Structure in North Pacific False Killer Whales (*Pseudorca crassidens*)', *Journal of Heredity*, 105(5), pp. 611–626. doi:10.5061/dryad.2pq32.

May-Collado, L. J. and Wartzok, D. (2008) 'A comparison of bottlenose dolphin whistles in the Atlantic Ocean: Factors promoting whistle variation', *Journal of Mammalogy*, 89(5), pp. 1229–1240. doi:10.1644/07-MAMM-A-310.1.

Mellinger, D. K., Stafford, K. M., Moore, S. E., Dziak, R. P. and Matsumoto, H. (2007) 'Fixed passive acoustic observation methods for cetaceans', *Oceanography*, 20(4), pp. 36–45. doi:10.5670/oceanog.2007.03.

Melo-Merino, S. M., Reyes-Bonilla, H. and Lira-Noriega, A. (2020) 'Ecological niche models and species distribution models in marine environments: A literature review and spatial analysis of evidence', *Ecological Modelling*, 415. doi:10.1016/j.ecolmodel.2019.108837.

Merkens, K., Mann, D., Janik, V. M., Claridge, D., Hill, M. and Oleson, E. (2018) 'Clicks of dwarf sperm whales (*Kogia sima*)', *Marine Mammal Science*, 34(4), pp. 963–978. doi:10.1111/mms.12488.

Mesnick, S. L., Taylor, B. L., Archer, F. I., Martien, K. K., Trevi??o, S. E., Hancock-Hanser, B. L., Moreno Medina, S. C., Pease, V. L., Robertson, K. M., Straley, J. M., Baird, R. W., Calambokidis, J., Schorr, G. S., Wade, P., Burkanov, V., Lunsford, C. R., Rendell, L. and Morin, P. A. (2011) 'Sperm whale population structure in the eastern and central North Pacific inferred by the use of single-nucleotide polymorphisms, microsatellites and mitochondrial DNA', *Molecular Ecology Resources*, 11(SUPPL. 1), pp. 278–298. doi:10.1111/j.1755-0998.2010.02973.x.

Mikkelsen, L., Rigét, F. F., Kyhn, L. A., Sveegaard, S., Dietz, R., Tougaard, J., Carlström, J. A. K., Carlén, I., Koblitz, J. C. and Teilmann, J. (2016) 'Comparing distribution of harbour porpoises (*Phocoena phocoena*) derived from satellite telemetry and passive acoustic monitoring', *PloS one*, 11(7), p. e0158788. doi:10.1371/journal.pone.0158788.

Miller, D. L., Burt, M. L., Rexstad, E. A. and Thomas, L. (2013) 'Spatial models for distance sampling data : recent developments and future directions', *Methods in Ecology and Evolution*,

4(11), pp. 1001–1010. doi:10.1111/2041-210X.12105.

Miller, D. L., Rexstad, E., Thomas, L., Laake, J. L. and Marshall, L. (2019) 'Distance sampling in R', *Journal of Statistical Software*, 89(1), pp. 1–28. doi:10.18637/jss.v089.i01.

Miller, P. J. O., Johnson, M. P. and Tyack, P. L. (2004) 'Sperm whale behaviour indicates the use of echolocation click buzzes "creaks" in prey capture.', *Proceedings Biological Sciences*, 271(1554), pp. 2239–47. doi:10.1098/rspb.2004.2863.

Møhl, B., Wahlberg, M., Madsen, P. T., Heerfordt, A. and Lund, A. (2003) 'The monopulsed nature of sperm whale clicks', *Journal of the Acoustical Society of America*, 114(2), pp. 1143–1154. doi:10.1121/1.1586258.

Moore, S. E. (2008) 'Marine mammals as ecosystem sentinels', *Journal of Mammalogy*, 89(3), pp. 534–540. doi:10.1644/07-MAMM-S-312R1.1.

Morisaka, T., Shinohara, M., Nakahara, F. and Akamatsu, T. (2005) 'Geographic variations in the whistles among three Indo-Pacific bottlenose dolphin (*Tursiops aduncus*) populations in Japan', *Fisheries Science*, 71(3), pp. 568–576. doi:10.1111/j.1444-2906.2005.01001.x.

Myrberg, A. A. (1980) 'Fish bio-acoustics: its relevance to the "not so silent world"', *Environmental Biology of Fishes*. Springer, 5(4), pp. 297–304.

Nitta, E. T. and Henderson, J. R. (1993) 'A review of interactions between Hawaii's fisheries and protected species', *Marine Fisheries Review*, 55(2), pp. 83–92.

Norris, K. S., Wursig, B., Wells, R. S. and Wursig, M. (1994) *The Hawaiian spinner dolphin*. Univ of California Press.

Nosal, E.-M. (2013) 'Chapter 8. Model-based marine mammal localization methods', in *DCL 2003-2013*, pp. 173–183.

Nosal, E.-M. and Frazer, L. N. (2006) 'Track of a sperm whale from delays between direct and surface-reflected clicks', *Applied Acoustics*, 67(11–12), pp. 1187–1201. doi:10.1016/j.apacoust.2006.05.005.

Nosal, E.-M. and Frazer, L. N. (2007) 'Sperm whale three-dimensional track, swim orientation, beam pattern, and click levels observed on bottom-mounted hydrophones.', *The Journal of the Acoustical Society of America*, 122(4), pp. 1969–1978. doi:10.1121/1.2775423.

Nowacek, D. P. (2005) 'Acoustic ecology of foraging bottlenose dolphins (*Tursiops truncatus*), habitat-specific use of three sound types', *Marine Mammal Science*, 21(4), pp. 587–602. doi:10.1111/j.1748-7692.2005.tb01253.x.

Olden, J. D., Jackson, D. A. and Peres-Neto, P. R. (2002) 'Predictive models of fish species distributions: A note on proper validation and chance predictions', *Transactions of the American Fisheries Society*, 131(2), pp. 329–336. doi:10.1577/1548-8659(2002)131<0329:pmofsd>2.0.co;2.

Oleson, E. M., Barlow, J. P., Barkley, Y., Becker, E. A. and Forney, K. A. (2015) *Stock Assessment Analytical Methods Annual Report: Incorporating passive acoustic detections into predictive models of cetacean abundance*.

Oleson, E. M., Boggs, C. H., Forney, K. A., Hanson, M. B., Knox, D., Taylor, B. L., Wade, P. R. and Ylitalo, G. M. (2010) 'Status review of Hawaiian insular false killer whales (*Pseudorca crassidens*) under the Endangered Species Act', *NOAA Technical Memorandum*, (NMFS-PIFSC-22), p. 140.

Oliveira, C., Wahlberg, M., Johnson, M., Miller, P. J. and Madsen, P. T. (2013) 'The function of male sperm whale slow clicks in a high latitude habitat: communication, echolocation, or prey debilitation?', *J Acoust Soc Am*, 133(5), pp. 3135–3144. doi:10.1121/1.4795798.

Oliveira, C., Wahlberg, M., Silva, M. A., Johnson, M., Antunes, R., Wisniewska, D. M., Fais, A., Gonçalves, J. and Madsen, P. T. (2016) 'Sperm whale codas may encode individuality as well as clan identity', *The Journal of the Acoustical Society of America*, 139(5), pp. 2860–2869. doi:10.1121/1.4949478.

Oswald, J. N. (2013) 'Development of a Classifier for the Acoustic Identification of Delphinid Species in the Northwest Atlantic Ocean'.

Oswald, J. N. and Oswald, M. (2013) 'ROCCA (Real-time Odontocete Call Classification Algorithm) User's Manual. Prepared for Naval Facilities Engineering Command Atlantic, Norfolk, Virginia under HDR Environmental, Operations and Construction, Inc. Contract CON005-4394-009, Subproject 1647'.

Oswald, J. N., Rankin, S. and Barlow, J. (2008) 'To whistle or not to whistle? Geographic variation in the whistling behavior of small odontocetes', *Aquatic Mammals*, 34(3), pp. 288–302. doi:10.1578/AM.34.3.2008.288.

Oswald, J. N., Rankin, S., Barlow, J. and Lammers, M. O. (2007) 'A tool for real-time acoustic species identification of delphinid whistles.', *The Journal of the Acoustical Society of America*, 122(1), pp. 587–595. doi:10.1121/1.2743157.

Owen, R. (1846) *A history of British fossil mammals and birds*. London: John Van Voorst.

Oyafuso, Z. S., Drazen, J. C., Moore, C. H. and Franklin, E. C. (2017) 'Habitat-based species distribution modelling of the Hawaiian deepwater snapper-grouper complex', *Fisheries Research*, 195, pp. 19–27. doi:10.1016/j.fishres.2017.06.011.

Pal, M. (2005) 'Random forest classifier for remote sensing classification', *International Journal of Remote Sensing*, 26(1), pp. 217–222. doi:10.1080/01431160412331269698.

Palacios, D. M., Baumgartner, M. F., Laidre, K. L. and Gregr, E. J. (2013) 'Beyond correlation: Integrating environmentally and behaviourally mediated processes in models of marine mammal distributions', *Endangered Species Research*, 22(3), pp. 191–203. doi:10.3354/esr00558.

Papale, E., Azzolin, M., Cascão, I., Gannier, A., Lammers, M. O., Martin, V. M., Oswald, J. N., Perez-Gil, M., Prieto, R., Silva, M. A. and Giacoma, C. (2013) 'Geographic variability in the acoustic parameters of striped dolphin's (*Stenella coeruleoalba*) whistles.', *The Journal of the Acoustical Society of America*, 133(2), pp. 1126–34. doi:10.1121/1.4774274.

Papale, E., Azzolin, M., Cascão, I., Gannier, A., Lammers, M. O., Martin, V. M., Oswald, J. N., Perez-Gil, M., Prieto, R., Silva, M. A. and Giacoma, C. (2014) 'Acoustic divergence between bottlenose dolphin whistles from the Central–Eastern North Atlantic and Mediterranean Sea', *Acta Ethologica*, 17(3), pp. 155–165. doi:10.1007/s10211-013-0172-2.

Papastavrou, V., Smith, S. C. and Whitehead, H. (1989) 'Diving behaviour of the sperm whale, *Physeter macrocephalus*, off the Galapagos Islands', *Canadian Journal of Zoology*, 67(1977), pp. 839–846.

Van Parijs, S. M., Clark, C. W., Sousa-Lima, R. S., Parks, S. E., Rankin, S., Risch, D. and Van Opzeeland, I. C. (2009) 'Management and research applications of real-time and archival passive acoustic sensors over varying temporal and spatial scales', *Marine Ecology Progress Series*, 395, pp. 21–36. doi:10.3354/meps08123.

Pebesma, E. (2018) 'Simple Features for R: Standardized Support for Spatial Vector Data', *The R Journal*, 10(1), pp. 439–446. doi:10.32614/RJ-2018-009.

Pirotta, E., Matthiopoulos, J., MacKenzie, M., Scott-Hayward, L. and Rendell, L. (2011) 'Modelling sperm whale habitat preference: A novel approach combining transect and follow data', *Marine Ecology Progress Series*, 436, pp. 257–272. doi:10.3354/meps09236.

Pitcher, T. J., Morato, T., Hart, P. J. B., Clark, M. R., Haggan, N. and Santos, R. S. (2007) *Seamounts: ecology, fisheries and conservation*, *Blackwell Fisheries and Aquatic Resources*

Series.

Polovina, J. J. and Howell, E. A. (2005) 'Ecosystem indicators derived from satellite remotely sensed oceanographic data for the North Pacific', *ICES Journal of Marine Science*, 62(3), pp. 319–327. doi:10.1016/j.icesjms.2004.07.031.

Polovina, J. J., Kobayashi, D. R., Parker, D. M., Seki, M. P. and Balazs, G. H. (2000) 'Turtles on the edge: Movement of loggerhead turtles (*Caretta caretta*) along oceanic fronts, spanning longline fishing grounds in the central North Pacific, 1997-1998', *Fisheries Oceanography*, 9(1), pp. 71–82. doi:10.1046/j.1365-2419.2000.00123.x.

Polovina, J., Uchida, I., Balazs, G., Howell, E. A., Parker, D. and Dutton, P. (2006) 'The Kuroshio Extension Bifurcation Region : A pelagic hotspot for juvenile loggerhead sea turtles', 53, pp. 326–339. doi:10.1016/j.dsr2.2006.01.006.

Porter, M. B. and Liu, Y.-C. (1994) 'Finite-element ray tracing', *Theoretical and Computational Acoustics*, 2, pp. 947–956.

Poulter, T. C. (1963) 'Sonar signals of the sea lion', *Science*, 139(3556), pp. 753–755.

Qiu, B. (1999) 'Seasonal eddy field modulation of the North Pacific Subtropical Countercurrent : TOPEX / Poseidon observations and theory', *Journal of Physical Oceanography*, 29, pp. 2471–2486.

Qiu, B., Koh, D. A., Lumpkin, C. and Flament, P. (1997) 'Existence and formation mechanism of the North Hawaiian Ridge Current', *American Meteorological Society*, 27, pp. 431–444.

Rankin, S., Archer, F., Keating, J. L., Oswald, J. N., Oswald, M., Curtis, A. and Barlow, J. (2017) 'Acoustic classification of dolphins in the California Current using whistles, echolocation clicks, and burst pulses', *Marine Mammal Science*, 33(2), pp. 520–540. doi:10.1111/mms.12381.

Rankin, S., Barlow, J., Barkley, Y. and Valtierra, R. (2013) 'A guide to constructing hydrophone arrays for passive acoustic data collection during NMFS shipboard cetacean surveys', *NOAA Technical Memorandum*, 511, p. 36.

Rankin, S., Barlow, J. and Oswald, J. N. (2008) 'An Assessment of the Accuracy and Precision of Localization of a Stationary Sound Source Using a Two-Element Towed Hydrophone Array', *NOAA Technical Memorandum*, 416, p. 35.

Rankin, S., Barlow, J., Oswald, J. N. and Ballance, L. (2008) 'Acoustic Studies of Marine Mammals During Seven Years of Combined Visual and Acoustic Line-Transect Surveys for

Cetaceans in the Eastern and Central Pacific Ocean', *NOAA Technical Memorandum*, (NMFS-SWFSC-429), p. 69.

Rankin, S., Oswald, J. N. and Barlow, J. (2008) 'Passive acoustic methods for population studies', *Canadian Acoustics*, 36(1), pp. 88–92.

Redfern, J. V., Ferguson, M. C., Becker, E. A., Hyrenbach, K. D., Good, C., Barlow, J., Kaschner, K., Baumgartner, M. F., Forney, K. A., Ballance, L. T., Fauchald, P., Halpin, P., Hamazaki, T., Pershing, A. J., Qian, S. S., Read, A., Reilly, S. B., Torres, L. and Werner, F. (2006) 'Techniques for cetacean-habitat modeling', *Marine Ecology Progress Series*, 310, pp. 271–295. doi:10.3354/meps310271.

Redfern, J. V., McKenna, M. F., Moore, T. J., Calambokidis, J., Deangelis, M. L., Becker, E. A., Barlow, J., Forney, K. A., Fiedler, P. C. and Chivers, S. J. (2013) 'Assessing the risk of ships striking large whales in marine spatial planning', *Conservation Biology*, 27(2), pp. 292–302. doi:10.1111/cobi.12029.

Rendell, L. E., Matthews, J. N., Gill, A., Gordon, J. C. D. and Macdonald, D. W. (1999) 'Quantitative analysis of tonal calls from five odontocete species, examining interspecific and intraspecific variation', *Journal of Zoology*. Blackwell Publishing Ltd, 249(4), pp. 403–410. doi:10.1111/j.1469-7998.1999.tb01209.x.

Rendell, L., Mesnick, S. L., Dalebout, M. L., Burtenshaw, J. and Whitehead, H. (2012) 'Can genetic differences explain vocal dialect variation in sperm whales, *Physeter macrocephalus*?', *Behavior Genetics*, 42(2), pp. 332–343. doi:10.1007/s10519-011-9513-y.

Rendell, L. and Whitehead, H. (2003) 'Vocal clans in sperm whales (*Physeter macrocephalus*).', *Proceedings of the Royal Society of London. Series B: Biological Sciences*, 270(1512), pp. 225–231. doi:10.1098/rspb.2002.2239.

Rendell, L. and Whitehead, H. (2004) 'Do sperm whales share coda vocalizations? Insights into coda usage from acoustic size measurement', *Animal Behaviour*, 67(5), pp. 865–874. doi:10.1016/j.anbehav.2003.04.018.

Riesch, R. and Deecke, V. B. (2011) 'Whistle communication in mammal-eating killer whales (*Orcinus orca*): Further evidence for acoustic divergence between ecotypes', *Behavioral Ecology and Sociobiology*, 65(7), pp. 1377–1387. doi:10.1007/s00265-011-1148-8.

Riesch, R., Ford, J. K. B. and Thomsen, F. (2006) 'Stability and group specificity of stereotyped whistles in resident killer whales, *Orcinus orca*, off British Columbia', *Animal Behaviour*,

71(1), pp. 79–91. doi:10.1016/j.anbehav.2005.03.026.

Roberts, J. J., Best, B. D., Mannocci, L., Fujioka, E., Halpin, P. N., Palka, D. L., Garrison, L. P., Mullin, K. D., Cole, T. V. N., Khan, C. B., Mclellan, W. A., Pabst, D. A. and Lockhart, G. G. (2016) 'Habitat-based cetacean density models for the U.S. Atlantic and Gulf of Mexico', *Scientific Reports*. Nature Publishing Group, 6(1), pp. 1–12. doi:10.1038/srep22615.

Robinson, N. M., Nelson, W. A., Costello, M. J., Sutherland, J. E. and Lundquist, C. J. (2017) 'A systematic review of marine-based Species Distribution Models (SDMs) with recommendations for best practice', *Frontiers in Marine Science*, 4(DEC), pp. 1–11. doi:10.3389/fmars.2017.00421.

Robinson, P. W., Costa, D. P., Crocker, D. E., Gallo-reynoso, J. P., Champagne, C. D., Fowler, M. A., Goetsch, C., Goetz, K. T., Hassrick, J. L., Kuhn, C. E., Maresh, J. L., Maxwell, S. M., Mcdonald, B. I., Hu, L. A., Peterson, S. H., Simmons, S. E., Teutschel, N. M., Villegas-amtmann, S. and Yoda, K. (2012) 'Foraging behavior and success of a mesopelagic predator in the Northeast Pacific Ocean : Insights from a data-rich species , the northern elephant seal', *PLoS ONE*, 7(5), p. e36728. doi:10.1371/journal.pone.0036728.

Roch, M. A., Scott Brandes, T., Patel, B., Barkley, Y., Baumann-Pickering, S. and Soldevilla, M. S. (2011) 'Automated extraction of odontocete whistle contours', *The Journal of the Acoustical Society of America*, p. 2212.

Roman, J., Estes, J. A., Morissette, L., Smith, C., Costa, D., McCarthy, J., Nation, J. B., Nicol, S., Pershing, A. and Smetacek, V. (2014) 'Whales as marine ecosystem engineers', *Frontiers in Ecology and the Environment*, 12(7), pp. 377–385. doi:10.1890/130220.

Roman, J. and McCarthy, J. J. (2010) 'The whale pump: Marine mammals enhance primary productivity in a coastal basin', *PLoS ONE*, 5(10). doi:10.1371/journal.pone.0013255.

Rossi-Santos, M. R. and Podos, J. (2006) 'Latitudinal variation in whistle structure of the estuarine dolphin *Sotalia guianensis*', *Behaviour*, 143(3), pp. 347–364.

Saha, S., Nadiga, S., Thiaw, C., Wang, J., Wang, W., Zhang, Q., Van den Dool, H. M., Pan, H.-L., Moorthi, S., Behringer, D., Stokes, D., Peña, M., Lord, S., White, G., Ebisuzaki, W., Peng, P. and Xie, P. (2006) 'The NCEP climate forecast system', *Journal of Climate*, 19(15), pp. 3483–3517. doi:10.1175/JCLI3812.1.

Sakai, T. (2020) 'PAMmisc: A collection of miscellaneous functions for passive acoustics'.

Saulitis, E. L., Matkin, C. O. and Fay, F. H. (2005) 'Vocal repertoire and acoustic behavior of

the isolated AT1 killer whale subpopulation in southern Alaska', *Canadian Journal of Zoology*, 83, pp. 1015–1029. doi:10.1139/z05-089.

Scales, K. L., Miller, P. I., Hawkes, L. A., Ingram, S. N., Sims, D. W. and Votier, S. C. (2014) 'On the front line: Frontal zones as priority at-sea conservation areas for mobile marine vertebrates', *Journal of Applied Ecology*, 51(6), pp. 1575–1583. doi:10.1111/1365-2664.12330.

Scarpaci, C., Bigger, S. W., Corkeron, P. J. and Nugegoda, D. (2000) 'Bottlenose dolphins (*Tursiops truncatus*) increase whistling in the presence of " swim-with-dolphin " tour operations', *Journal of Cetacean Research and Management*, 2(3), pp. 183–185.

Schevill, W. E. and Lawrence, B. (1949) 'Underwater listening to the white porpoise (*Delphinapterus leucas*)', *Science*, 109(2824), pp. 143–144.

Schorr, G. S., Falcone, E. A., Moretti, D. J. and Andrews, R. D. (2014) 'First long-term behavioral records from Cuvier's beaked whales (*Ziphius cavirostris*) reveal record-breaking dives', *PLoS ONE*, 9(3). doi:10.1371/journal.pone.0092633.

Seki, M. P., Polovina, J. J., Kobayashi, D. R., Robert, R. and Mitchum, G. T. (2002) 'An oceanographic characterization of swordfish (*Xiphias gladius*) longline fishing grounds in the springtime subtropical North Pacific', *Fisheries Oceanography*, 11(5), pp. 251–266.

Shallenberger, E. W. (1981) *The status of Hawaiian Cetaceans. Final report to US Marine Mammal Commission*.

Silva, T. L., Mooney, T. A., Sayigh, L. S., Tyack, P. L., Baird, R. W. and Oswald, J. N. (2016) 'Whistle characteristics and daytime dive behavior in pantropical spotted dolphins (*Stenella attenuata*) in Hawai'i measured using digital acoustic recording tags (DTAGs)', *The Journal of the Acoustical Society of America*, 140(1), pp. 421–429. doi:10.1121/1.4955081.

Simmons, J. A. and Stein, R. A. (1980) 'Acoustic imaging in bat sonar: echolocation signals and the evolution of echolocation', *Journal of comparative physiology*. Springer, 135(1), pp. 61–84.

Smotherman, M., Knörnschild, M., Smarsh, G. and Bohn, K. (2016) 'The origins and diversity of bat songs', *Journal of Comparative Physiology A: Neuroethology, Sensory, Neural, and Behavioral Physiology*. Springer Berlin Heidelberg, 202(8), pp. 535–554. doi:10.1007/s00359-016-1105-0.

Soldevilla, M. S., Henderson, E. E., Campbell, G. S., Wiggins, S. M., Hildebrand, J. A. and

Roch, M. A. (2008) ‘Classification of Risso’s and Pacific white-sided dolphins using spectral properties of echolocation clicks.’, *The Journal of the Acoustical Society of America*, 124(1), pp. 609–624. doi:10.1121/1.2932059.

Southall, B. L., Nowacek, D. P., Miller, P. J. O. and Tyack, P. L. (2016) ‘Experimental field studies to measure behavioral responses of cetaceans to sonar’, *Endangered Species Research*, 31(1), pp. 293–315. doi:10.3354/esr00764.

Stafford, K. M., Fox, C. G. and Clark, D. S. (1998) ‘Long-range acoustic detection and localization of blue whale calls in the northeast Pacific Ocean’, *The Journal of the Acoustical Society of America*, 104(6), pp. 3616–3625. doi:10.1121/1.423944.

Staudigel, H., Koppers, A. A. P., William Lavelle, J., Pitcher, T. J. and Shank, T. M. (2010) ‘Box 1: Defining the word “seamount”’, *Oceanography*, 23(1), pp. 20–21. doi:10.5670/oceanog.2010.85.

Straley, J. M., Schorr, G. S., Thode, A. M., Calambokidis, J., Lunsford, C. R., Chenoweth, E. M., O’Connell, V. M. and Andrews, R. D. (2014) ‘Depredating sperm whales in the Gulf of Alaska: Local habitat use and long distance movements across putative population boundaries’, *Endangered Species Research*, 24(2), pp. 125–135. doi:10.3354/esr00595.

Strobl, C., Boulesteix, A. L., Kneib, T., Augustin, T. and Zeileis, A. (2008) ‘Conditional variable importance for random forests’, *BMC Bioinformatics*, 9, pp. 1–11. doi:10.1186/1471-2105-9-307.

Sveegaard, S., Galatius, A., Dietz, R., Kyhn, L., Koblitz, J. C., Amundin, M., Nabe-Nielsen, J., Sinding, M. H. S., Andersen, L. W. and Teilmann, J. (2015) ‘Defining management units for cetaceans by combining genetics, morphology, acoustics and satellite tracking’, *Global Ecology and Conservation*. Elsevier B.V., 3(May), pp. 839–850. doi:10.1016/j.gecco.2015.04.002.

Taylor, B. L., Baird, R., Barlow, J., Dawson, S. M., Ford, J., Mead, J. G., Notarbartolo di Sciara, G., Wade, P. and Pitman, R. L. (2019) ‘*Physeter macrocephalus* , Sperm Whale (Amended version)’, *The IUCN Red List of Threatened Species*, 8235. doi:e.T41755A160983555.

Taylor, B. L., Wade, P. R., Master, D. P. D. E. and Barlow, J. A. Y. (2000) ‘Incorporating Uncertainty into Management Models for Marine Mammals’, 14(5), pp. 1243–1252.

Team, R. C. (2018) ‘R: A language and environment for statistical computing’. Vienna, Austria: R Foundation for Statistical Computing.

Team, R. C. (2020) ‘R: A language and environment for statistical computing’. Vienna, Austria: R Foundation for Statistical Computing.

Teloni, V., Johnson, M. P., Miller, P. J. O. and Madsen, P. T. (2008) ‘Shallow food for deep divers: Dynamic foraging behavior of male sperm whales in a high latitude habitat’, *Journal of Experimental Marine Biology and Ecology*, 354(1), pp. 119–131. doi:10.1016/j.jembe.2007.10.010.

Thode, A. (2004) ‘Tracking sperm whale (*Physeter macrocephalus*) dive profiles using a towed passive acoustic array’, *Journal of the Acoustical Society of America*, 116(1), pp. 245–253. doi:10.1121/1.1758972.

Thode, A. (2005) ‘Three-dimensional passive acoustic tracking of sperm whales (*Physeter macrocephalus*) in ray-refracting environments’, *Journal of the Acoustical Society of America*, 118(6), pp. 3575–3584. doi:10.1121/1.2049068.

Thomas, L., Buckland, S. T., Burnham, K. P., Anderson, D. R., Laake, J. L., Borchers, D. L. and Strindberg, S. (2006) ‘Distance sampling’, *Encyclopedia of …*, 1, pp. 544–552. doi:10.2307/2532812.

Thompson, P. O. and Friedl, W. A. (1982) ‘A long term study of low frequency sounds from several species of whales off Oahu, Hawaii’. Biological Systems.

Thomsen, F., Franck, D. and Ford, J. K. (2002) ‘On the communicative significance of whistles in wild killer whales (*Orcinus orca*)’, *Naturwissenschaften*, 89(9), pp. 404–407. doi:10.1007/s00114-002-0351-x.

Tiemann, C. O., Porter, M. B. and Frazer, L. N. (2004) ‘Localization of marine mammals near Hawaii using an acoustic propagation model.’, *The Journal of the Acoustical Society of America*, 115(6), pp. 2834–2843. doi:10.1121/1.1643368.

Timmel, G., Courbis, S., Sargeant-Green, H. and Markowitz, H. (2008) ‘Effects of human traffic on the movement patterns of Hawaiian spinner dolphins (*Stenella longirostris*) in Kealakekua Bay , Hawaii’, *Aquatic Mammals*, 34(4), pp. 402–411. doi:10.1578/AM.34.4.2008.402.

Tishechkin, D. Y. (2014) ‘The use of bioacoustic characters for distinguishing between cryptic species in insects: Potentials, restrictions, and prospects’, *Entomological review*. Springer, 94(3), pp. 289–309.

Titus, K., Mosher, J. A. and Williams, B. K. (1984) ‘Chance-corrected classification for use in discriminant analysis: Ecological applications’, *The American Midland Naturalist*, 111(1), pp.

1–7.

Torres, L. G., Nieukirk, S. L., Lemos, L. and Chandler, T. E. (2018) ‘Drone up! Quantifying whale behavior from a new perspective improves pbservational capacity’, *Frontiers in Marine Science*, 5(319), pp. 1–14. doi:10.3389/fmars.2018.00319.

Tozer, B., Sandwell, D. T., Smith, W. H. F., Olson, C., Beale, J. R. and Wessel, P. (2019) ‘Global Bathymetry and Topography at 15 Arc Sec: SRTM15+’, *Earth and Space Science*, 6(10), pp. 1847–1864. doi:10.1029/2019EA000658.

Tyack, P. L., Zimmer, W. M. X., Moretti, D., Southall, B. L., Claridge, D. E., Durban, J. W., Clark, C. W., D’Amico, A., DiMarzio, N., Jarvis, S., McCarthy, E., Morrissey, R., Ward, J. and Boyd, I. L. (2011) ‘Beaked whales respond to simulated and actual navy sonar’, *PLoS ONE*, 6(3). doi:10.1371/journal.pone.0017009.

Urian, K., Gorgone, A., Read, A., Balmer, B., Wells, R. S., Berggren, P., Durban, J., Eguchi, T., Rayment, W. and Hammond, P. S. (2015) ‘Recommendations for photo-identification methods used in capture-recapture models with cetaceans’, *Marine Mammal Science*, 31(1), pp. 298–321. doi:10.1111/mms.12141.

Van Cise, A. M., Mahaffy, S. D., Baird, R. W., Mooney, T. A. and Barlow, J. (2018) ‘Song of my people: dialect differences among sympatric social groups of short-finned pilot whales in Hawai’i’, *Behavioral Ecology and Sociobiology*, 72(193), pp. 1–13. doi:10.1007/s00265-018-2596-1.

Van Cise, A. M., Roch, M. A., Baird, R. W., Mooney, T. A. and Barlow, J. (2017) ‘Acoustic differentiation of Shiho- and Naisa-type short-finned pilot whales in the Pacific Ocean’, *The Journal of the Acoustical Society of America*, 141(2), pp. 737–748. doi:10.1121/1.4974858.

Virgili, A., Authier, M., Boisseau, O., Cañadas, A., Claridge, D., Cole, T., Corkeron, P., Dorémus, G., David, L., Di-Méglio, N., Dunn, C., Dunn, T. E., García-Barón, I., Laran, S., Lauriano, G., Lewis, M., Louzao, M., Mannocci, L., Martínez-Cedeira, J., Palka, D., Panigada, S., Pettex, E., Roberts, J. J., Ruiz, L., Saavedra, C., Santos, M. B., Van Canneyt, O., Vázquez Bonales, J. A., Monestiez, P. and Ridoux, V. (2019) ‘Combining multiple visual surveys to model the habitat of deep-diving cetaceans at the basin scale: Large-scale modelling of deep-diving cetacean habitats’, *Global Ecology and Biogeography*, 28(3), pp. 300–314. doi:10.1111/geb.12850.

von Benda-Beckmann, A. M., Thomas, L., Tyack, P. L. and Ainslie, M. A. (2018) ‘Modelling

the broadband propagation of marine mammal echolocation clicks for click-based population density estimates', *The Journal of the Acoustical Society of America*, 143(2), pp. 954–967. doi:10.1121/1.5023220.

Wahlberg, M. (2002) 'The acoustic behaviour of diving sperm whales observed with a hydrophone array', *Journal of Experimental Marine Biology and Ecology*, 281(1–2), pp. 53–62. doi:10.1016/S0022-0981(02)00411-2.

Wang, B., Wu, R. and Lukas, R. (2000) 'Annual adjustment of the thermocline in the tropical Pacific Ocean', *Journal of Climate*, 13(3), pp. 596–616. doi:10.1175/1520-0442(2000)013<0596:AAOTTI>2.0.CO;2.

Watanabe, H., Kubodera, T., Moku, M. and Kawaguchi, K. (2006) 'Diel vertical migration of squid in the warm core ring and cold water masses in the transition region of the western North Pacific', *Marine Ecology Progress Series*, 315, pp. 187–197. doi:10.3354/meps315187.

Watwood, S. L., Miller, P. J. O., Johnson, M., Madsen, P. T. and Tyack, P. L. (2006) 'Deep-diving foraging behaviour of sperm whales (*Physeter macrocephalus*)', *Journal of Animal Ecology*, 75(3), pp. 814–825. doi:10.1111/j.1365-2656.2006.01101.x.

Weilgart, L. S. (2007) 'The impacts of anthropogenic ocean noise on cetaceans and implications for management', *Canadian Journal of Zoology*, 85(11), pp. 1091–1116. doi:10.1139/Z07-101.

Weilgart, L. and Whitehead, H. (1993) 'Coda communication by sperm whales (*Physeter macrocephalus*) off the Galapagos Islands', *Canadian Journal of Zoology*. NRC Research Press, 71(4), pp. 744–752.

Wessel, P. and Smith, W. H. F. (1996) 'A global, self-consistent, hierarchical, high-resolution shoreline database', *Journal of Geophysical Research B: Solid Earth*, 101(4), pp. 8741–8743. doi:10.1029/96jb00104.

Whitehead, H. (1996) 'Babysitting, dive synchrony, and indications of alloparental care in sperm whales', *Behavioral Ecology and Sociobiology*, 38(4), pp. 237–244.

Whitehead, H. (2003) *Sperm Whales: Social Evolution in the Ocean*. Chicago: University of Chicago Press.

Whitehead, H. and Weilgart, L. (1990) 'Click rates from sperm whales', *Journal of the Acoustical Society of America*, 87(4), pp. 1798–1806. doi:10.1121/1.399376.

Wiener, C., Insitute, S. O. and Needham, M. D. (2009) 'Hawaii's real life marine park : Interpretation and impacts of commercial marine tourism in the Hawaiian Islands', *Current*

Issues in Tourism, 12(5–6), pp. 489–504. doi:10.1080/13683500902736855.

Wild, L., Straley, J. and Gordon, J. (2017) *Real Time Localization of Sperm Whales Using a Towed Array Hydrophone*. Sitka, Alaska.

Wong, S. N. P. and Whitehead, H. (2014) 'Seasonal occurrence of sperm whales (*Physeter macrocephalus*) around Kelvin Seamount in the Sargasso Sea in relation to oceanographic processes', *Deep-Sea Research Part I: Oceanographic Research Papers*. Elsevier, 91, pp. 10–16. doi:10.1016/j.dsr.2014.05.001.

Wood, S. N. (2011) 'Fast stable restricted maximum likelihood and marginal likelihood estimation of semiparametric generalized linear models', *Journal of the Royal Statistical Society*, 73(1), pp. 3–36.

Woodworth, P. A., Schorr, G. S., Baird, R. W., Webster, D. L., Mcsweeney, D. J., Hanson, M. B., Andrews, R. D. and Polovina, J. J. (2012) 'Eddies as offshore foraging grounds for melon-headed whales (*Peponocephala electra*)', *Marine Mammal Science*, 28(3), pp. 638–647. doi:10.1111/j.1748-7692.2011.00509.x.

Yack, T. M., Norris, T. N. and Novak, N. (2016) *Acoustic Based Habitat Models for Sperm Whales in the Mariana Islands Region*. Arlington, VA.

Yano, K. M., Oleson, E. M., Keating, J. L., Ballance, L. T., Hill, M. C., Bradford, A. L., Allen, A. N., Joyce, T. W., Moore, E. and Henry, A. (2018) 'Cetacean and seabird data collected during the Hawaiian Islands Cetacean and Ecosystem Assessment Survey (HICEAS), July – December 2017', *NOAA Technical Memorandum*, 72, p. 110.

Ylitalo, G. M., Baird, R. W., Yanagida, G. K., Webster, D. L., Chivers, S. J., Bolton, J. L., Schorr, G. S. and McSweeney, D. J. (2009) 'High levels of persistent organic pollutants measured in blubber of island-associated false killer whales (*Pseudorca crassidens*) around the main Hawaiian Islands', *Marine Pollution Bulletin*, 58(12), pp. 1932–1937. doi:10.1016/j.marpolbul.2009.08.029.

Young, R. E. (1978) 'Vertical distribution and photosensitive vesicles of pelagic cephalopods from Hawaiian waters', *Fishery Bulletin*, 76(3), pp. 583–615.

Yurk, H., Barrett-Lennard, L., Ford, J. K. B. and Matkin, C. O. (2002) 'Cultural transmission within maternal lineages: Vocal clans in resident killer whales in southern Alaska', *Animal Behaviour*, 63(6), pp. 1103–1119. doi:10.1006/anbe.2002.3012.

Zapetis, M. and Szesciorka, A. R. (2018) 'Cetacean Navigation', *Encyclopedia of Animal*

Cognition and Behavior. Springer International Publishing.

Zhang, H., Ludsin, S. A., Mason, D. M., Adamack, A. T., Brandt, S. B., Zhang, X., Kimmel, D. G., Roman, M. R. and Boicourt, W. C. (2009) 'Hypoxia-driven changes in the behavior and spatial distribution of pelagic fi sh and mesozooplankton in the northern Gulf of Mexico', *Journal of Experimental Marine Biology and Ecology*, 381, pp. 80–91. doi:10.1016/j.jembe.2009.07.014.

Zimmer, W. M. X. (2013) 'Range estimation of cetaceans with compact volumetric arrays.', *The Journal of the Acoustical Society of America*, 134(3), pp. 2610–2618. doi:10.1121/1.4817892.

Zimmer, W. M. X., Harwood, J., Tyack, P. L., Johnson, M. P. and Madsen, P. T. (2008) 'Passive acoustic detection of deep-diving beaked whales', *Journal of the Acoustical Society of America*, 124(5), pp. 2823–2832. doi:10.1121/1.2988277.